

Mechanistic Aspects of RAFT Mediated (Co) Polymerization by *In situ* ^1H NMR

by

Mpho Mothunya

*This thesis is submitted in partial fulfilment of the requirements of
MSc degree in polymer science at the University of Stellenbosch*



Supervisor: Prof. Bert Klumperman

Faculty of Science

Department of Chemistry and Polymer Science

March 2013

Declaration

I, the under-signed, hereby declare that the work submitted in this thesis is original and is my own work; this work has not been submitted to acquire any other degree or qualification.

Mpho Mothunya

.....

Stellenbosch, March 2013

"

"

"

"

"

"

"

"

"

"

"

"

"

"

"

"

"

"

"

"

"

"

"

"

Eqr {tki j vÍ "4235"Ugmgpdquej "Wpłxgtukv{
Cmłtki j w'tgugt xgf

Abstract

In this study the kinetic and mechanistic aspects of the Reversible Addition Fragmentation Chain Transfer (RAFT) process on the copolymerization of acrylonitrile (AN) and vinyl acetate (VAc) are investigated by application of *in situ* ^1H nuclear magnetic resonance (NMR) spectroscopy. The focus is on the early stages of the reaction where the first few monomer (M) additions occur; the change in concentration of the leaving group of RAFT species as a function of time is followed. Cumyl dithiobenzoate (CDB), *S*-*sec* propionic acid *O*-ethyl xanthate (PEX) and *O*-ethyl cumyl xanthate (ECX) were selected for use in this study. The basis for RAFT agent selection was solely the fact that more activated monomers, e.g. acrylonitrile (AN) are controlled by dithiobenzoates while the less activated monomers, e.g. VAc, are controlled by xanthates. Furthermore, the behaviour of the copolymerization, where the reaction medium is composed of a RAFT agent preferring one monomer in the reaction, is largely unexplored in the literature.

First, the homopolymerization of each of these monomers was studied. In accordance with the literature, the AN showed good control when CDB was used as the chain transfer agent, whereas VAc showed good control when using PEX to mediate the polymerization. More emphasis is however placed on the CDB-mediated copolymerization as it still showed some preferential consumption of AN even in the presence of the VAc comonomer, although the reaction was retarded. The copolymerization mixtures comprised the monomer pair, the RAFT agent, and the 2,2'-azobis(isobutyronitrile) (AIBN) in mole ratios as specified for each experiment. When using the total monomer to RAFT to initiator ([M]:[CDB]:[AIBN]) ratio of 5:1:0.2, the AN initialization time was found to be 150 min at 60 °C. Copolymerization of AN with VAc under similar conditions resulted in retardation of the initialization reaction; the initialization period was now about 600 min at $f_{\text{VAc}} = 0.1$. In all the copolymerization reactions undertaken under the conditions described, the VAc monomer conversion was 4–6%. This means that VAc, possibly, retards the copolymerization by binding to the cumyl radicals of the CDB, which it then releases due to weak bonds formed with CDB.

Second, reactivity ratios were later determined, using the non-linear least squares fitting method. The results showed excellent correlation between the experimental and fitted data for the CDB- and PEX-mediated systems, but within a narrow experimental data region for ECX at $f_{AN}=0.5$, thus for [AN]/[VAc] ratios 0.65–0.93.

Opsomming

In hierdie studie word die kinetiese en meganitiese aspekte van die proses van die kopolimerisasie van akrilonitriël (AN) en vinielasetaat (VAs) ondersoek met behulp van *in situ* ^1H KMR. Die fokus is op die vroeë stadiums van die reaksie waar addisie van die eerste paar monomere (M) plaasvind. Die verandering in konsentrasie van die verlatende groep as 'n funksie van tyd is tydens hierdie stadium gemeet. Kumielditiobensoaat (KDB), *S*-sek-propiëlsuur-*O*-etiel-xantaat (PEX) en *O*-etiel-kumiel-xantaat (ECX) is vir hierdie studie gekies. Die keuses is gebaseer op die feit dat meer geaktiveerde monomere, bv. AN, deur ditiobensoaat beheer word, terwyl die minder geaktiveerde monomere, bv. VAs, deur xantate beheer word. Daar is nie baie voorbeelde in die literatuur oor die gedrag van die kopolimerisasie waar een van die monomere deur die RAFT-agent bevoordeel word nie.

Eerstens is die homopolimerisasie van elk van hierdie monomeerpere (AN en VAs) bestudeer. In ooreenstemming met die literatuur, het die AN goeie beheer getoon wanneer KDB gebruik is as die kettingoordragmiddel, terwyl VAs goeie beheer in die polimerisasie getoon het in die teenwoordigheid van PEX as bemiddelingsagent. Meer klem word egter geplaas op die KDB-bemiddelde kopolimerisasie omdat dit AN by voorkeur gebruik, selfs in die teenwoordigheid van die VAs komonomeer, alhoewel daar 'n vertraging in die reaksie is. Die reaksiemengsel het bestaan uit die monomeepaar, die RAFT-agent en die afsetter (AIBN), in verhoudings soos uiteengesit vir elke eksperiment. Vir 'n totale monomeer tot RAFT tot afsetter ($[\text{M}]:[\text{KDB}]:[\text{AIBN}]$) verhouding van 5:1:0.2 was die afsettingstyd vir AN 150 min by $60\text{ }^\circ\text{C}$. Kopolimerisasie van AN en VAs onder dieselfde omstandighede het tot 'n vertraging in die afsettingstyd gelei. Die periode was 600 min by $f_{\text{VAs}} = 0.1$. Die omsetting van VAs in al die kopolimerisasiereaksies was 4–6%, wat beteken dat VAs die reaksie vertraag deur aan die kumielradikale van die KDB te bind. Die radikale word weer vrygestel a.g.v. die swak bindings tussen die twee vorms.

Tweedens is die reaktiwiteitsverhoudings bepaal deur middel van die nie-lineêre kleinstekwadrate passingsmetode. Die resultate het uitstekende ooreenstemming tussen die

eksperimentele en gepaste data vir die KBD- en PEX-bemiddelde sisteme getoon. Dit was egter slegs vir 'n kort eksperimentele area vir ECX by $f_{AN} = 0.5$, dus vir $[AN]/[VAs]$ verhoudings 0.65–0.93.

Acknowledgements

Prof. B. Klumperman for giving me a chance to study in his research group and also for invaluable advice and support he offered throughout this study. I thank you for giving me the freedom to learn and grow as an independent researcher. I would like to thank Stellenbosch University and the NRF SARChI for funding my MSc Study.

Dr. L. Hlalele, thank you for being a tolerant mentor and for teaching me so much regarding data analysis and also for proof reading my work, I am forever grateful for that. Dr. E. van den Dungen is thanked for helping with processing *in situ* ^1H NMR experiments and for teaching me how to use the HPLC instrument. Dr. R. Pfukwa, thank you for helping me feel like I belong, for teasing me whenever wherever, and for proof reading my work and valuable suggestions you always gave me.

To, soon to be Dr., ‘the Magnificent-Kay’ Khotso Mpitso thank you for the friendship and all the frank advices offered and for always listening attentively to my whining and complaining.

To Waled Hadasha, thank you for always checking up on me when doing my distillations and making sure everything goes well, I appreciated all of your contributions. Khumo Maiko, thank you for being a friend and for advice on how to interpret LCMS data. Freda Meltz, Welmarie Van Schalkwyk and Dr.Hurndall are thanked for abstract translation

CAF staff: Dr. M. Stander for LCMS analysis, Dr. D. J. Brand and Elsa Malherbe are acknowledged for continuously running my *in situ* ^1H NMR experiments and for their continuous support and advice on how to get more out of NMR techniques.

To my husband, Mohau Phiri, thank you for support and allowing me to follow my passion, to my son, Poloko Phiri, thank you for not crying too much at night. And for all the smiles and laughter that you welcomed with every time I came back home from school, this really kept me going even during stressful times. I also most importantly would like to thank my aunt, Nkileng Mothunya, for putting her life on hold and taking care of my son while I was studying and also for making sure that I ate healthy throughout my MSc study.

I would like to thank fellow Basotho at Stellenbosch University, all members of LESA-SU for their support and for creating a homey environment away from home. Last but not least, I acknowledge the entire free radical group.

Above it all, I want to thank God almighty for having given me the strength to endure all the challenges I encountered throughout the completion of this work. I know without Him I wouldn't have made it.

Table of Contents

Declaration.....	ii
Abstract.....	iii
Opsomming.....	v
Acknowledgements.....	vii
Table of Contents.....	ix
List of Symbols.....	xii
List of Acronyms.....	xiv
List of Schemes.....	xvii
List of Tables.....	xviii
List of Figures.....	xix
Chapter 1: INTRODUCTION.....	1
1.1 Free Radical Polymerization.....	1
1.2 Controlled/Living Radical Polymerization (CLRP).....	4
1.2.1 Atom Transfer Radical Polymerization (ATRP).....	5
1.2.2 Nitroxide Mediated Polymerization (NMP).....	5
1.3 Background to the Project.....	6
1.4 Objectives.....	7
1.5 References.....	8
Chapter 2: LITERATURE REVIEW.....	10
2.1 RAFT Mediated Polymerization: Overview.....	10
2.1.1. The Leaving (R) Group.....	10
2.1.2. The Stabilizing/Destabilizing (Z) Group.....	11
2.2 Initiation in RAFT Process.....	12
2.2.1. 2,2'-Azobis(isobutyronitrile) (AIBN) Decomposition.....	12
2.3 Kinetic and Mechanistic Aspects of the RAFT Process.....	14
2.3.1 Selective and Non-Selective Initialization in RAFT Mediated Polymerization.....	16
2.4 Drawbacks of RAFT Polymerization.....	18
2.5 <i>In Situ</i> Proton (¹ H) NMR Analysis.....	19
2.6 References.....	20

Chapter 3: EXPERIMENTAL	23
3.1 RAFT Agent Synthesis	23
3.1.1 Procedure for Drying THF	23
3.1.2 Chemicals	23
3.1.3 Synthesis of Cumyl Dithiobenzoate (CDB)	24
3.1.4 Synthesis of <i>S</i> -sec Propionic Acid <i>O</i> -Ethyl Xanthate (PEX)	25
3.1.5 Synthesis of <i>O</i> -Ethyl Cumyl Xanthate (ECX).....	27
3.2 <i>In Situ</i> Proton NMR Analysis.....	28
3.2.1 Sample Preparation.....	28
3.2.2 <i>In situ</i> ¹ H NMR Experiments.....	28
3.2.3 Data Normalization.....	29
3.3 Size exclusion chromatographic (SEC) analysis.....	30
3.4 HPLC-MS analysis	31
3.5 References.....	32
Chapter 4: RAFT MEDIATED HOMOPOLYMERIZATION	33
4.1 Introduction	33
4.1.1 Controlled features	33
4.1.2 Living features	33
4.2 Properties of PAN and PVAc.....	34
4.3 Experimental	34
4.3.1 Chemicals	34
4.3.2 Sample Preparation.....	35
4.3.3 <i>In Situ</i> Proton NMR experiments	35
4.4 Results and Discussions	36
4.4.1 CDB mediated homopolymerization	36
4.4.2 ECX mediated homopolymerization	44
4.4.3 PEX mediated homopolymerization.....	48
4.4.4 Side reactions in CDB and ECX homopolymerization	52
4.4 Conclusion.....	53
4.5 References	55
CHAPTER 5: RAFT MEDIATED COPOLYMERIZATION	56

5.1 Introduction	56
5.2 Determination of Reactivity Ratios	57
5.3 Experimental	59
5.4 Results and Discussions	59
5.4.1 CDB-Mediated Acrylonitrile-Vinyl Acetate (AN/VAc) Copolymerization	60
5.4.1.1 Temperature effect study	62
5.4.1.2 Increased chain length study.....	63
5.4.1.3 Variation of monomer conversion with temperature and chain length	64
5.4.1.4 Higher temperature and longer chain length studies	66
5.4.1.5 Variation of initialization time as a function of VAc feed composition	68
5.4.1.6 Selectivity Studies with CDB	70
5.4.2 <i>S</i> -Cumyl- <i>O</i> -Ethyl Xanthate (ECX) Mediated Copolymerization.....	72
5.4.3 <i>S-sec</i> Propionic acid <i>O</i> -Ethyl Xanthate (PEX) Mediated AN-VAc Copolymerization	74
5.4.4 Evaluation of the Reactivity Ratios	76
5.4.5 LC-MS Analysis for RAFT Mediated Copolymerization	80
5.4.6 High molecular weight RAFT-mediated AN/VAc copolymerization.....	84
5.5 Conclusion.....	88
5.6 References	90
Chapter 6: Conclusions and Recommendations	91
6.1 Overall conclusions	91
6.2 Recommendations	92
APPENDIX.....	93

List of Symbols

$[I_2]_0$	Initial concentration of initiator
$[M]_0$	Initial concentration of Monomer
$[P^*]$	Propagating radical concentration
$[RAFT]_0$	Initial concentration of RAFT agent
C_T	Rate transfer coefficient
D	Dispersity
f	Initiator efficiency factor
I^*	Initiator radical
I_2	Initiator molecule
$k_{a,i,j}$	Rate coefficient of addition during main equilibrium in RAFT process
$k_{a,i,o}$	Rate coefficient of addition during pre-equilibrium in RAFT process
k_{act}	Rate coefficient for activation cycle in ATRP process
k_c	Rate coefficient for combination in NMP equilibrium
k_c	Rate coefficient for combination in NMP process
k_d	Initiator decomposition rate coefficient
k_{deact}	Rate coefficient for deactivation cycle in ATRP process
k_{dec}	Rate coefficient for decomposition in NMP equilibrium
k_{dec}	Rate coefficient for decomposition in NMP process
$k_{f,i,j}$	Rate coefficient of fragmentation during main equilibrium in RAFT process

$k_{f,i,o}$	Rate coefficient of fragmentation during pre-equilibrium in RAFT process
$k_{in,I}$	Rate coefficient of re-initiation during main equilibrium in RAFT process
k_p	Propagation rate coefficient
k_t	Overall rate coefficient for termination
k_{tc}	Rate coefficient for termination by combination
k_{td}	Rate coefficient for termination by disproportionation
k_{trT}	Overall coefficient for chain transfer
M	Monomer
M_{Monomer}	Monomer molar mass
M_n	Number average molecular
M_{RAFT}	RAFT agent molar mass
$P_n\text{-X}$	Dormant chain in ATRP process
$P_n\text{-Y}$	Dormant chain in NMP equilibrium
R	Gas constant
r	Reactivity ratio
R_p	Propagation rate
t	time
X	Halogen
Y	Nitroxide
χ	Monomer fractional conversion

List of Acronyms

AIBN	2,2'-azobis(isobutyronitrile)
AN	Acrylonitrile
ARGET	Activator regenerated by electron transfer
ATRP	Atom transfer radical polymerization
BA	Butyl acrylate
BPO	Benzoyl peroxide
C ₆ D ₆	Benzene d ₆
CCl ₄	Carbon tetrachloride
CDB	Cumyl dithiobenzoate
CIPDB	Cyano-isopropyl dithiobenzoate
CPDA	Cumyl phenyl dithioacetate
CS ₂	Carbon disulfide
CT	Chain transfer
CTA	Chain transfer agent
DCM	Dichloromethane
DMAc	Dimethyl acetamide
DMF	Dimethyl formamide
ECX	<i>O</i> -ethyl cumyl xanthate
ESR	Electron spin resonance

FTIR	Fourier transform infra-red spectroscopy
HPLC-MS	High performance liquid chromatography-mass spectrometry
ICAR	Initiator for continuous activator regeneration
LAM	Less activated monomer
MA	Methyl acrylate
MADIX	Macromolecular design by interchange of xanthate
MAM	More activated monomer
MAN	Methacrylonitrile
Mg	Magnesium
MMA	methyl methacrylate
NaCl	Sodium chloride
NaHCO ₃	Sodium hydrogen carbonate
NIPAAm	N-isopropyl acrylamide
NMP	Nitroxide mediated polymerization
NVP	<i>N</i> -vinyl pyrrolidone
PAN	Poly(acrylonitrile)
PEX	<i>S</i> - <i>Sec</i> propionic acid <i>O</i> -ethyl xanthate
RAFT	Reversible addition fragmentation chain transfer
SEC	Size exclusion chromatography
Sty	Styrene
Sty-NIPAAm	Styrene- <i>N</i> -isopropyl acrylamide

TEMPO	2,2,6,6-tetramethyl-1-piperidinyloxy free radical
THF	Tetrahydrofuran
TMSN	Tetramethyl succinonitrile
TTC-CIP	<i>S</i> -butyl- <i>S'</i> -cyano isopropyl trithiocarbonate
UV	Ultra-violet
VAc	Vinyl acetate

List of Schemes

Scheme 1.1: Conventional Radical Polymerization elementary reactions	2
Scheme 1.2: ATRP Equilibrium	5
Scheme 1.3: Equilibrium step in NMP process	6
Scheme 3.1: Reaction steps in the cumyl dithiobenzoate (CDB) synthesis	24
Scheme 3.2: Reaction steps in the synthesis <i>S</i> - <i>sec</i> propionic acid <i>O</i> -ethyl xanthate (PEX)	25
Scheme 3.3: Reaction steps in the <i>O</i> -ethyl cumyl xanthate (ECX) synthesis	27
Scheme 4.1: PEX mediated VAc homopolymerization.....	35
Scheme 5.1: Reaction pathway for RAFT-mediated copolymerization showing the first two monomer insertions.....	57

List of Tables

Table 3.1: Amounts of Components used in the RAFT Mediated Polymerization 30

Table 5.1: DMAc SEC analysis against polymethyl methacrylate (PMMA) standards 86

List of Figures

Figure 3.1: FTIR spectra of <i>S-sec</i> propionic acid <i>O</i> -ethyl xanthate (PEX)	27
Figure 4.1: The ^1H NMR spectra of the AN polymerization showing the instantaneous spectra taken at 20 minutes intervals from the beginning of the reaction up to 5 hours at 60 °C monitored by <i>in situ</i> proton NMR	37
Figure 4.2: Enlarged first AN adduct region	38
Figure 4.3: The relative concentration of all the RAFT species for CDB AN homopolymerization at 60 °C monitored by <i>in situ</i> ^1H NMR run for 10 hours	39
Figure 4.4: Fractional conversion as a function of time for the CDB mediated AN homopolymerization at 60 °C monitored by <i>in situ</i> ^1H NMR run for 10 hours in C_6D_6	40
Figure 4.5: The VAc CDB-mediated homopolymerization monitored by <i>in situ</i> ^1H NMR at [VAc]:[CDB]:[AIBN] ratio of 5:1:0.2 at 60 °C in C_6D_6 showing 1.14-1.16 ppm and 1.24-1.26 ppm region	41
Figure 4.6: Comparison between the fractional conversion of AIBN and CDB for CDB mediated VAc homopolymerization at 60 °C monitored by <i>in situ</i> proton NMR in C_6D_6	42
Figure 4.7: VAc Fractional conversion as a function of time for CDB mediated homopolymerization at 60 °C by <i>in situ</i> ^1H NMR in C_6D_6 run for 14 hours at [VAc]:[CDB]:[AIBN] ratios of 5:1:0.2.	43
Figure 4.8: a)The variation of the relative concentration of CDB, CVAcD and CIPVAcD as a function of time for VAc homopolymerization at 60 °C monitored by <i>in situ</i> ^1H NMR run for 14 hours at [VAc]:[CDB]:[AIBN] ratios of 5:1:0.2. b) Shows the zoomed CVAcD concentration as a function of time.	43

Figure 4.9: VAc fractional conversion as a function of time for the ECX mediated homopolymerization at 60 °C monitored via <i>in situ</i> ^1H in C_6D_6 at [VAc]:[ECX]:[AIBN] ratios of 5:1:0.2	45
Figure 4.10: Comparison of fractional conversion of ECX and AIBN for the ECX mediated VAc homopolymerization at 60 °C monitored by <i>in situ</i> ^1H NMR in C_6D_6 at [VAc]:[ECX]:[AIBN] ratios of 5:1:0.2	45
Figure 4.11: Relative concentration of CiPVAcX as a function of time for the ECX mediated VAc homopolymerization at 60 °C monitored by <i>in situ</i> ^1H NMR in C_6D_6 at [VAc]:[ECX]:[AIBN] ratios of 5:1:0.2.....	46
Figure 4.12: AN fractional conversion as a function of time for the ECX mediated homopolymerization at 60 °C monitored by <i>in situ</i> ^1H in C_6D_6 at [AN]:[ECX]:[AIBN] ratios of 5:1:0.2	47
Figure 4. 13: Fractional conversion of ECX for the ECX mediated AN homopolymerization at 60 °C monitored by <i>in situ</i> ^1H in C_6D_6 at [AN]:[ECX]:[AIBN] ratios of 5:1:0.2	48
Figure 4.14: The snap short of the <i>in situ</i> ^1H NMR spectra during the PEX mediated VAc homopolymerization at [VAc]:[PEX]:[AIBN] ratios of 5:1:0.2 from 100 minutes after commencement of the reaction	49
Figure 4.15: The relative concentration of species in the PEX mediated VAc homopolymerization at 60 °C monitored by <i>in situ</i> ^1H NMR run for 14 hours at [VAc]:[PEX]:[AIBN] ratios of 5:1:0.2 valuable	50
Figure 4.16: VAc fractional conversion as a function of time for the PEX mediated VAc homopolymerization at 60 °C monitored by <i>in situ</i> ^1H NMR run for 14 hours at [VAc]:[PEX]:[AIBN] ratios of 5:1:0.2.....	51
Figure 4.17: Evolution of the acetaldehyde relative to the total ECX concentration as a function of time for the CDB mediated VAc homopolymerization at 60 °C monitored by <i>in situ</i> ^1H NMR run for 14 hours at [CDB]:[VAc]:[AIBN] ratios of 5:1:0.2.....	52

Figure 4.18: Evolution of the acetaldehyde relative to the total ECX concentration as a function of time for the ECX mediated VAc homopolymerization at [ECX]:[VAc]:[AIBN] ratios of 5:1:0.2 53

Figure 5.1: The relative concentration of the RAFT species for CDB mediated AN/VAc copolymerization with [M]:[CDB]:[AIBN] ratios of 5:1:0.2 monitored via *in situ* ^1H NMR for 10 hours. at 60 °C a) $f_{\text{AN}}=0.9$, b) $f_{\text{AN}}=0.5$, c) $f_{\text{AN}}=0.25$ 61

Figure 5.2: The evolution of AIBN fractional conversion with time as a function AN feed compositions for the polymerization reactions with [M]:[CDB]:[AIBN] ratios of 5:1:0.2 monitored via *in situ* ^1H NMR conducted at 60 °C for 10 hours..... 62

Figure 5.3: The plot of the relative concentration of the RAFT species for the CDB mediated AN/VAc copolymerization at 70 °C and at [M]:[CDB]:[AIBN] ratios monitored by *in situ* ^1H NMR run for 14 hours, $f_{\text{AN}}=0.25$ 63

Figure 5.4: The plot of the relative concentration of the RAFT species for the CDB mediated AN/VAc copolymerization at 60 °C and at [M]:[CDB]:[AIBN] ratios of 10:1:0.1 monitored by *in situ* ^1H NMR run for 14 hours, $f_{\text{AN}}=0.25$ 64

Figure 5.5: a) The evolution of AN and VAc fractional conversion as a function of time for CDB mediated AN/VAc copolymerization at 60 °C monitored by *in situ* ^1H NMR run for 10 hours. $f_{\text{AN}}=0.25$ b) an enlargement in the region of the VAc fractional conversion for the [M]:[CDB]:[AIBN] ratios of 5:1:0.2. 65

Figure 5.6:a) The evolution of AN and VAc fractional conversion as a function of time for CDB mediated AN/VAc comopolymerization at 70 °C monitored by *in situ* ^1H NMR run for 14 hours. $f_{\text{AN}}=0.25$ b) an enlargement in the region of the VAc fractional conversion at [M]:[CDB]:[AIBN] ratios of 5:1:0.2. 66

Figure 5.7: The evolution of AN and VAc fractional conversion as a function of time for CDB mediated AN/VAc copolymerization at 60 °C and at [M]:[CDB]:[AIBN] ratios of 10:1:0.1 monitored by *in situ* ^1H NMR run for 14 hours. $f_{\text{AN}}=0.25$ b) an enlargement in the region of the AN fractional conversion..... 66

Figure 5.8: The relative concentration of the RAFT species for CDB-mediated AN/VAc copolymerization at 70 °C monitored by *in situ* ^1H NMR run for 14 hours at $[\text{M}]:[\text{CDB}]:[\text{AIBN}]$ ratios of 10:1:0.1 a) $f_{\text{AN}} = 0.9$, b) $f_{\text{AN}} = 0.5$, c) $f_{\text{AN}} = 0.10$ 68

Figure 5.9: The CDB fractional conversion as a function of time at various f_{AN} for the polymerization reactions undertaken at 60 °C and at $[\text{M}]:[\text{CDB}]:[\text{AIBN}]$ ratios of 5:1:0.2 as monitored by *in situ* ^1H NMR. Where total $[\text{M}]_{\text{oTotal}} = 2 \text{ M}$, $[\text{CDB}]_{\text{o}} = 3.5 \times 10^{-1} - 4.5 \times 10^{-1} \text{ M}$ and $[\text{AIBN}]_{\text{o}} = 7.5 \times 10^{-2} - 9.0 \times 10^{-2} \text{ M}$ 69

Figure 5.10: The CDB fractional conversion as a function of time at various f_{AN} for the copolymerization reactions at 70 °C and at $[\text{M}]:[\text{CDB}]:[\text{AIBN}]$ ratios of 10:1:0.1 as monitored by *in situ* ^1H NMR. Where total $[\text{M}]_{\text{oTotal}} = 3 \text{ M}$, $[\text{CDB}]_{\text{o}} = 3.1 \times 10^{-1} \text{ M}$ and $[\text{AIBN}]_{\text{o}} = 3.1 \times 10^{-2} \text{ M}$ 70

Figure 5.11: Relative concentration of CDB adducts versus time for CDB mediated polymerization at 70 °C and 10:1:0.1 $[\text{M}]:[\text{CDB}]:[\text{AIBN}]$ ratios (a) MA CDB-mediated homopolymerization and (b) MA/VAc CDB-mediated copolymerization, $f_{\text{MA}}=0.5$ 71

Figure 5.12: Relative concentration CDB adducts versus time CDB mediated polymerization at 70 °C and 10:1:0.1 $[\text{M}]:[\text{CDB}]:[\text{AIBN}]$ ratios a) AN CDB-mediated homopolymerization and b) AN/VAc CDB-mediated copolymerization, $f_{\text{MA}}=0.5$ 72

Figure 5.13: a) The fractional monomer conversion as a function of time for ECX-ediated AN/VAc comopolymerization at 60 °C monitored via *in situ* ^1H NMR for 10 hours. $f_{\text{AN}} = 0.5$ b) shows an enlargement in the region of the VAc fractional conversion. 73

Figure 5.14: ECX fractional conversion for the ECX mediated polymerization at 60 °C in C_6D_6 at $[\text{Monomer}]:[\text{ECX}]:[\text{AIBN}]$ ratios of 5:1:0.2 at 0, 0.5 and 1 AN feed compositions 74

Figure 5.15: The relative concentration versus time for the PEX mediated copolymerization of AN and VAc at 60 °C monitored by *in situ* ^1H NMR using $f_{\text{AN}} = f_{\text{VAc}}$ where $[\text{M}]:[\text{PEX}]:[\text{AIBN}]$ is 5:1:0.2 75

Figure 5.16: Fractional monomer conversion for the PEX-mediated copolymerization of AN and VAc at 60 °C using $f_{\text{AN}} = f_{\text{VAc}}$ where $[\text{M}]:[\text{PEX}]:[\text{AIBN}]$ is 5:1:0.2 76

Figure 5.17: Relative concentration of vinyl acetate [VAc] versus the ratio [AN]/ [VAc] for the PEX mediated AN/VAc copolymerization at $f_{AN} = 0.5$ and at [M]:[PEX]:[AIBN] = 5:1:0.2 for the polymerization undertaken at 60 °C by *in situ* ^1H NMR ($r_{AN} = 2.45$ and $r_{VAc} = 0.156$) 78

Figure 5.18: Relative concentration of vinyl acetate [VAc] versus the ratio [AN]/ [VAc] for the CDB mediated AN/VAc copolymerization at $f_{AN} = 0.5$ and at [M]:[CDB]:[AIBN] = 5:1:0.2 for the polymerization undertaken at 60 °C by *in situ* ^1H NMR ($r_{AN} = 22.7$ and $r_{VAc} = 0.118$) 79

Figure 5.19: Relative concentration of vinyl acetate [VAc] versus the ratio [AN]/ [VAc] for the ECX mediated AN/VAc copolymerization at $f_{AN} = 0.5$ and at [M]:[ECX]:[AIBN] = 5:1:0.2 for the polymerization undertaken at 60 °C by *in situ* ^1H NMR ($r_{AN} = 5.53$ and $r_{VAc} = 0.046$) 80

Figure 5.20: LC-MS analysis of ECX-mediated AN homopolymerization at [AN]:[ECX]:[AIBN] ratios of 5:1:0.2 at 60 °C monitored via *in situ* ^1H NMR. The ionization source was ESI+, Capillary voltage 3 kV, Cone Voltage 25 V and the analysis was calibrated against Sodium formate and Lock mass against Leucine enkaphalin. Waters UPLC flow rate of 1 mL/min, 100% methanol (Romil), Ascentis[®] C18 column. 81

Figure 5.21: LC-MS analysis of ECX-mediated AN/VAc copolymerization at [AN]:[ECX]:[AIBN] ratios of 5:1:0.2 at 60 °C monitored via *in situ* ^1H NMR. The ionization source was ESI+, Capillary voltage 3 kV, Cone Voltage 25 V and the analysis was calibrated against Sodium formate and Lock mass against Leucine enkaphalin. Waters UPLC flow rate of 1 mL/min, 100% methanol (Romil), Ascentis[®] C18 column. 82

Figure 5.22: LC-MS analysis of CDB-mediated AN/VAc copolymerization at [AN]:[ECX]:[AIBN] ratios of 5:1:0.2 at 60 °C monitored via *in situ* ^1H NMR. The ionization source was ESI+, Capillary voltage 3 kV, Cone Voltage 15 V and the analysis was calibrated against Sodium formate and Lock mass against Leucine enkaphalin. Waters UPLC in methanol at a flow rate of 0.2 mL/min using Phenomenex Nucleosil 5 C18, 150x2mm 83

Figure 5.23: LC-MS analysis of PEX mediated AN/VAc copolymerization at [AN]:[ECX]:[AIBN] ratios of 5:1:0.2 at 60 °C monitored via *in situ* ^1H NMR. The ionization source was ESI+, Capillary voltage 3 kV, Cone Voltage 15 V and the analysis was calibrated against Sodium formate and Lock mass against Leucine enkaphalin. Waters UPLC in methanol at a flow rate of 0.2 mL/min using Phenomenex Nucleosil 5 C18, 150x2mm 84

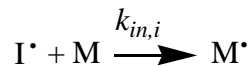
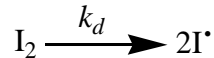
Figure 5.24: DMAc SEC analysis of AN/VAc copolymers produced using different RAFT agents at [M]:[RAFT]:[AIBN] ratios of 100:1:0.1 and [M]:[AIBN] ratio of 100:0.1 in absence of RAFT agent at 70 °C. 86

Chapter 1: INTRODUCTION

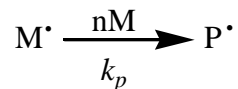
1.1 Free Radical Polymerization

Conventional free radical polymerization is a type of chain polymerization process whereby free radical initiators (or any source of free radicals) are employed as the active species to initiate the polymerization reaction¹. The two most commonly used initiators are peroxides, *e.g.* benzoyl peroxide (BPO) and azo compounds, *e.g.* 2, 2-azobisisobutyronitrile (AIBN). The free radical polymerization process allows for polymerization of almost all known monomers for chain growth processes (*i.e.* vinyl monomers). It permits a wide working temperature range in bulk, solution or emulsion where solvent choices are numerous, tolerating even water and protic solvents. On the downside, this process results in the formation of polymers with broad molecular weight distributions due to limited control over the polymerization process. The reason behind the poor control has been explained by the fact that free radicals are highly reactive to any vinyl center. Consequently, once generated, these radicals undergo propagation and termination in a matter of seconds.² This means that the chain length distribution becomes larger since the cycle of growth and termination takes place continuously. Due to this occurrence of simultaneous initiation, propagation and termination processes, polymer chains grow to different lengths depending on the probability of chain growth relative to chain termination events. The three elementary reaction steps, initiation, propagation and termination, of free radical polymerization are depicted in Scheme 1.1.

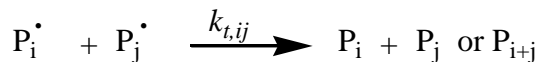
i) Initiation



ii) Propagation



iii) Termination



Scheme 1.1: Conventional Radical Polymerization elementary reactions

In Scheme 1.1, the initiator molecule (I_2) decomposes at a rate determined by the decomposition rate coefficient (k_d). The value of k_d is determined by the conditions under which decomposition is taking place. In thermal decomposition, the initiator I_2 undergoes homolytic cleavage to give two radical fragments and the rate of radical formation is described by equation 1.1.

$$\frac{d[I^\bullet]}{dt} = -\frac{d[I_2]}{dt} = 2k_d[I_2] \quad (1.1)$$

At any time t during the polymerization process, the instantaneous concentration of the initiator is defined by equation 1.2.

$$[I_2] = [I_2]_o \cdot e^{-k_d t} \quad (1.2)$$

Where $[I_2]_o$ is the initial concentration of the initiator while $[I_2]$ is its concentration at any time t .

Polymer chain growth occurs in the propagation step through addition of the active radicals to monomer (M), resulting in chain extension. The rate of addition of the propagating radical to monomer is primarily governed by the rate coefficient of propagation (k_p). However, it is

important to consider that the initiator fragment may influence the reactivity of short chain radicals more than their longer counterparts. In simple terms, ignoring the chain length dependency, the rate of polymerization (change of monomer concentration as a function of time) can be expressed as illustrated by equation 1.3.

$$R_p = -\frac{d[M]}{dt} = k_p[P\cdot][M] \quad (1.3)$$

Termination in free radical polymerization occurs through two main processes, combination and disproportionation (reaction iii), scheme 1.1). The rate coefficient k_t , similarly to the k_p , is chain length dependent.³ Thus, during the start of the polymerization reaction, termination rates are higher as compared to when majority of the chains have considerably grown longer and hence their diffusion rates lowered. The gel effect is a good example of build-up of radicals due to decrease in termination rate. The rate of termination by disproportionation is given by equation 1.4, however if termination occurs by combination, then the factor of 2 should be excluded.

$$R_t = -\frac{d[P\cdot]}{dt} = 2k_t[P\cdot]^2 \quad (1.4)$$

In most cases, both kinds of termination occur in one polymerization reaction hence the overall termination rate coefficient is defined as:

$$k_t = k_{td} + k_{tc} \quad (1.5)$$

It is worth mentioning that other reactions do occur in the polymerization that competes with propagation, and these include chain transfer (CT) reactions. During a CT reaction, a radical on one polymer chain can be transferred to another carbon center within the same chain (intra-molecular CT) or to a different polymer chain (inter-molecular CT). Chain transfer reactions can also occur to monomer, solvent and other species (such as thiols) in the polymerization mixture. The rate at which the transfer reactions occur can, jointly be described by the transfer coefficient (C_T) which is expressed as:

$$C_T = \frac{k_{trT}}{k_p} \quad (1.6)$$

where k_{trT} is the rate coefficient for chain transfer to compound T.

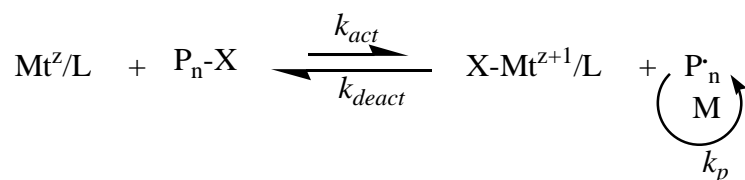
1.2 Controlled/Living Radical Polymerization (CLRP)

The advent of the controlled radical polymerization techniques has been of great value to polymer chemists as it has enabled the ease of production of well-designed materials. Thus, predetermined polymer molecular weights of narrow distribution are accessible. In general, the radical flux is kept low in these CLRP processes so as to minimize the undesired bimolecular termination as the main shortcoming of conventional radical polymerization process. Consequently, a large majority of the chains grow throughout the entire reaction time while in the conventional radical process the chain growth life is in order of one second (1 s). All the CLRP techniques rely on the equilibrium whereby the active propagating radicals are converted to some form of dormant species that are reversibly revived to the active form in situ. For a well-controlled process, the equilibrium is ideally shifted to the dormant side, such that the instantaneous radical concentration remains low. On average, an active polymer chain should add one or two monomer units before it is transformed into a dormant species.

Recalling equations 1.3 and 1.4, and also the fact that the radical concentration is low in controlled radical polymerization processes, the active to dormant species ratio is inevitably small. It is hence not surprising that the termination rate is significantly minimized as termination is second order in radical concentration. The low radical concentration means a sacrifice on the propagation rate but since propagation is first order in radical concentration, there will not be major drop in the rate^{2,4,5}. Mechanistically, two classes of controlled radical polymerizations are distinguishable i.e. reversible deactivation (persistent radical effect) and degenerative chain transfer⁶⁻⁸. Preeminent examples of reversible deactivation techniques include Nitroxide Mediated Polymerization (NMP) and Atom Transfer Radical Polymerization (ATRP) and for degenerative chain transfer mechanism it is the so called Reversible Addition Fragmentation Chain Transfer (RAFT). A detailed discussion of the RAFT process follows in Chapter 2 and only a brief overview of ATRP and NMP is given in subsections 1.2.1 and 1.2.2, respectively.

1.2.1 Atom Transfer Radical Polymerization (ATRP)

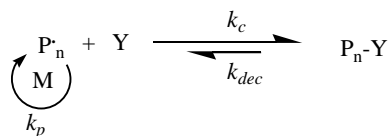
Atom Transfer Radical Polymerization is based on reversible deactivation by halogen atom (X) transfer between a transition metal complex (M^z/L) (usually copper) and the alkyl halide ($P-X$).⁹⁻
¹² ATRP has been applied successfully to acrylic and styrenic monomers and recently it has been extended to acidic monomers.¹³ The catalyst poisoning in protic solvents and solvent induced side reactions with the transition metal complex^{14, 15} were overcome by the development of activator regenerated by electron transfer (ARGET) and initiators for continuous activator regeneration (ICAR) ATRP processes. These new processes utilize low concentrations (parts per million) transition metal catalyst content in the polymerization reactions hence isolation from the polymer matrix and side reactions are significantly minimized.¹⁶ The ATRP equilibrium is shown in Scheme 1.2.



Scheme 1.2: ATRP Equilibrium

1.2.2 Nitroxide Mediated Polymerization (NMP)

Nitroxide mediated polymerization is based on reversible deactivation of a propagating alkyl radical ($P_n\cdot$) with a persistent radical (nitroxide, Y) to form a dormant chain (P_n-Y), as illustrated in Scheme 1.3.^{9, 17} A drawback with NMP, however, has been the lability of the newly formed nitroxide to carbon (NO-C) bond in the dormant species for typical 1st generation nitroxides such as TEMPO and its derivatives. The relatively stable adducts (dormant chains) formed by these nitroxides require high reaction temperatures in order to ensure sufficient dissociation of dormant moiety to result in chain growth. In the past decade, there have been significant advances in synthesizing 2nd generation nitroxides *e.g.* SG1, whose dormant species can be activated at reasonably low temperatures.^{18, 19}



Scheme 1.3: Equilibrium step in NMP process

1.3 Background to the Project

RAFT mediated homopolymerization of vinyl acetate (VAc) using xanthates as chain transfer agents has been well documented in literature.²⁰⁻²² Dithiobenzoate based RAFT agents however are known to inhibit/retard RAFT mediated polymerization of VAc. On the other hand, the RAFT mediated polymerization of methyl acrylate (MA) and acrylonitrile (AN) using dithiobenzoate RAFT agents have been widely studied and good control of both molecular weight and dispersity (\mathcal{D}) has been realised.²³⁻²⁵ Under conventional free radical polymerization conditions, both MA and AN have been found to readily copolymerize with VAc to give statistical copolymers.^{26, 27} Thus, the copolymer obtained under equimolar quantities of monomers is richer in acrylate or acrylonitrile monomer sequence. The reactivity ratios reported for AN/VAc system are $r_{AN}=2.7$ and $r_{VAc}=0.05$ ²⁶ and for MA/VAc system are $r_{MA}=6.72$ and $r_{VAc}=0.04$ as determined by non-linear error-in-variable method.²⁷

To the best of our knowledge, there is no literature reports on the RAFT mediated copolymerizations of MA/VAc and AN/VAc using cumyl dithiobenzoate (CDB), *O*-ethyl cumyl xanthate (ECX) and *S*-*sec* propionic acid *O*-ethyl xanthate (PEX). The present study is conducted to see how VAc will affect the polymerization of the comonomer when using CDB, PEX and ECX as RAFT agents. Also, if VAc gets consumed, if at all, to form the copolymer or if VAc will behaves more like a diluent in the copolymerization system. The similar study is also

conducted but now using PEX, which controls VAc homopolymerization. Then the effect of the comonomer on VAc consumption is studied while using PEX.

1.4 Objectives

The focus of this study is on the mechanism as well as the kinetics of RAFT mediated AN/VAc copolymerization. This will be achieved by assessing the selectivity of cumyl dithiobenzoate (CDB), *O*-ethyl cumyl xanthate (ECX) and *S*-sec propionic acid *O*-ethyl xanthate (PEX) in the AN/VAc and MA/VAc copolymerization systems. *In situ* ^1H NMR will be used as a main tool to follow the polymerization reactions as a function of time, monitoring the consumption of reactants and the formation of products in real time. The selectivity of CDB in AN/VAc and MA/VAc copolymerization systems will be studied and the initialization times will be compared. Finally, the reactivity ratios will be estimated for the AN/VAc system when different RAFT agents are used to mediate the polymerization reaction.

1.5 References

1. Odian, G., *Principles of Polymerization*. 4th ed.; John Wiley & Sons, Inc.: New Jersey, 2004.
2. Van Herk, A., Introduction to Radical (co)Polymerization. In *Chemistry and Technology of Emulsion Polymerization*, Van Herk, A., Ed. Blackwell Publishing Ltd: 2005; pp 25-45.
3. Scheren, P. A. G. M.; Russell, G. T.; Sangster, D. F.; Gilbert, R. G.; German, A. L. *Macromolecules* **1995**, *28*, 3637-3749.
4. Russell, G. T.; Gilbert, R. G.; Napper, D. H. *Macromolecules* **1993**, *26*, 3538-3552.
5. Heuts, J. P. A.; Davis, T. P.; Russell, G.T. *Macromolecules* **1999**, *32*, 6019-6030
6. Fischer, H. *Chem. Rev.* **2001**, *101*, 3581-3610.
7. Fischer, H. *Macromolecules* **1997**, *30*, 5666-5672.
8. Fischer, H. *J Polym Sci. Part A: Polym Chem* **1999**, *37*, 1885-1901.
9. Chiefari, J.; Chong, Y. K. B.; Ercole, F.; Krstina, J.; Jeffery, J.; Le, T. P. T.; Mayadunne, R. T. A.; Meijs, G. F.; Moad, C. L.; Moad, G.; Rizzardo, E.; Thang, S. H. *Macromolecules* **1998**, *31*, 5559-5562.
10. Wang, J. S.; Matyjaszewski, K. *J. Am. Chem. Soc.* **1995**, *117*, 5614-5615.
11. Kato, M.; Kamigaito, M.; Sawamoto, M.; Higashimura, T. *Macromolecules* **1995**, *28*, 1721-1723.
12. Wang, J. S.; Matyjaszewski, K. *J. Am. Chem. Soc.* **1995**, *117*, 5614.
13. Jana, S.; Parthiban, A.; Choo, F. M. *Chem. Commun* **2012**, *48*, 4256-4258.
14. Matyjaszewski, K.; Patten, T. E.; Xia, J. *J. Am. Chem. Soc.* **1997**, *119*, 674.
15. Matyjaszewski, K.; Davis, T. P.; Patten, T. E.; Wei, M. *Tetrahedron* **1997**, *53*, 15321.
16. Matyjaszewski, K. *Macromolecules* **2012**, *45*, 4015-4039.
17. Connolly, T. J.; Scaiano, J. C. *Tetr. Lett* **1997**, *38*, 1133-1136.
18. Farcet, C.; Lansalot, M.; Charleux, B.; Pirri, R.; Vairon, J. P. *Macromolecules* **2000**, *33*, 8559-8570.
19. Hawker, C. J.; Bosman, A. W.; Harth, E. *Chemical Reviews* **2001**, *101*, 3661-3688.
20. Postma, A.; Davis, T. P.; Li, G.; Moad, G.; O'shea, M. S.; . *Macromolecules* **2006**, *39*, 5307-5318.

21. Nguyen, T. L. U.; Eagles, K.; Davis, T. P.; Barner-Kowollik, C.; Stenzel, M. H. *J Polym Sci. Part A: Polym Chem* **2006**, *44*, 4372-4383.
22. Quiclet-Sire, B.; Zard, S. Z. *Chem. Eur. J.* **2006**, *12*, 6002-6016.
23. McLeary, J. B. Reversible Addition-Fragmentation Transfer Polymerization in Heterogeneous Aqueous Media. PhD thesis, Stellenbosch University, Stellenbosch, South Africa, 2004.
24. Xiao-Hui, L.; Yan-Guo, L.; Ying, L.; Yue-Sheng, L. *J Polym Sci. Part A: Polym Chem* **2006**, *45*, 1272-1281.
25. Van den Dungen, E. T. A.; Matahwa, H.; McLeary, J. B.; Sanderson, R. D.; Klumperman, B. *J Polym Sci: Part A: Polym Chem* **2008**, *46*, 2500-2509.
26. Cheetham, P. F.; Huckerby, T. N.; Tabner, B. J. *Eur. Polym. J.* **1994**, *30*, 581-587.
27. Brar, A. S.; Goyal, A. K.; Ganai, A.; Hooda, S. *J. Mol. Struct.* **2008**, *888*, 257-265.

Chapter 2: LITERATURE REVIEW

2.1 RAFT Mediated Polymerization: Overview

Reversible addition-fragmentation chain transfer (RAFT) mediated polymerization process is one of the well-known and widely applied methods among controlled radical polymerization techniques. This is attributable to the extensive range of monomers, the wide temperature window and various initiation techniques that can be used with RAFT procedure. A vast variety of RAFT agents available allow for synthesis of a variety of α , ω -functional polymers. The RAFT process is based on degenerative chain transfer mechanism, taking place between the propagating radical and dithio-ester, thiocarbamate, trithio-carbonate or xanthate compounds. RAFT agents consist of the general structure R-S-C(=S)-Z or R-S-C(=S)-S-R where R is defined as the reinitiating/leaving group and Z is the (de)stabilizing group.¹ It is evident that RAFT process can be tuned for a certain monomer or monomer system by simply changing the stabilizing Z-group and/or the leaving group (R). In a typical RAFT mediated polymerization, like in other CLRP processes, tuning the molar ratio of monomer(s) to RAFT agent allows for preparation (synthesis) of polymers with predetermined molecular weights (Equation 2.1).

$$M_n = \left(\frac{x M_{Monomer} [Monomer]_0}{[RAFT]_0} \right) + M_{RAFT} \quad (2.1)$$

Where M_n is number average molecular weight, x is monomer fractional conversion, $M_{Monomer}$ is monomer molar mass, $[Monomer]_0$ is the monomer initial concentration and $[RAFT]_0$ is the initial concentration of the RAFT agent. Equation 2.1, however, holds when assuming that the entire transfer agent has been used up and further, ignoring chains initiated by the initiator derived radicals.²

2.1.1. The Leaving (R) Group

As pointed out earlier, the leaving R-group and the stabilizing/destabilizing Z-group are of prime importance towards proper functioning of the RAFT agent. For RAFT mechanism to take effect,

the leaving group in the original transfer agent should be more labile than the monomer derived propagating radical. Nonetheless, the latter should still have reasonable leaving ability in order for the polymer to grow in a controlled manner after complete conversion of the original RAFT agent into the oligomeric form. The role of the leaving group is crucial to the reactivity of the RAFT agent with monomer during initialization period. The properties of the R-group govern whether the initial chain growth will take place on the leaving group radical of the transfer agent or the initiator derived radicals. Moad et al credited the selective initialization to the fast addition of the leaving group radical to monomer and to huge transfer constant of the RAFT agent.³ O-ethyl xanthates have been shown to give three distinct initialization behaviours from selective, non-selective and selective with slow initiation process for vinylpyrrolidone (NVP) while changing the R-group.⁴ The cumyl dithiobenzoate (CDB) and cyano-iso-propyl dithiobenzoate (CIPDB) have been reported to give similar initialization intervals in high target molecular weight methyl acrylate (MA) polymerization.⁵ On the contrary, earlier studies done by the same group on MA polymerization employing high concentrations of both CDB and CIPDB, five monomer units chain length targeted, the initialization was longer for CDB.⁶

2.1.2. The Stabilizing/Destabilizing (Z) Group

The stabilizing/destabilizing Z-group is responsible for controlling the fragmentation rate of the intermediate radical adduct species. Therefore, the stability properties of the z-group should be coordinated to those of the monomer in question for the process to be efficient. Thus, poorly stabilized monomers will require the use of poorly stabilizing (destabilizing) Z-groups. In the case of vinyl acetate (VAc) and N-vinyl pyrrolidone (NVP), xanthates and thiocarbamates have been shown to result in highly selective initialization with fast fragmentation rates of the intermediate radical.^{7, 8} Cumyl phenyl dithioacetate (CPDA) resulted in fast polymerization of MA after initialization than in the case of CDB, even though both CPDA and CDB have the same leaving group. This discrepancy in the rate of polymerization of MA was explained to be a consequence of the destabilizing benzyl group of CPDA prompting the intermediate radical unstable. As a result, fragmentation rate of the intermediate radical hence increased drastically in the case of CPDA, after completion of the initialization period.^{5, 6}

2.2 Initiation in RAFT Process

The initiation modes compatible with RAFT mediated polymerization range from the use of thermal and photo-induced initiator decomposition, microwave irradiation,⁹ to room temperature laser induced initiated polymerization reactions using ultra-violet (UV) and gamma radiation sources.¹⁰ The initiation brought about by using radiation as a source of radicals has the advantage of supplying a constant radical flux during the progress of polymerization reaction. It has been reported that initiation by gamma radiation in the presence of a high concentration of cumyldithiobenzoate (CDB) exhibited fairly long initialization times at ambient temperatures. The contrasting behavior for the initialization periods has been observed for CDB mediated styrene polymerization initiated by 2, 2'-azoisobutyronitrile (AIBN) at 70 °C. In the same study, cyanoisopropyl dithiobenzoate (CIPD) and S-butyl-S-cyaono isopropyl trithiobenzoate (TTC-CIP) were found to give similar initialization periods in AIBN initiated systems at 70 °C while in gamma irradiated experiments, TTC-CIP showed faster initialization periods at lower irradiation power of 25 kGy than CIPD 150 kGy. However, the RAFT agent concentration decreased in a similar linear trend for both initiation methods.¹⁰

In most RAFT polymerization procedures, the same initiators used in conventional radical polymerization are employed because their mechanism of initiation is well understood even though they may pose some problems for this process. These initiators are known to generate radicals throughout the polymerization reaction period and undergo a number of side reactions especially when polymerization is done in solution. However, considerably low concentration of the initiator is usually employed in RAFT mediated systems and thus undesired side products of decomposition are minimized.¹¹⁻¹³ For the purposes on the present work, only the AIBN thermal decomposition mechanism is discussed.

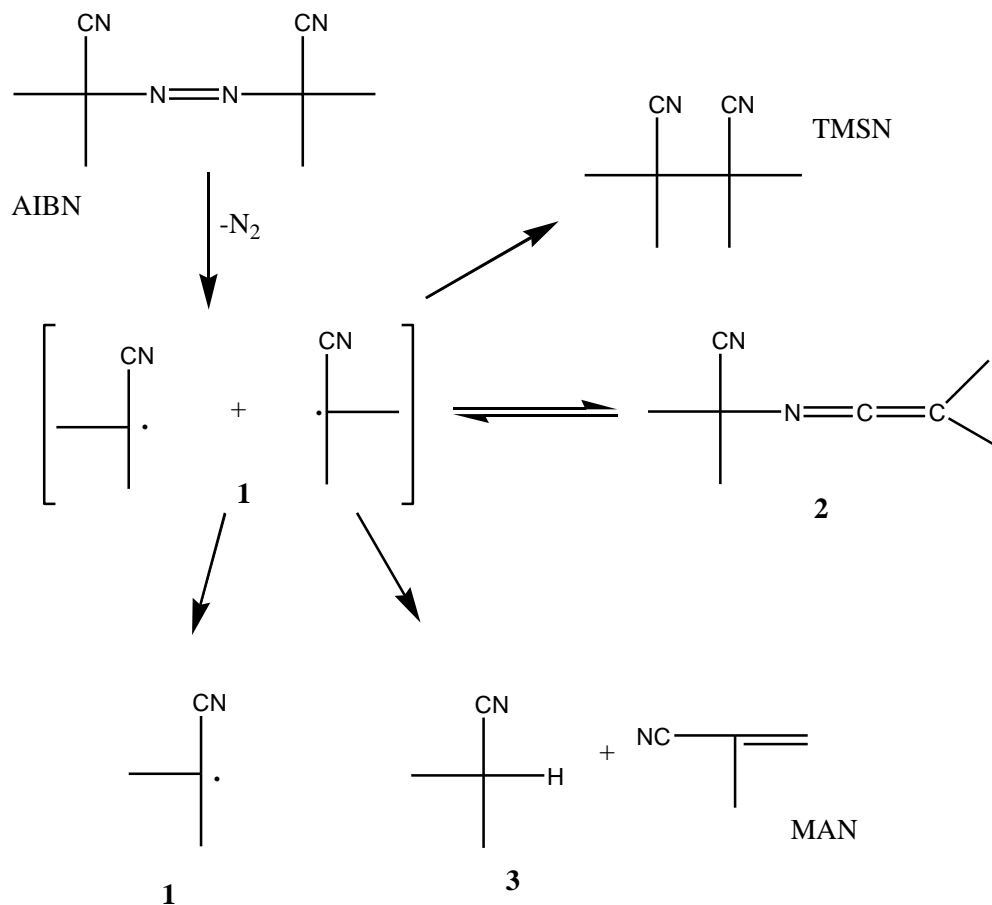
2.2.1. 2,2'-Azobis(isobutyronitrile) (AIBN) Decomposition

AIBN has been reported to undergo homolytic cleavage by thermal or photolytic stimulus to give two primary radicals (compound 1 in Scheme 2.1). However, like other conventional free radical

polymerization initiators, under the solvent cage, these primary radicals can undergo a series of side reactions, including among others, fragmentation, rearrangement to secondary radicals and β -scission reactions. According to Scheme 2.1, AIBN has been found to disintegrate to give tetramethylsuccinonitrile (TMSN) as the major product. Other products of AIBN decomposition include isobutyronitrile¹⁴ (4) and dimethyl ketene cyanoisopropylimine (2) which decomposes further to give methacrylonitrile (MAN).^{3, 15} The rate coefficient of dissociation of AIBN, k_d , is described by Equation 2.2 in benzene and toluene in the temperature range of 310-373 K.¹³

$$k_d(s^{-1}) = 1.5 \times 10^{15} e^{-218750/RT} \quad (2.2)$$

Where, R is the gas constant in $J K^{-1} mol^{-1}$ and T is temperature in K. However, a certain proportion of initiator derived radicals (1) may escape the solvent cage to initiate the polymerization reaction through addition to monomer. This fraction is described by an additional parameter f , called the initiator efficiency and describes the actual fraction of AIBN derived radicals which initiate the polymerization.



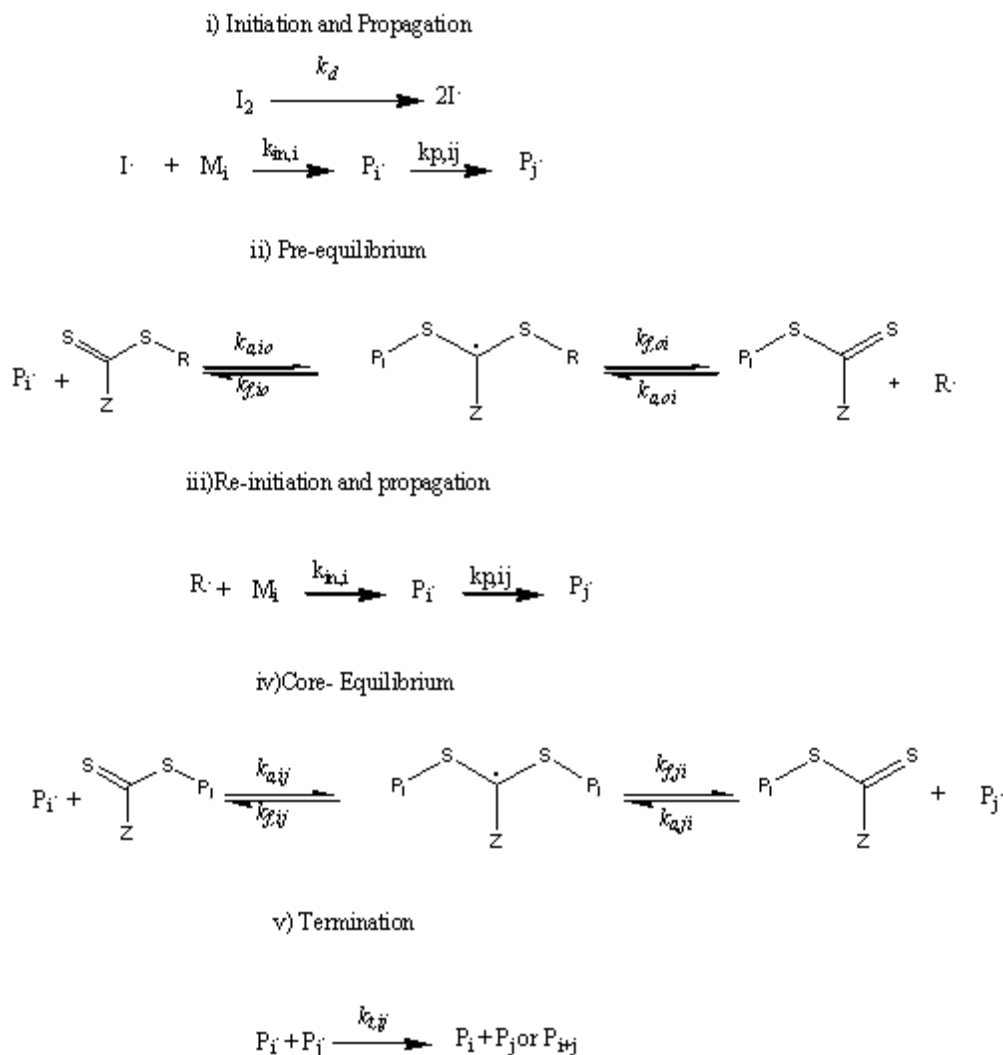
Scheme 2.1: AIBN thermal decomposition products

2.3 Kinetic and Mechanistic Aspects of the RAFT Process

The process consists of five elementary reactions initiation, pre-equilibrium propagation, main equilibrium and termination. However, initiation, propagation, and termination occur in the similar way as in the conventional free radical polymerization process. The two additional stages called the pre-equilibrium, also called initialization³⁰, and the main equilibrium are unique to RAFT process. Extensive studies have been devoted to understanding the kinetic as well as the mechanic features of each of these equilibriums especially for homopolymerizations.^{5, 31} Scheme 2.2 illustrates the proposed mechanism for a RAFT mediated polymerization. The kinetics of RAFT mediated polymerization was first described in the late 20th century after discovery of the

RAFT process.^{32, 33} They are based on the high affinity of carbon radicals towards sulphur atom of the dithio or trithio moiety of the RAFT transfer agent.³⁴

In an ideal RAFT process, during pre-equilibrium, the original RAFT agent is consumed to form the single monomer adduct of the RAFT agent until it is almost entirely consumed before insertion of the second and subsequent monomer units. Thus, monomer consumption during initialization is by addition to the leaving group primary radicals and once the initialization is complete, the propagating radicals undergo further monomer addition to grow. During both equilibria, the radical addition to the C=S of the RAFT agent goes through an intermediate radical formation step and this has been detected and ascertained by electron spin resonance spectroscopy (ESR).³⁵ This intermediate radical then undergoes fragmentation to release the R-group or the propagating radical (P) which then adds monomer to grow. The rate coefficients $k_{a,i0}$ and $k_{f,i0}$ in (Scheme 2.2, reaction (ii)) pertain to addition and fragmentation steps, respectively, during initialization while $k_{a,ij}$, $k_{a,ji}$, and $k_{f,ij}$, $k_{f,ji}$ relate to the addition and fragmentation steps, respectively, in the main equilibrium (iv). The subscripts i and j denote different degrees of polymerization. Bimolecular termination still occurs under RAFT polymerization conditions but to a limited extent. In addition, intermediate radical termination has been subject of discussion in the literature. A number of authors have shown that apart from fragmentation reactions, the intermediate radical may undergo site reactions through coupling reactions with the propagating radicals to result in the formation of 3-arm and 4-arm dead star polymers.³⁶⁻³⁸



Scheme 2.2: RAFT mechanism

2.3.1 Selective and Non-Selective Initialization in RAFT Mediated Polymerization

The degree of control in RAFT mediated polymerization depends mostly on the strong selectivity of the transfer agent to monomer. But then again, reasonable fragmentation rate of the intermediate radical should be maintained such that only an average of one monomer unit or less is added per addition-fragmentation cycle. This is governed by a number of factors including the quality of the leaving group,^{3, 16} the stabilizing group features, method of initiation and radical flux as already discussed. Pound G. *et al.* reported that *S*-cyano isopropyl-*O*-ethyl xanthate

resulted in the selective initialization of *N*-vinylpyrrolidone (NVP) homopolymerization.¹⁷ MA also showed selective initialization when CDB was used as the chain transfer agent.⁶

The attractiveness of the RAFT process lies in the range of possibilities from chain extension to copolymerization to result in the preparation of various copolymer architectures. A lot of RAFT copolymer architectures are documented in the literature, including among others block¹⁸⁻²¹, graft²², stars²³, random (MMA-BA)²⁴ and statistical²⁴ copolymers. In most common cases, the RAFT agent used is found to control both monomers employed in the experiment. However, very little work has been done on the RAFT copolymerization in relation to individual monomer selectivity. Feldermann *et al.* studied the RAFT copolymerization of the methyl methacrylate with styrene (MMA-Sty), methyl acrylate with styrene (MA-Sty) and methyl acrylate with butyl acrylate (MA-BA) and used ¹H NMR at less than 5% monomer conversion and terminal model reactivity ratios to obtain copolymer composition.²⁴ They observed an increased reactivity of the monomer with the higher reactivity ratio. Thus, the reactivity of Sty was found to be higher than that of MA and MMA was found to be more reactive than BA for RAFT mediated process with increased RAFT agent concentration than in the absence of the RAFT agent. This phenomenon was explained by the fact that high RAFT agent concentrations support formation of short chain length radicals, see equation 2.1. Hence the monomer with the high reactivity will be preferentially consumed during early stages of polymerization at the expense of the one with low reactivity, thus reactivity ratios here were calculated at short chain lengths. Klumperman has previously reported on short chain length styrene-acrylonitrile random copolymer block formation employing RAFT agents with different reinitiating leaving groups.²⁵

Initialization experiments for styrene-maleic anhydride copolymerization have also been performed at high monomer to RAFT agent molar ratios in order to study the sequential addition of comonomers to the leaving group of either CDB or CIPD. Styrene was reported to be preferentially added as the first unit to the leaving group of CIPD while maleic anhydride was the first unit to attach to the leaving group of CDB as followed by real time (*in situ*) ¹H NMR studies.²⁶ Two sequential additions of electron poor vinyl phthalimide followed by electron rich

less activated monomer has been reported.²⁷ Houshyar *et al.* successfully achieved sequential addition of styrene – N-isopropylacrylamide (Sty-NIPAM) while using *S*-2-cyanopropan-2-yl-*S*'-decyl carbonotrithioate at 2:1 monomer to RAFT agent or Sty macro-RAFT agent ratio.²⁸ Nonetheless, the reverse order of the sequence was not achievable as the resulting intermediate radical fragmentation was in favor of formation of the original NIPAM macro-RAFT agent.

Non-selective initialization in RAFT mediated process simply can be described as a situation where the RAFT agent's leaving group is poorer than the oligomeric counterpart. Thus, the addition rate of propagating radicals to the RAFT agent is slower than the propagation rate. In this case longer oligomer chains will be formed prior to consumption of the chain transfer agent. However, other factors like the Z-group properties and monomer nucleophilicity/electrophilicity need to be taken into consideration. Quiclet-Sire *et al.* reported that use of a series of *O*-ethyl xanthates resulted in oligomer formation in *N*-vinyl phthalimides (NVPh) polymerization with the exception of AIBN derived *O*-ethyl xanthate.²⁹ However, vinyl acetate (VAc) and *N*-vinyl pyrrolidone (NVP) formed single monomer adduct with ease when using the same RAFT agents. They explained the results by showing that the adduct radical (R-NVPh radical) undergoes resonance stabilization. This imparted allylic attribute to this adduct radical making it prone to monomer addition as its lifetime was longer than in the case of VAc and NVP. The successful single monomer adduct formation of NVPh was achieved by use of excess *O*-ethyl xanthates in slightly diluted reaction mixtures.²⁷

2.4 Drawbacks of RAFT Polymerization

One of the major shortcomings of the conventional RAFT process is the fact that there is no universal RAFT agent. Hence, more activated monomers (MAMs) and less activated monomers (LAMs) are controlled by RAFT agents of different properties. These present major limitations when it comes to application of RAFT in copolymerization of a dissimilar monomer pair. Recently, switchable RAFT agents have been developed for polymerization of both MAMs and LAMs through application of the single RAFT agent. Simple protonation or de-protonation

makes the transfer agent suited for each monomer type (MAM or LAM). However, such strategies are limited to block copolymerization of these incompatible monomer pairs.^{19-21, 39}

Slower rates of polymerization are also an issue with RAFT mediated polymerization, necessitating lengthy polymerization times compared to the times it would take for the same polymerization reaction under conventional radical system to achieve the same monomer conversion. These slow rates are, however, still acceptable as weighed against the excellent properties of the polymer product obtainable by RAFT process. A number of authors have opted for microwave irradiated RAFT polymerization as it demonstrated high polymerization rates while maintaining good control over molecular weight.^{40, 41} Modelling studies of microwave irradiated polymerization of styrene revealed that microwave enhanced propagation and enhancement of addition rate coefficient to RAFT moiety was responsible for the increase in polymerization rates.⁹

2.5 *In Situ* Proton (¹H) NMR Analysis

In situ ¹H NMR has been widely applied in the study of controlled radical (co)polymerization reactions. This technique has been applied successfully in NMP⁴² and in RAFT^{11, 43} polymerization systems. It permits real time analysis of polymerization reactants and products as the reaction proceeds. This eliminates the problems associated with the use of gravimetric methods when determining polymerization reaction kinetics. Apart from providing less detailed information, the latter is time consuming and may result in erroneous data due to loss of polymer either during precipitation or purification process.

2.6 References

1. Chiefari, J.; Rizzardo, E., Control of Free-Radical Polymerization by Chain Transfer Methods. In *Handbook of Radical Polymerization*, Matyjaszewski, K.; Davis, T. P., Eds. A John Wiley & Sons, Inc. Publication: Hoboken, 2002.
2. Perrier, S.; Takolpuckdee, P. *J. Polym. Sci. Part A: Polym. Chem.* **2005**, 43, 5347-5393.
3. Moad, G.; Chong, Y. K.; Mulder, R.; Rizzardo, E.; Thang, S. H., New Features of the Mechanism of RAFT Polymerization. In *Controlled/Living Radical Polymerization: progress in RAFT, DT,NMP & OMRP* Matyjaszewski, K., Ed. American Chemical Society: Washington DC, 2009 pp 3-16.
4. Pound-Lana, G.; Klumperman, B., Reversible Addition Fragmentation Chain Transfer (RAFT) Mediated Polymerization of N-Vinylpyrrolidone: RAFT Agent Design. In *Controlled/Living Radical Polymerization: progress in RAFT, DT,NMP & OMRP* Matyjaszewski, K., Ed. American Chemical Society: : Washington DC, 2009; pp 167-179.
5. Van den Dungen, E. T. A.; Matahwa, H.; McLeary, J. B.; Sanderson, R. D.; Klumperman, B. *J Polym Sci: Part A: Polym Chem* **2008**, 46, 2500–2509.
6. McLeary, J. B.; McKenzie, J. M.; Tonge, M. P.; Sanderson, R. D.; Klumperman, B. *Chem Commun* **2004**, 1950-1951.
7. Postma, A.; Davis, T. P.; Li, G.; Moad, G.; O'shea, M. S.; . *Macromolecules* **2006**, 39, 5307-5318.
8. Nguyen, T. L. U.; Eagles, K.; Davis, T. P.; Barner-Kowollik, C.; Stenzel, M. H. *J Polym Sci. Part A: Polym Chem* **2006**, 44, 4372-4383.
9. Zetterlund, P. B.; Perrier, S. *Macromolecules* **2011**, 1340-1346.
10. Klumperman, B.; Van den Dungen, E. T. A.; Heuts, J. P. A.; Monteiro, M. J. *macromol. Rapid Commun.* **2010**, 31, 1846-1862.
11. McLeary, J. B. Reversible Addition-Fragmentation Transfer Polymerization in Heterogeneous Aqueous Media. Stellenbosch University, Stellenbosch, 2004.
12. Kucera, M., *Mechanism and Kinetics of Addition Polymerization*. Elsevier Science Publishing Company, Inc.: USA, 1992; Vol. 31, p 85-86.

13. Chahykian, R. H.; Beylerian, N. M., Lasers Application Boundaries to Stimulate Photochemical processes. In *Morden Tendencies in Organic and Biorganic Chemistry: Today and Tomorrow*, Nova Science Publishers, Inc: New York, 2008; p 296.
14. Moad, G.; Solomon, D. H.; Johns, S. R.; Willing, R. I. *Macromolecules* **1984**, *17*, 1094-1099.
15. Pound, G.; McLeary, J. B.; McKenzie, J. M.; and, R. F. M. L.; Klumperman, B. *Macromolecules* **2006**, *39*, 7796-7797.
16. Pound, G.; Eksteen, Z.; Barnard, D.; Klumperman, B. *Polymer* **2008**, *39*, 256-257.
17. Chiefari, J.; Chong, Y. K.; Ercole, F.; Krstina, J.; Jeffery, J.; Le, T. P. T.; Mayadunne, R. T. A.; Gordon, F. M.; Moad, C. L.; Moad, G.; Rizzardo, E.; Thang, S. H. *Macromolecules* **1998**, *31*, 5559-5562.
18. Chong, Y. K.; Le, T. P.; Moad, G.; Rizzardo, E.; Thang, S. H. *Macromolecules* **1999**, *32*, 2071-2074.
19. Coote, M. L.; Wood, G. P. F.; Random, L. *J. Physic. Chem. A* **2002**, *106*, 12124-12138.
20. Tonge, M. P.; Calitz, F. M.; Sanderson, R. D. *Macromol. Chem. Phys.* **2006**, *207*, 1852-1860.
21. Barner-Kowollik, C.; Buback, M.; Charleux, B.; Coote, M. L.; Drache, M.; Fukuda, T.; Goto, A.; Klumperman, B.; Lowe, A. B.; McLeary, J. B.; Moad, G.; Monteiro, M. J.; Sanderson, R. D.; Tonge, M. P.; Vana, P. *J Polym Sci. Part A: Polym Chem* **2006**, *44*, 5809-5831.
22. konkolewicz, D.; Hawkett, B. S.; Gray-Weale, A.; Perrier, S. *Macromolecules* **2008**, *41*, 6400-6412.
23. konkolewicz, D.; Hawkett, B. S.; Gray-Weale, A.; Perrier, S. *J Polym Sci. Part A: Polym Chem* **2009**, *47*, 3455-3466.
24. McLeary, J. B.; Calitz, F. M.; McKenzie, J. M.; Tonge, M. P.; Sanderson, R. D.; Klumperman, B. *Macromolecules* **2004**, *37*, 2383-2394.
25. Pound, G.; Eksteen, Z.; Barnard, D.; Klumperman, B. *Polymer Preprints* **2008**, *49*, 256-257.
26. de Lambert, B.; Charreyre, M.; Chaix, C.; Pichot, C. *Polymer* **2007**, *48*, 437-447.
27. Benaglia, M.; Chen, M.; Chong, Y. K.; Moad, G.; Rizzardo, E.; Thang, S. H. *Macromolecules* **2009**, *42*, 9384-9386.

28. Keddie, D. J.; Guerrero-Sanchez, C.; Moad, G.; Rizzardo, E.; Thang, S. H. *Macromolecules* **2011**, *44*, 6738-6745.
29. Benaglia, M.; Chiefari, J.; Chong, Y. K.; Moad, G.; Rizzardo, E.; Thang, S. H. *J. Am. Chem. Soc.* **2009**, *131*, 6914-6915.
30. Stenzel-Rosenbaum, M.; Davis, T. P.; Fane, A. G.; Chen, V. *Angew Chem. Int Ed* **2001**, *40*, 3428-3432.
31. Stenzel-Rosenbaum, M.; Davis, T. P.; Fane, A. G.; Chen, V. *J Polym Sci. Part A: Polym Chem* **2001**, *39*, 2777-2783.
32. Feldermann, A.; Toy, A. A.; Phan, H.; Stenzel, M. H.; Davis, T. P.; Barner-Kowollik, C. *Polymer* **2004**, *45*, 3997-4007.
33. Klumperman, B.; McLeary, J. B.; Van den Dungen, E. T. A.; Soer, W. J.; Bozovic, J. *ACS symp. ser.* **2006**, *944*, 501-513.
34. Van den Dungen, E. T. A.; Rinqwest, J.; Pretorius, N. O.; McKenzie, J. M.; McLeary, J. B.; Sanderson, R. D.; Klumperman, B. *Aus. J. Chem* **2006**, *59*, 742-748.
35. Quiclet-Sire, B.; Revol, G.; Zard, S. Z. *Tetrahedron* **2010**, *66*, 6656-6666.
36. Houshyar, S.; Keddie, D. J.; Moad, G.; Mulder, R. J.; Saubern, S.; Tsanaktsidis, J. *Polym. Chem.* **2012**, *3*, 1879-1889.
37. Quiclet-Sire, B.; Zard, S. Z. *Chem. Euro. J.* **2006**, *12*, 6002-6016.
38. Moad, G.; Benaglia, M.; Chen, J.; Chiefari, J.; Chong, Y.; Keddie, D. J.; Rizzardo, E.; Thang, S. H. *ACS symp. ser.* **2011**, *1066*, 81-102.
39. Brown, S. L.; Rayner, C. M.; Graham, S.; Cooper, A.; Rannard, S.; Perrier, S. *Chem. Commun.* **2007**, 2145-2147.
40. Roy, D.; Ullah, A.; Sumerlin, B. S. *Macromolecules* **2009**, *42*, 7701-7708.
41. Hlalele, L. Kinetic and Mechanistic Features of Nitroxide Mediated (CO)polymerization. Stellenbosch University, Stellenbosch, 2011.
42. Pound, G.; McLeary, J. B.; McKenzie, J. M.; Lange, R. F. M.; Klumperman, B. *Macromolecules* **2006**, *39*, 7796-7797.

Chapter 3: EXPERIMENTAL

3.1 RAFT Agent Synthesis

In this chapter, the synthesis of the RAFT agents is dealt with comprehensively. In the case of CDB preparation, all glassware, magnetic stirrer and magnesium turnings were dried overnight in a 150 °C oven. Another important issue is that most reagents were used as received unless otherwise stated.

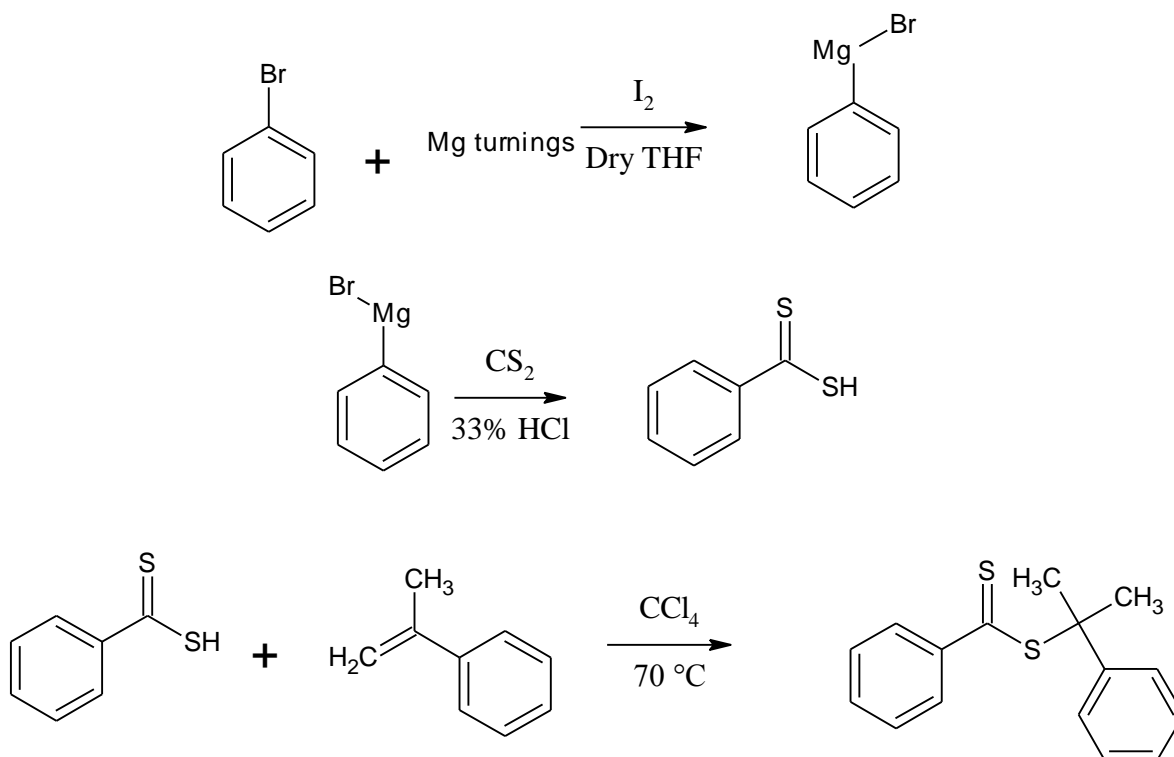
3.1.1 Procedure for Drying THF

Benzophenone (10 g), about 500 mL THF and two sodium crystals (cut under silicon oil or paraffin oil) were added in a 1 L two neck round bottom flask. The mixture was refluxed at 80 °C using a heating mantle until the THF mixture turned dark blue. The flask was also fitted with the nitrogen gas tubing, such that the refluxing was done under nitrogen environment.

3.1.2 Chemicals

Iodine (ANALAR), carbon tetrachloride (Merck, 99.8%), bromo-benzene dried over molecular sieves (Acros Organics, 99%), anhydrous magnesium sulphate (Science world, 99%), magnesium turnings (Acros Organics, 99.9%), para-toluene sulphonic acid (FLUKA, 97%), alpha methyl styrene (Sigma-Aldrich, 99%), hydrochloric acid (KIMIX, 33%), hexane (Merck, 98%), deuterated chloroform with 0.03% TMS (Sigma-Aldrich, 99.8%).

3.1.3 Synthesis of Cumyl Dithiobenzoate (CDB)

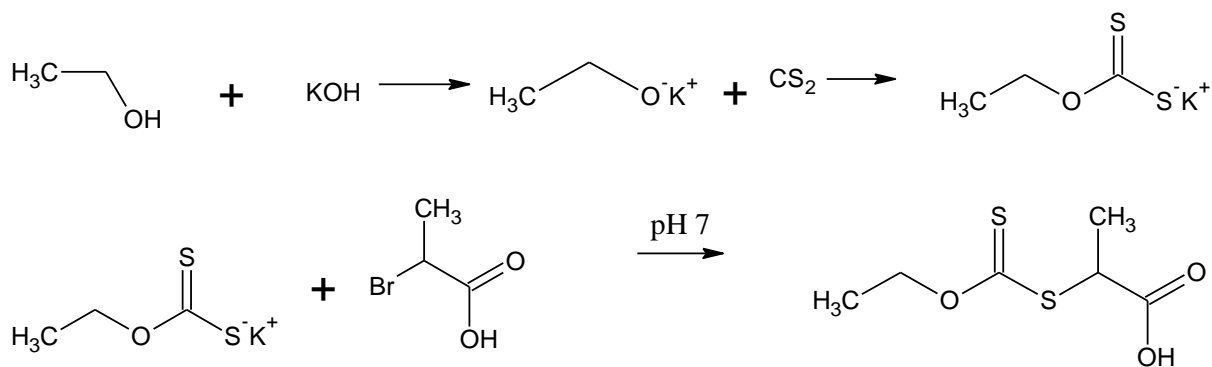


Scheme 3.1: Reaction steps in the cumyl dithiobenzoate (CDB) synthesis

Magnesium turnings (1.254 g, 51 mmol), magnetic stirrer bar, a crystal of iodine and tetrahydrofuran (THF, 20 mL) were added in a 250 mL three neck round bottom flask fitted with a condenser, a thermometer and two dropping funnels and stirring was started at room temperature. The flask was immersed in an ice bath and about 2 mL of bromo-benzene/THF solution (7.85 g, 50 mmol in 40 mL THF) was added to the flask contents through one of the dropping funnels. The reaction was then started by heating the bottom of the flask with the hair dryer (the mixture turned transparent). The remaining bromo-benzene/THF solution was added drop-wise such that the temperature of the reaction is, at all times, kept below 40 °C. The reaction mixture was stirred until all the magnesium had been consumed and the reaction was allowed to cool to room temperature on its own. Then the flask was placed in the ice bath. Carbon disulphide (3.00 mL, 50 mmol) was added drop-wise making sure that the temperature stays below 40 °C. The reaction was stirred for 30 minutes.

The Grignard reagent was hydrolyzed by slow addition of 50 mL distilled water until no more heat was generated by the reaction indicating that hydrolysis was complete. The mixture was concentrated by use of rotary evaporator (to remove the THF) at 40 °C. Then 33 % hydrochloric acid (HCl) was added slowly using a pipette to acidify the mixture to form the dithio acid and the reaction remained purple when acidification was complete. The dithio acid was extracted several times from the rest of the reaction mixture with 50 mL portions diethyl ether. The organic layer was washed once with water and then concentrated on the rotary evaporator after drying for 30 minutes with anhydrous magnesium sulphate. 1.3 equivalents of dithio acid to 1 equivalent of alpha methyl styrene, carbon tetra chloride (30 % V/V to reagents) and a catalytic amount of *para*-toluene sulphonic acid were added to a 100 mL one neck round bottom flask. The mixture was refluxed at 70 °C for 24 hours, concentrated by vacuum and then purified by application of two column chromatography on silica gel followed by one on neutral alumina. The purity was estimated at > 95% by proton NMR at 300 MHz in deuterated chloroform¹. The reaction steps of the CDB synthesis through the Grignard route are depicted in Scheme 3.1. ¹H NMR signals in CDCl₃ δ: 1.8 ppm, s, 6H, H_{cumyl methyl protons}; 7.1-7.4, m, H_{aromatic protons}; 7.5, dd, 2H, H_{ortho protons of cumyl ring}; 7.8, dd, 2H, H_{orthoprotons of dithiobenzoate ring}.

3.1.4 Synthesis of *S*-sec Propionic Acid *O*-Ethyl Xanthate (PEX)



Scheme 3.2: Reaction steps in the synthesis *S*-sec propionic acid *O*-ethyl xanthate (PEX)

Potassium hydroxide (21.02 g, 0.375 mol), ethanol (76 mL, 60 g) and a stirrer bar were added in a 250 mL three-neck round bottom flask. The mixture was refluxed for one hour at 80 °C. CS₂ (23 mL, 28.5 g, 0.375 mol) was added drop-wise over an hour to the refluxed mixture. The yellow solid (potassium *O*-ethyl dithio carbonate crystals) formed were filtered off and washed with 20 mL portions of diethyl ether. The potassium *O*-ethyl dithio carbonate was then recrystallized twice from absolute ethanol (99 % pure).² Potassium *O*-ethyl dithiocarbonate (5.18 g) was dissolved in distilled water (10 mL) with stirring until complete dissolution of the solid. The solution was cooled in an ice bath to below 10 °C (ammonium chloride was used to lower the ice temperature). 2-Bromopropionic acid (2.6 mL) was added drop-wise ensuring the reaction temperature does not exceed 30 °C. It was followed up by addition of 50% sodium hydroxide solution (1.50 mL) under similar temperature conditions.

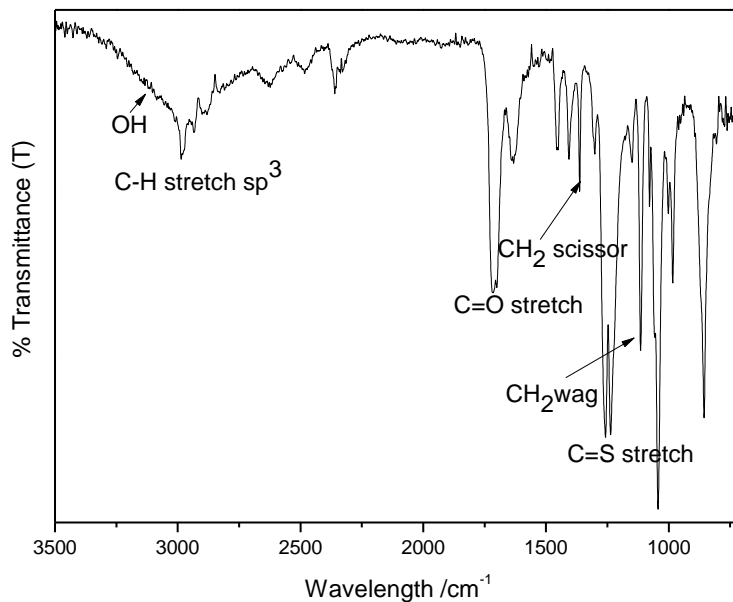
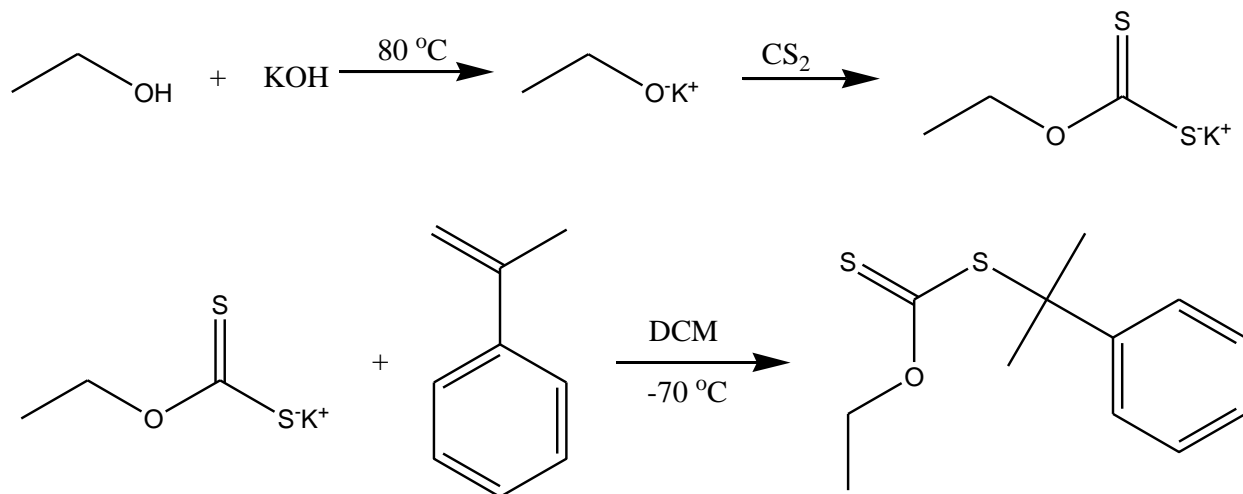
The ice bath was removed when the exotherm stopped and 10 mL water was added and then left to stir for 24 hours. After 24 hours stirring, the reaction mixture was cooled in an ice bath, 10 M HCl added drop-wise (about 20 mL) while keeping temperature below 10 °C until the pH is closer to 1 as measured by the universal indicator paper. The yellow crystals formed were washed twice with cold water, dried and then recrystallized from hexane.³ The purity was estimated to be >98% by ¹H NMR on the 300 MHz instrument in deuterated chloroform.

¹H NMR signals in CDCl₃ δ: 1.4 ppm, t, 3H, H_{methyl} protons of *o*-ethyl group; 1.6 ppm, d, 3H, H_{methyl} protons of close to dithio group; 4.4 ppm, 1H, q, H_{methylilydenyl} protons close to dithio group; 4.6 ppm, 2H, q, H_{methylene} protons of *o*-ethyl group.

¹³C NMR signals in CDCl₃ δ: 13.5 ppm, C_{methyl} of *o*-ethyl group; 16.5 ppm, C_{methyl} close to dithio group; 46.6 ppm, C H_{methylene} of *o*-ethyl group; 70.5 ppm, C_{methylilydenyl} close to dithio group; 176.5 ppm, C_{carbonyl} group; 212 ppm, C_{dithio} group.

FTIR signal

The FTIR spectrum of PEX is shown in Figure 3.1 and the characteristic peaks are labeled.

Figure 3.1: FTIR spectra of *S-sec* propionic acid *O*-ethyl xanthate (PEX)3.1.5 Synthesis of *O*-Ethyl Cumyl Xanthate (ECX)Scheme 3.3: Reaction steps in the *O*-ethyl cumyl xanthate (ECX) synthesis

The potassium *O*-ethyl dithio carbonate salt was prepared similarly to section 3.1.4 above. Alpha methyl styrene (3 mL, 0.028 mol) was dissolved in 50 mL dichloromethane (DCM) and then *O*-

ethyl xanthinic acid potassium salt (4.48 g, 0.028 mol) was added. The mixture was cooled to -70 °C in dry ice for about 30 minutes and then 95% sulphuric acid (0.86 mL, 0.033 mol) was added slowly and the reaction was stirred at room temperature for an hour. The reaction mixture was poured into distilled water. The organic layer was washed twice with distilled water, followed by sodium hydrogen carbonate (NaHCO₃) and the sodium chloride (NaCl) aqueous solutions respectively. The organic layer was then dried over anhydrous magnesium sulphate, DCM removed by vacuum and columned using pentane/diethyl-ether solution (99:1) first on alumina and then on silica to purify the product.⁴ The fraction containing ECX was left in the freezer for several days while the ECX crystallized out of solution as cream-white crystals. The purity was estimated as >98% by ¹H NMR on the 300 MHz instrument in deuterated chloroform. ¹H NMR signals in CDCl₃ δ: 7.55–7.00 ppm, m, 5H, H_{aromatic} protons; 4.42 ppm q, 2H, H_{methylene} protons of *o*-ethyl group; 1.82 ppm s, 6H, H_{cumyl} methyl protons, 1.07 ppm t, 3H, H_{methyl} protons of *o*-ethyl group.

3.2 *In Situ* Proton NMR Analysis

3.2.1 Sample Preparation

In situ proton NMR samples were prepared by mixing the weighed desired amount of monomer, RAFT agent to AIBN (molar ratio 5:1:0.2 or 10:1:0.1 respectively) and the volume of deuterated benzene (C₆D₆) was used as shown in Table 3.1. The reaction mixture was transferred to the NMR tube (5 mm in diameter) where the final reaction volume in the tube was about 0.5 mL. The reaction solution was degassed via application of several freeze-pump-thaw cycles and the reaction was carried out under ultra-high purity argon blanket.

3.2.2 *In situ* ¹H NMR Experiments

All *in situ* ¹H NMR experiments were run on the 400 MHz Varian Unity Inova spectrometer. The spectra were acquired using 3 μs (40°) pulse width with acquisition time of 4 s. For the present study, the NMR tube containing the sample was inserted in the magnet cavity, the instrument shimmed and then the reference spectrum obtained at 25 °C. Following this, the sample was removed and then the magnet's cavity heated to the required reaction temperature (60 °C or 70 °C) and once the temperature was steady, the sample was introduced again.

Shimming was repeated to optimize the conditions and an initial spectrum was collected 2-9 minutes after the insertion. Subsequent spectra were obtained at specified time intervals (4 or 5 minutes) for the duration of the experiment (10 and 14 hours). ACD labs 10.0 ^1H NMR processor[®] was used to process the resulting NMR data. Auto phase correction was performed on individual spectrum followed by baseline correction of grouped spectrum array while integration was done manually. The spectrum obtained after the instrument was heated was considered to be the start point and monomer conversion taken as zero at that point. Table 3.1 shows the actual amounts of reagents used in *in situ* ^1H NMR experiments.

3.2.3 Data Normalization

The *in situ* ^1H NMR data were normalized relative to the total phenyl protons of the CDB and ECX RAFT agents. Thus, the integrals of all the phenyl protons belonging to the RAFT agent were added together and that total used to divide all other integrals. PEX mediated systems were normalized by setting the doublet (1.3 ppm) belonging to the methyl protons of the leaving group to 3 by use of version 10.0 of ACD labs ^1H NMR processor[®].

Table 3.1: Amounts of Components used in the RAFT Mediated Polymerization

Sample	AN		VAc		RAFT Agent		AIBN		C ₆ D ₆	
	Mass (g)	Conc. (M)	Mass (g)	Conc. (M)	Mass (g)	Conc. (M)	Mass (g)	Conc. (M)	Volume (mL)	M:RAFT:AIBN calculated at 25 °C
1 ^a $f_{AN}=1.0$	0.41	2.21	0		0.43	0.44	0.049	0.088	2.56	4:1:0.2
2 ^a $f_{AN}=0.90$	0.060	1.64	0.01	0.18	0.067	0.37	0.0076	0.073	0.50	4:1:0.2
3 ^a $f_{AN}=0.50$	0.037	1.06	0.050	1.06	0.081	0.42	0.0079	0.085	0.40	2.5:1:0.2
4 ^a $f_{AN}=0.25$	0.019	0.44	0.066	1.33	0.051	0.35	0.0063	0.071	0.40	4:1:0.2
5 ^a $f_{AN}=0.0$	0		0.098	1.75	0.064	0.35	0.0076	0.070	0.50	4:1:0.2
6 ^a $f_{AN}=1.0$	0.11	3.03	0		0.057	0.30	0.0034	0.030	0.50	8:1:0.1
7 ^a $f_{AN}=0.50$	0.058	1.51	0.94	1.51	0.060	0.30	0.0036	0.030	0.50	9:1:0.1
8 ^a $f_{AN}=0.90$	0.10	2.77	0.019	0.31	0.059	0.31	0.0035	0.031	0.50	8:1:0.1
9 ^a $f_{AN}=0.10$	0.012	0.30	0.18	2.74	0.064	0.30	0.0038	0.030	0.50	9:1:0.1
10 ^b $f_{AN}=0.5$	0.034	0.98	0.055	0.98	0.057	0.39	0.0084	0.079	0.50	4:1:0.2
11 ^b $f_{AN}=0.0$	0		0.12	2.04	0.062	0.41	0.0091	0.082	0.50	5:1:0.3
12 ^b $f_{AN}=1.0$	0.070	2.07	0		0.059	0.41	0.0086	0.083	0.50	5:1:0.3
13 ^c $f_{AN}=0.0$	0		0.12	2.06	0.054	0.41	0.0092	0.082	0.50	5:1:0.3
14 ^c $f_{AN}=0.5$	0.034	0.99	0.055	0.99	0.050	0.40	0.0084	0.079	0.50	4:1:0.2
15 ^c $f_{AN}=1.0$	0.063	2.05	0		0.046	0.41	0.0078	0.082	0.50	4:1:0.2

^a Cumyl dithiobenzoate (CDB)^b *O*-ethyl cumyl xanthate (ECX)^c *S*-*sec* propionic acid *O*-ethyl xanthate (PEX)

3.3 Size exclusion chromatographic (SEC) analysis

Molecular weight and molecular weight distribution was determined using THF and dimethyl acetamide (DMAc) SEC. The Shimadzu DMAc SEC instrument setup consisting of a Shimadzu LC-10AD pump, a Waters 717Plus autosampler, a column system fitted with a 50x8

mm guard column in series with three 300x8 mm, 10 μm particle size GRAM columns (2 x 3000 \AA and 100 \AA) obtained from PSS. A Waters 2487 dual wavelength UV detector and a Waters 410 differential refractive index (DRI) detector all in series. The system is calibrated against narrow molecular weight poly(methylmethacrylate) (PMMA) standards and 1 mg/mL polymer solution concentrations were prepared in DMAc with 3% BHT.

For the THF-SEC instrumental set up consisted of a Shimadzu LC-10AT isocratic pump, a Waters 717 plus auto-sampler, a refractive index detector, a Waters 2487 dual wavelength UV detector, Waters Alliance apparatus fitted with a 50 \times 8 mm guard column connected in series with three 300 \times 8 mm, 10 μm particle size, GRAM columns (2 \times 3000 \AA and 100 \AA). The instrument calibration was done using polystyrene standard (PSty) of narrow molecular weights distribution and 1 mg/mL polymer solution concentrations were prepared in THF with 3% BHT.

3.4 HPLC-MS analysis

The Waters Synapt G2 Liquid chromatography Column (LC) instrument was used to identify short chain polymers prepared. The ionization source was ESI+, Capillary voltage 3 kV, Cone Voltage 15 V and 25 V and the analysis was calibrated against sodium formate and lock mass against Leucine enkephalin. Waters UPLC flow rate of 0.2 mL/min and 1 mL/min using 100 % methanol (Romil) as the mobile phase and a 25 cm \times 4.6 mm, 5 μm Ascentis[®] C18-column and a 150 \times 2 mm Phenomenex Nucleosil 5 C18 column.

3.5 References

1. McLeary, J. B. Reversible Addition-Fragmentation Transfer Polymerization in Heterogeneous Aqueous Media. PhD Thesis, Stellenbosch University, Stellenbosch, South Africa, **2004**.
2. Fleet, R.; McLeary, J. B.; Grumel, V.; Weber, W. G.; Matahwa, H.; Sanderson, R. D. *Macromol. Symp.* **2007**, *255*, 8–19.
3. Ferguson, C. J.; Hughes, R. J.; Nguyen, D.; Pham, B. T. T.; Gilbert, R. G.; Serelis, A. K.; C. H. Such; Hawkett, B. S. *Macromolecules* **2005**, *38*, 2191-2204.
4. Destarac, M.; Brochon, C.; Catala, J. M.; Wilczewska, A.; Zard, S. Z. *Macromol. Chem. Phys.* **2002**, *203*, 2281-2289.

Chapter 4: RAFT MEDIATED HOMOPOLYMERIZATION

4.1 Introduction

In order to understand the complex RAFT copolymerization reaction, it is necessary to study the RAFT homopolymerization of the relevant monomers so as to comprehend the kind of products obtainable and to use them as a point of reference for copolymerization. In a living radical polymerization process such as RAFT, it is important to study the nature and type of products, including side products; and the reaction rates of formation or consumption of each component in the polymerization mixture. However, the living and controlled characteristics of the polymer product are dependent on the properties of the monomer in question and of the transfer agent employed in the reaction. These two polymer characteristics, usually used interchangeably, are discussed below.

4.1.1 Controlled features

The polymerization reaction is said to be controlled when the resulting polymer product have narrow molecular weight distribution ($D < 1.5$). In addition, the evolution of molecular weight should be linear as a function of monomer conversion with minimal bimolecular termination. For the case of a RAFT mediated system, this means that the exchange process between the propagating radical and the dormant must be efficient. That is, it is desirable that only one monomer unit is added to the propagating radical per transfer cycle.

4.1.2 Living features

The livingness of the polymer is usually associated with the possibility of extending the polymer chain in the presence of more monomer under polymerization conditions. Thus, the RAFT chain-ends in the polymer are retained such that under polymerization conditions, when initiator and monomer are added, the polymer acts as the macro-RAFT agent to control further

polymerization. This block formation ability and also the end-group analysis are the techniques used to experimentally determine the living characteristics of the polymer sample in the literature to date.^{1,2}

4.2 Properties of PAN and PVAc

High molecular weight polyacrylonitrile (PAN) is known for its poor solubility in most organic solvents. Dimethyl formamide (DMF), dimethyl sulphoxide (DMSO) and ethylene carbonate (EC) have been reported to be good solvents for PAN, but EC was found to give ideal conditions for RAFT produced polymer with good control over molecular weight (up to 32800 g mol⁻¹) and dispersity (\bar{D}) values of 1.29 were reported.³ Vinyl acetate (VAc), on the other hand, has a fast growing radical and as a result is prone to side reactions including termination, transfer and head to head propagation. This renders VAc not easy to copolymerize. Successful RAFT controlled polymerization of VAc has been reported for the system using xanthate-mediated RAFT/MADIX systems. Molecular weight of up to 40 000 g·mol⁻¹ and \bar{D} values of less than 1.3 have been reported for xanthate mediated VAc homopolymerization.² For the experiments in the current study, deuterated benzene was used and the [M]:[RAFT]:[AIBN] mole ratio of 5:1:0.2 and 10:1:0.1 were chosen to enable initialization studies hence solubility of the PAN is no longer an issue at these short chains lengths.

4.3 Experimental

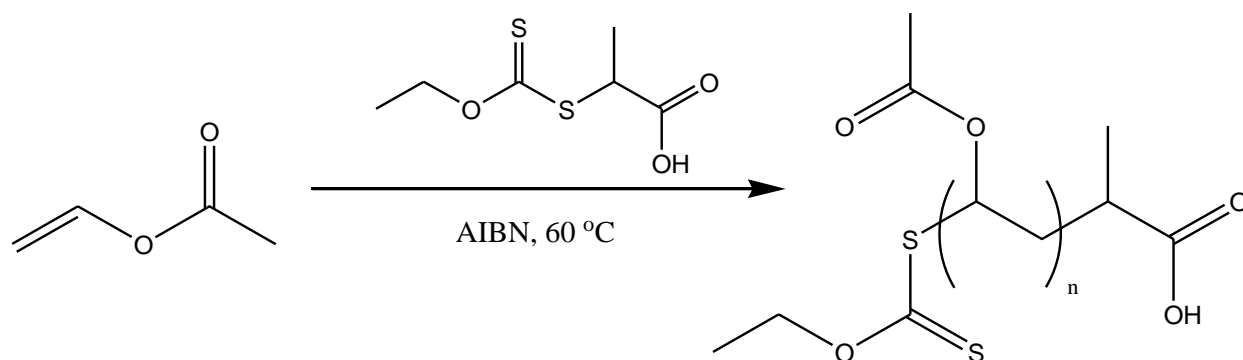
4.3.1 Chemicals

Cumyl dithiobenzoate (CDB), *S-sec* propionic acid *O*-ethyl xanthate (PEX) and *O*-ethyl-*S*-cumyl xanthate (ECX) were synthesized as outlined in Chapter 3 subsections 3.13, 3.14 and 3.15 respectively. Acrylonitrile (AN, Sigma-Aldrich) was purified by filtering or passing it through inhibitor remover (FLUKA, ≥99% assay) stabilized with 0.04% hydroquinone monomethyl ether, and vinyl acetate (VAc, Sigma-Aldrich) was washed several times with 5 % aqueous solution of sodium hydroxide to remove the inhibitor, dried over anhydrous magnesium sulphate

then distilled under vacuum at 50 °C. Benzene-d₆ solvent was used as received while AIBN (Sigma-Aldrich, 98% assay) was recrystallized from ethanol whereby it was dissolved at 50 °C and then allowed to slowly cool down to room temperature.

4.3.2 Sample Preparation

See section 3.2.1 of Chapter 3. Scheme 4.1 shows the PEX mediated VAc homopolymerization.



Scheme 4.1: PEX mediated VAc homopolymerization

4.3.3 In Situ Proton NMR experiments

NMR data was normalized by dividing all the peaks by the integral of the total phenyl protons on the RAFT agent (this was fairly constant over the reaction time and represents total concentration of the transfer agent for CDB and ECX). PEX mediated reaction data was normalised by setting the integrals of the methyl protons of the *S-sec* propionic acid leaving group to 3.

For calculation of monomer conversion, the average monomer concentration (residual concentration) was computed and then the conversion was calculated on the basis of equation 4.1.

$$x = \left(\frac{\text{initial conc} - \text{final conc}}{\text{initial conc}} \right) \times 100\% \quad (4.1)$$

Where x is the conversion

All polymerization reactions were carried out in the cavity of the 400 MHz spectrometer at 60 °C or at 70 °C. The ^1H NMR spectra were recorded every 4 and 5 minutes for the entire reaction time (10-14 hours).

4.4 Results and Discussions

4.4.1 CDB mediated homopolymerization

The acrylonitrile (AN) and vinyl acetate (VAc) homopolymerizations were undertaken by *in-situ* proton NMR using cumyl dithiobenzoate (CDB) at 60 °C and the reactions were run for 10 and 14 hours in C_6D_6 using a monomer to RAFT to initiator mole ratio of 5:1:0.2. Figure 4.1 shows the typical stacked proton NMR spectrum of the cumyl dithiobenzoate mediated homopolymerization of acrylonitrile at 60 °C in the first five hours of the reaction. The region labeled A denotes the aromatic protons region used for normalization of the experimental data (represents the total RAFT agent). Region B shows the resonance frequency area of vinylic protons belonging to AN used to compute the instantaneous monomer concentration and monomer conversion. The singlet of methyl protons of the leaving cumyl group of CDB, which resonates around 1.80 ppm, was followed since these protons become de-shielded and shift to lower chemical shifts (up field) when attached to the AN monomer.

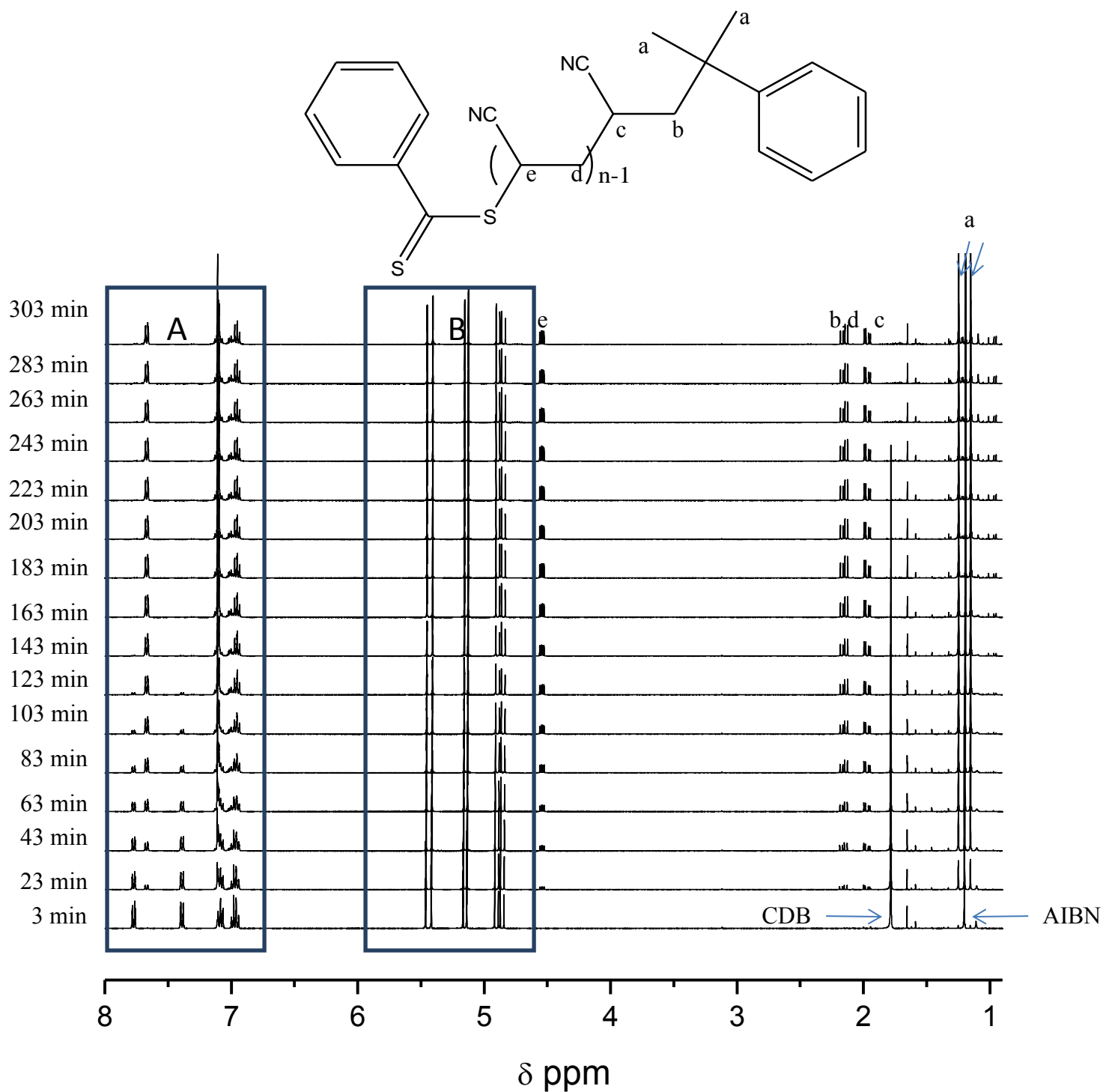


Figure 4.1: The ^1H NMR spectra of the AN polymerization showing the instantaneous spectra taken at 20 minutes intervals from the beginning of the reaction up to 5 hours at 60°C monitored by in situ ^1H NMR

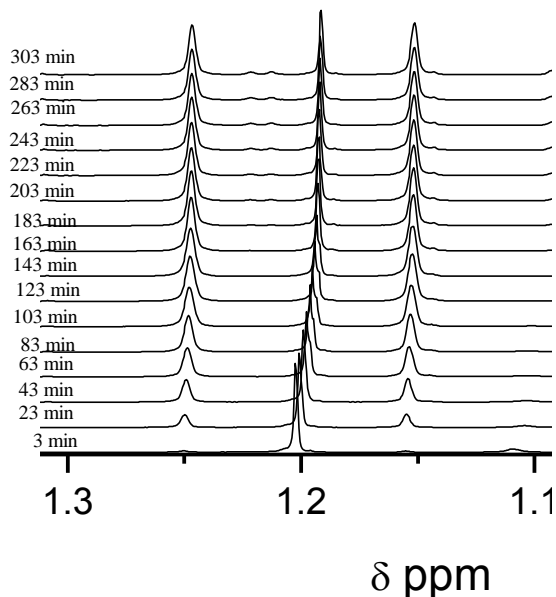


Figure 4.2: Enlarged first AN adduct region

The methylene (b, d) and methine protons (c-chains longer than one AN unit and e-for the proton close to dithio moiety in cumyl-AN-dithiobenzoate, CAND, species) belonging to acrylonitrile monomer after one insertion into the CDB, are observed to shift to lower chemical shifts. Whereas, (a) refer to the methyl protons of the cumyl leaving group after insertion of a single AN monomer unit (two stereo isomeric structures obtained). Upon expansion of the first adduct peaks region, Figure 4.2, it was observed that two stereo isomeric structures appear as two peaks of equal intensity at 1.13-1.16 ppm and 1.23-1.26 ppm. Also, these stereo isomers were observed fairly early in the polymerization reaction (earlier than 20 minutes), which was not the case for VAc mediated by CDB as will be shown later. Figure 4.3 shows the relative concentration of CDB and its derivatives as a function of time and it illustrates that the initialization period, about 150 minutes long, precedes the formation of higher monomer adducts.

Thus, the entire RAFT agent is consumed at the same rate as the appearance of the species where only one AN monomer unit is attached to the leaving group of the CDB. The minimum concentration of CDB coincides with the maximum concentration of the CAND species. This phenomenon was first established and explained by McLeary *et al.* for the RAFT mechanism of

methyl acrylate homopolymerization^{4, 5}. Thus, the CDB is completely consumed to form single monomer adducts and then second monomer is added, as indicated by its increasing relative concentration once the first adduct concentration reaches the maximum value. Examination of the slope of the first adduct (CAND), during and after initialization period, the formation of first monomer adduct seems to be faster than its consumption to form second and higher adducts. This could be explained by the fact that the leaving group properties of the CAND species, as compared to the cumyl leaving group are not so good, as a result, the reaction slows down to some extent.

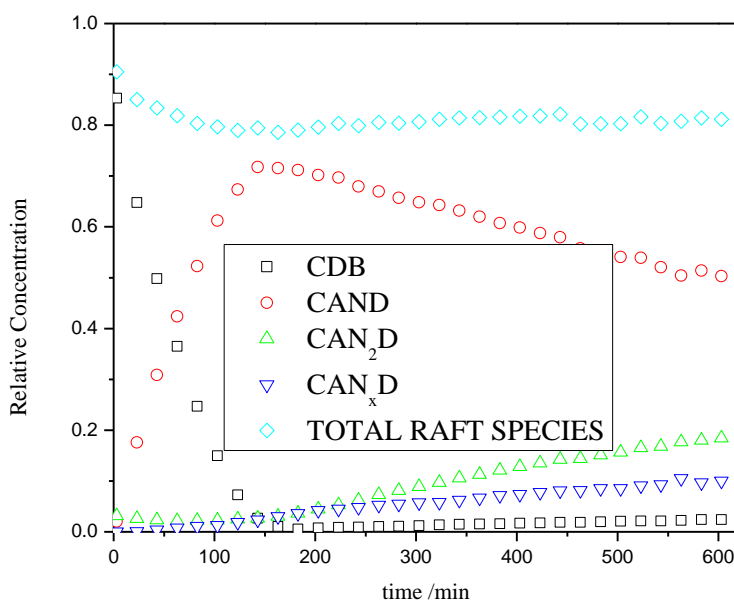


Figure 4.3: The relative concentration of all the RAFT species for CDB AN homopolymerization at 60 °C monitored by *in situ* ¹H NMR run for 10 hours

The conversion computed for the CDB mediated AN homopolymerization, Figures 4.4, further shows that the polymerization rate is faster during the initialization stage, up to 150 minutes, then decreased when formation of higher adducts commenced as indicated by decrease in the slope of the curve. Accordingly, it is shown that cumyl radicals are more reactive towards AN monomer than the oligomeric radicals. This is a perfect feature towards attaining well controlled polymer since the rate coefficient of re-initiation is greater than that of propagation ($k_{pi} > k_p$).

The maximum AN conversion was found to be 17% as observed from Figure 4.4, and the conversion was calculated based on equation 4.1.

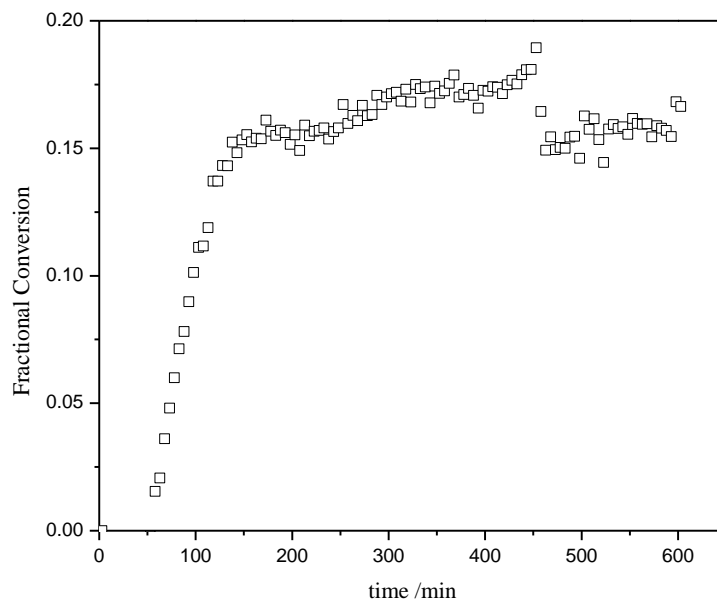


Figure 4.4: Fractional conversion as a function of time for the CDB mediated AN homopolymerization at 60 °C monitored by *in situ* ^1H NMR run for 10 hours in C_6D_6

For comparison sake, vinyl acetate homopolymerization was done under the same reaction conditions at 60 °C by *in situ* ^1H NMR run for 14 hours in C_6D_6 using the monomer to RAFT to initiator mole ratio of 5:1:0.2 (the same ratios used in AN CDB mediated homopolymerization). In Figure 4.5, the stacked *in situ* proton NMR spectra for VAc CDB mediated homopolymerization showing the expanded region between 1.14-1.16 ppm to 1.24-1.26 ppm where the peaks belonging to the appearance of the first VAc adduct with the cumyl leaving group of CDB (CVAcD) is seen. It takes about ten hours (600 minutes) for VAc to start showing first adduct peaks with CDB. Therefore, VAc does react with CDB, but the reaction is strongly retarded. The long retardation can most probably be due to the fact that the electron density difference between the VAc monomer and the cumyl radical is very small. Thus, VAc has an electron rich double bond due to high electron density around the oxygen atom attached directly

to the VAc carbon-carbon double bond, as a result, the electron rich cumyl radical does not prefer to react with it. This means that addition rate of VAc to CDB will be very slow as fragmentation is favoured over addition. Once in a while, successful addition of VAc may occur resulting in the formation of the first CVAcD adduct. One important issue to note from this study is that the first adduct peaks of CVAcD appear at the exact same resonance frequencies reported for CAND adduct peaks.

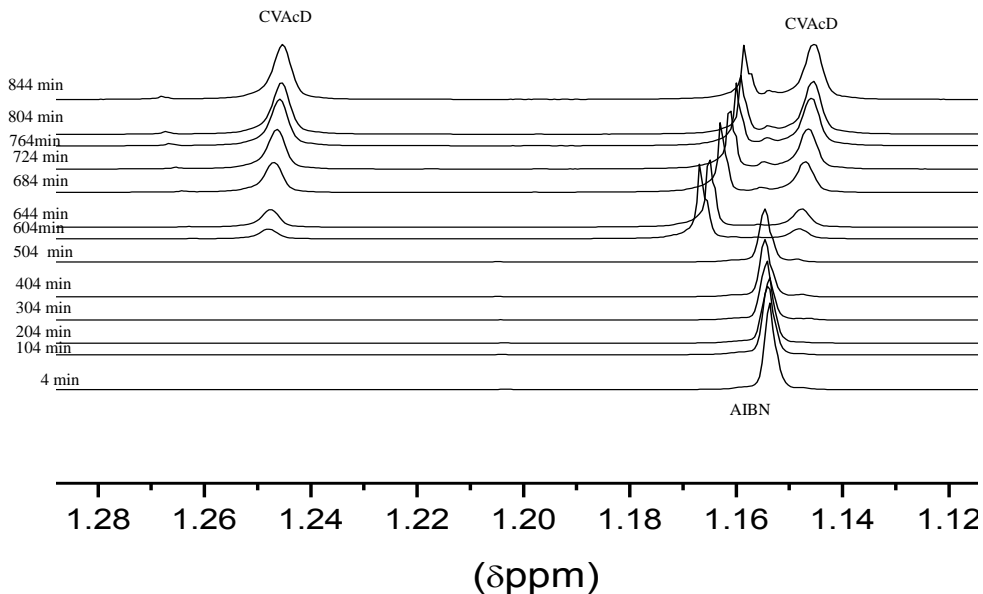


Figure 4.5: The VAc CDB-mediated homopolymerization monitored by *in situ* ¹H NMR at [VAc]:[CDB]:[AIBN] ratio of 5:1:0.2 at 60 °C in C₆D₆ showing 1.14-1.16 ppm and 1.24-1.26 ppm region

Figure 4.6 depicts comparison of the fractional conversion of AIBN and CDB over the reaction time. It is observed that final percentage conversion of AIBN (30 %) is higher than that of CDB (20 %). In the first 200 minutes, both species conversion seems to increase steadily at the same rate. Then, the rate of CDB conversion drops while AIBN conversion continues to increase with time. However, studying the VAc conversion with time (Figure 4.7), only 6% of the monomer is consumed in 14 hours of reaction time. On the other hand, Figure 4.8 shows the evolution of CVAcD adducts, CIPVAcD (AIBN initiated VAc) and CDB as a function of time. Only about 1% of the 20% converted CDB seems to have formed the first monomer adduct with VAc while

CiPVAcD, whose methyl protons resonate between 0.93-0.94 ppm, constitutes 11% of the used up CDB. The remaining 8% of the used up CDB could not be accounted for but it is believed that there might have been other side reactions including the formation of CIPDB when cyano isopropyl radicals of AIBN add to CDB replacing cumyl leaving group.

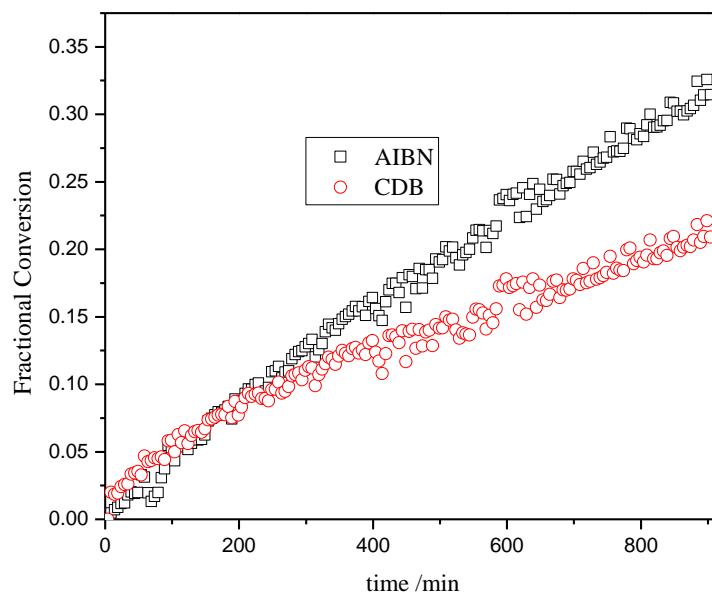


Figure 4.6: Comparison between the fractional conversion of AIBN and CDB for CDB mediated VAc homopolymerization at 60 °C monitored by *in situ* ^1H NMR in C_6D_6

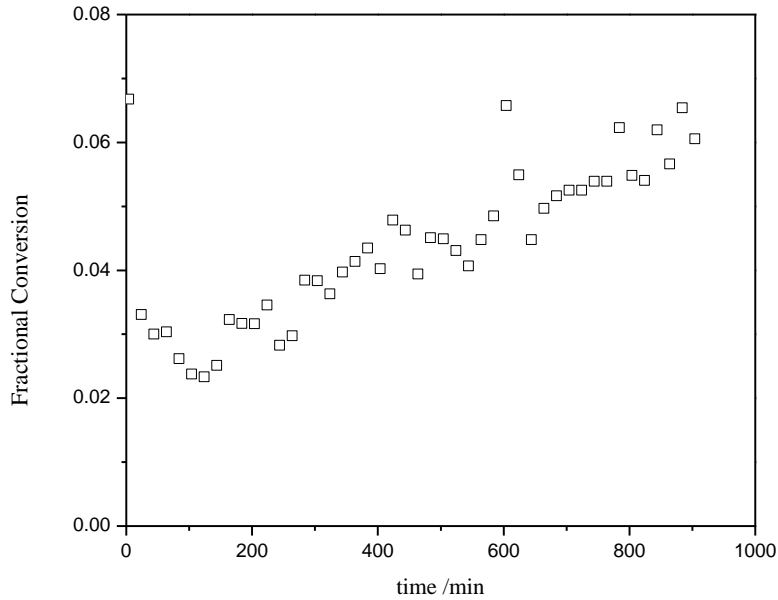


Figure 4.7: VAc Fractional conversion as a function of time for CDB mediated homopolymerization at 60 °C by *in situ* ^1H NMR in C_6D_6 run for 14 hours at [VAc]:[CDB]:[AIBN] ratios of 5:1:0.2.

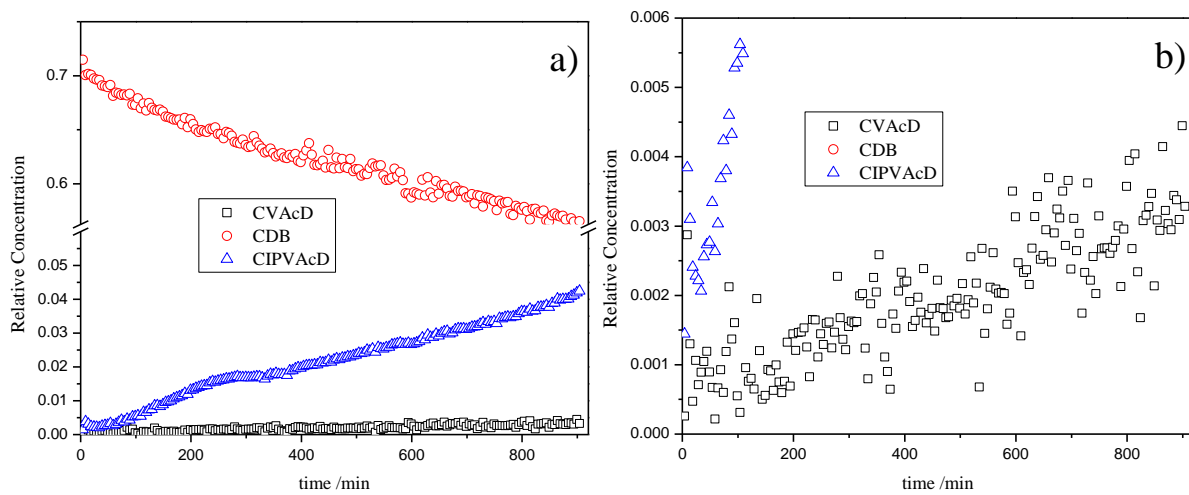


Figure 4.8: a) The variation of the relative concentration of CDB, CVAcD and CIPVAcD as a function of time for VAc homopolymerization at 60 °C monitored by *in situ* ^1H NMR run for 14 hours at [VAc]:[CDB]:[AIBN] ratios of 5:1:0.2. b) Shows the zoomed CVAcD concentration as a function of time.

4.4.2 ECX mediated homopolymerization

The ECX mediated homopolymerizations of VAc and of AN were done at 60 °C in C₆D₆ at [monomer]:[ECX]:[AIBN] ratios of 5:1:0.2 and the reactions were run for 14 hours. Figure 4.9 shows the fractional conversion of VAc homopolymerization as followed by *in situ* ¹H NMR. The VAc was consumed very quickly with the final fractional conversion of 17% in a matter of 50 minutes. Then no more VAc seems to be reacting after this time as indicated by plateau shape of the fractional conversion curve. It is of importance to note that the VAc conversion in this case is higher than when VAc was homopolymerized in the presence of CDB. The possible explanation for high VAc conversions could be related to the fact that the C=S of ECX is more active towards radical addition due to the electron affinity of the oxygen atom of the *O*-ethyl *Z*-group. It should also be noted that both ECX and CDB have cumyl as the leaving group while the CDB's *Z*-group is a stabilizing phenyl group whereas the *Z*-group of ECX is a destabilizing *O*-ethyl group hence renders the C=S bond of ECX more prone to radical attack. Thus, ECX will be susceptible to VAc centered radicals addition better than in the previous case of CDB. Beyond initialization, since the secondary leaving group derived from VAc has poor leaving properties as opposed to the tertiary cumyl leaving group, the reaction is extremely slowed down. The final percentage conversion of ECX is 25% in 14 hours of the reaction time (Figure 4.10). This low ECX conversion maybe due to the low addition rate of cumyl radical to VAc monomer due to the same reasons explained earlier in CDB mediated VAc homopolymerization. However, in the current case, 11.6% of the used up RAFT agent formed CiPVAcX (AIBN initiated VAc with xanthate moiety at the ω-chain end). The plot of the relative concentration of CIPVAcX as a function of time is shown in Figure 4.11 below.

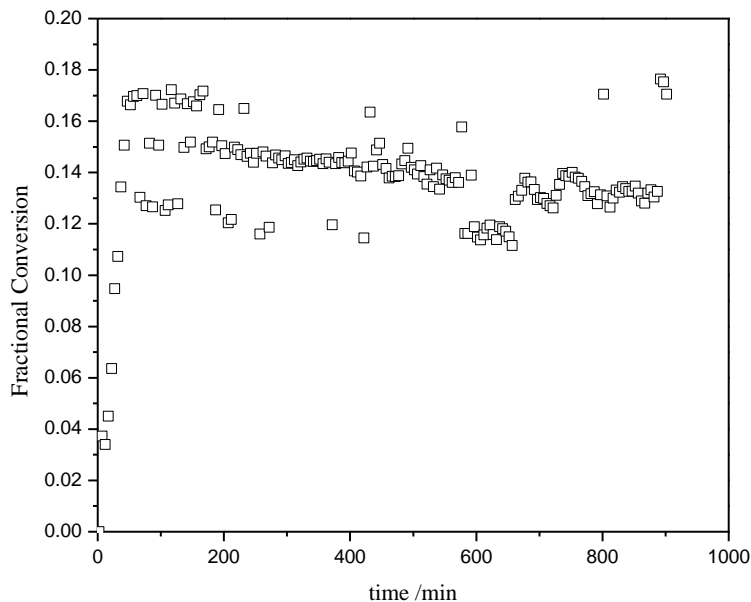


Figure 4.9: VAc fractional conversion as a function of time for the ECX mediated homopolymerization at 60 °C monitored via *in situ* ^1H in C_6D_6 at $[\text{VAc}]:[\text{ECX}]:[\text{AIBN}]$ ratios of 5:1:0.2

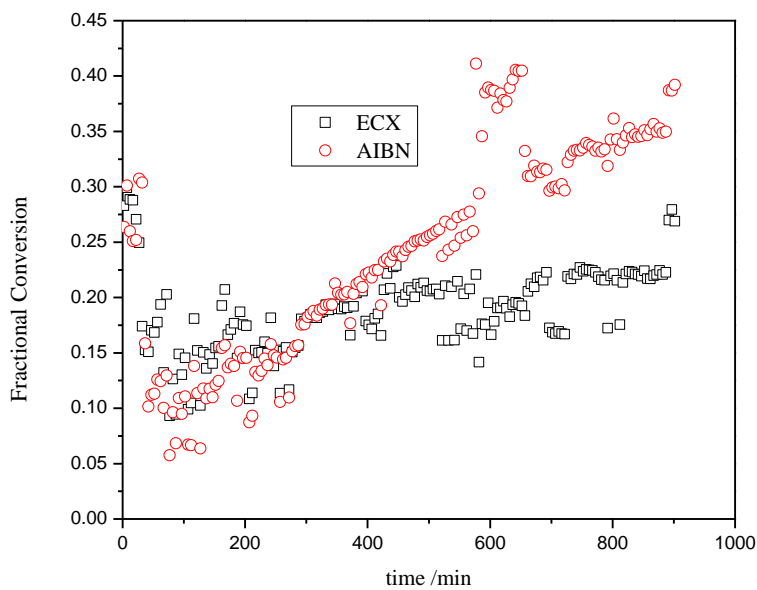


Figure 4.10: Comparison of fractional conversion of ECX and AIBN for the ECX mediated VAc homopolymerization at 60 °C monitored by *in situ* ^1H NMR in C_6D_6 at $[\text{VAc}]:[\text{ECX}]:[\text{AIBN}]$ ratios of 5:1:0.2

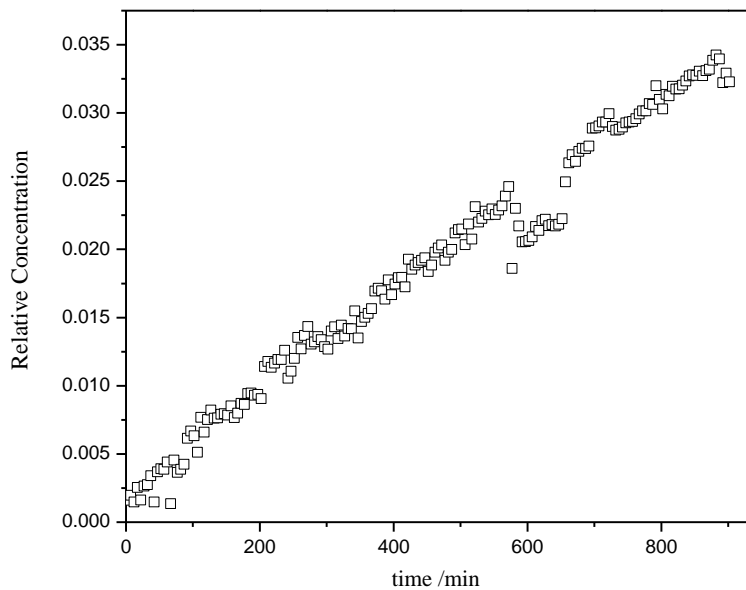


Figure 4.11: Relative concentration of CiPVAcX as a function of time for the ECX mediated VAc homopolymerization at 60 °C monitored by *in situ* ^1H NMR in C_6D_6 at [VAc]:[ECX]:[AIBN] ratios of 5:1:0.2

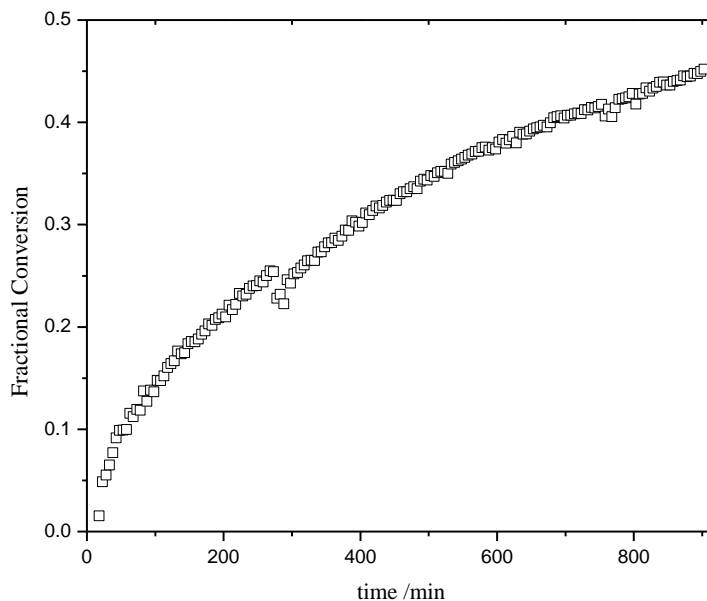


Figure 4.12: AN fractional conversion as a function of time for the ECX mediated homopolymerization at 60 °C monitored by *in situ* ^1H in C_6D_6 at $[\text{AN}]:[\text{ECX}]:[\text{AIBN}]$ ratios of 5:1:0.2

The homopolymerization of AN with ECX on the other hand resulted in 45 % monomer conversion in the 14 hours of reaction time (Figure 4.12) as opposed to the 17% monomer conversion obtained in the CDB mediated homopolymerization. However, no precipitation was observed in the AN homopolymerization which was a sign that only oligomer type products were formed. HPLC-MS analysis (Chapter 5 Figure 5.20) confirmed the results showing that the majority of chains were one to five monomer units long. The high AN conversion may be explained by the fact that there is a combination of two aspects. First, the cumyl radical of the ECX prefers to add AN due to large electron density difference between the two species. Secondly, the *O*-ethyl Z-group renders the C=S moiety of ECX more prone towards radical addition. However, this *O*-ethyl Z-group destabilizes the intermediate radical so much so that the AN monomer adducts are fragmented even before the original transfer agent is completely consumed. Thus, some kind of hybrid behaviour is suspected, where propagation and initialization reactions occur simultaneously.

The monomer fractional conversion achieved in the first 50 minutes of the polymerization reaction for both AN and VAc homopolymerizations mediated by ECX was found to be approximately the same, thus VAc is 17% while AN is 20%. The only divergence is that AN continues to grow while VAc seems to have completely stopped growing. It must be noted that cumyl radical does not prefer VAc and also that *O*-ethyl *Z*-group has good transfer properties for VAc hence adduct intermediate radical in this case will have low fragmentation rates. Examination of the ECX conversion in the AN homopolymerization, Figure 4.13, does not show any kind of selective conversion of ECX to single AN monomer unit adducts and was ascribed to the hybrid behavior described earlier.

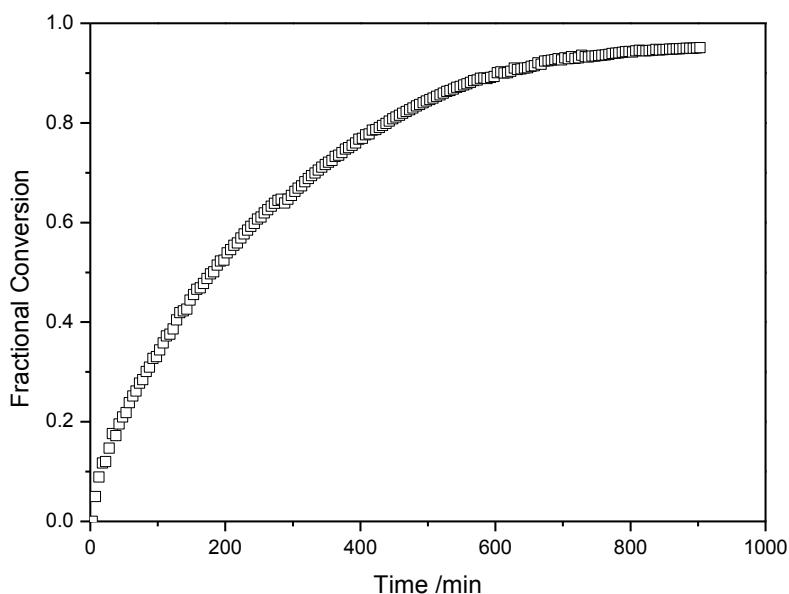


Figure 4. 13: Fractional conversion of ECX for the ECX mediated AN homopolymerization at 60 °C monitored by *in situ* ^1H in C_6D_6 at [AN]:[ECX]:[AIBN] ratios of 5:1:0.2

4.4.3 PEX mediated homopolymerization

The VAc and AN homopolymerizations were undertaken at 60 °C using the monomer to RAFT agent to AIBN ratio of 5:1:0.2 as done previously with CDB. The correlation of the RAFT species as a function of time was done by following the methyl protons of the PEX leaving group. These methyl protons give resonance signals between 1.285-1.340 ppm and appear as a

doublet with a J-coupling of 7 Hz (normalization done by setting their signal to 3 using ACD labs 10.0 ^1H NMR processor[®]). Figure 4.14 shows the snap shot of ^1H NMR spectra of PEX mediated VAc homopolymerization.

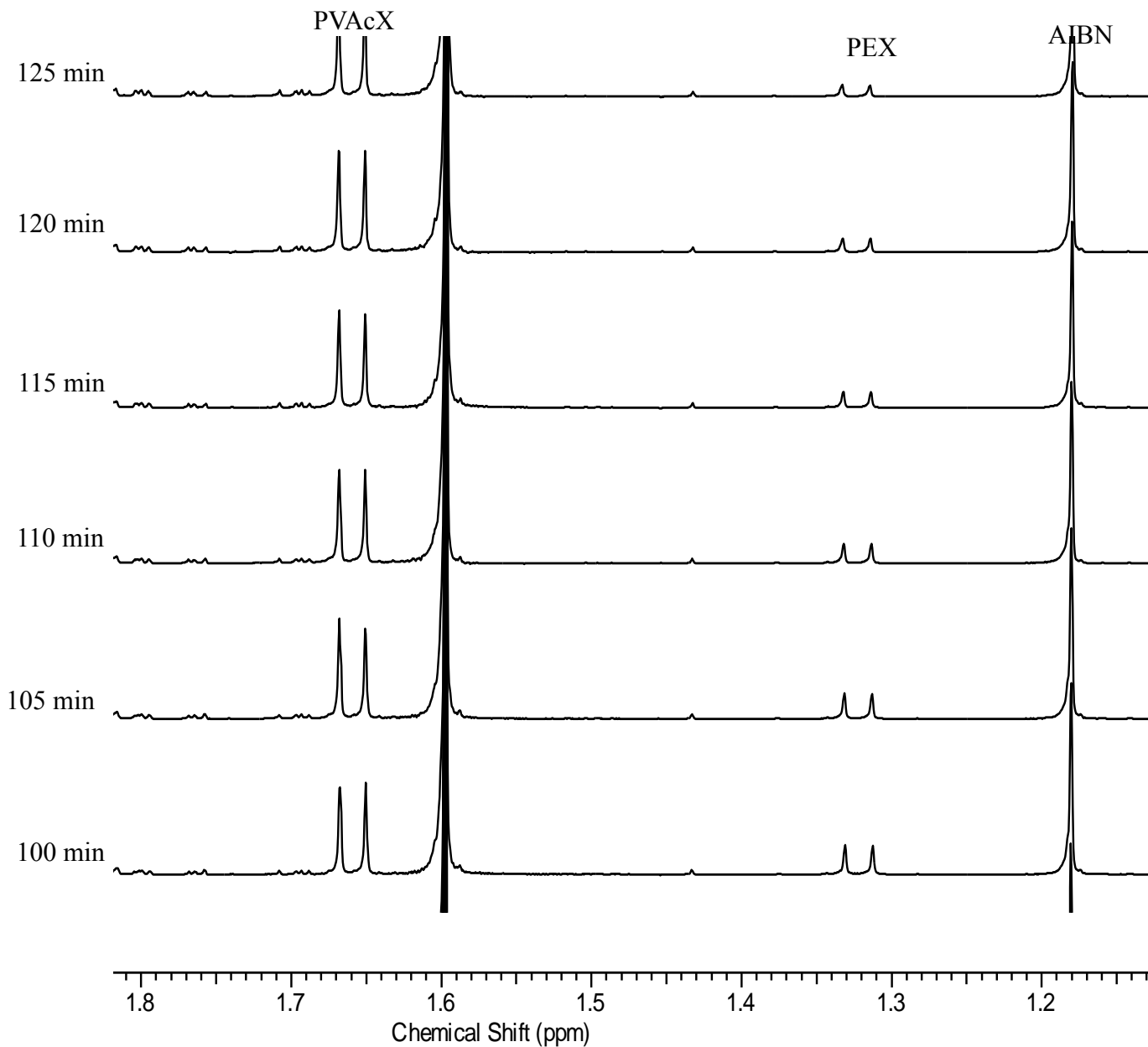


Figure 4.14: The snap short of the *in situ* ^1H NMR spectra during the PEX mediated VAc homopolymerization at [VAc]:[PEX]:[AIBN] ratios of 5:1:0.2 from 100 minutes after commencement of the reaction

In this case, PEX shows high selectivity for VAc, as observed from Figure 4.15 the transfer agent (PEX) is converted to the first monomer adduct (PVAcX). The first VAc adduct is observed as a doublet with 7 Hz J-coupling, which increases to give a maximum point after 162 minutes at higher resonance frequency (1.637-1.678 ppm). Once the PVAcX has reached maximum concentration, the second VAc adduct oligomers (PVAc₂X) can be seen. These appear at even higher frequencies, around 1.687-1.723ppm as a doublet of doublets. This doublet of doublets has J-coupling constants of 6.0 Hz, 5.0 Hz, 4.0 Hz and 3.2 Hz. The doublet of doublets can be explained to be due to two stereo-isomeric structures formed when the second VAc unit is added to the PVAcX adduct. However, the chemical shift of the methyl protons of the *S-sec* propionic group in these two isomers does not differ much, an accidental superposition of the lines occurs in the doublet of doublets such that the 1:1:1:1 ratios no longer exist.

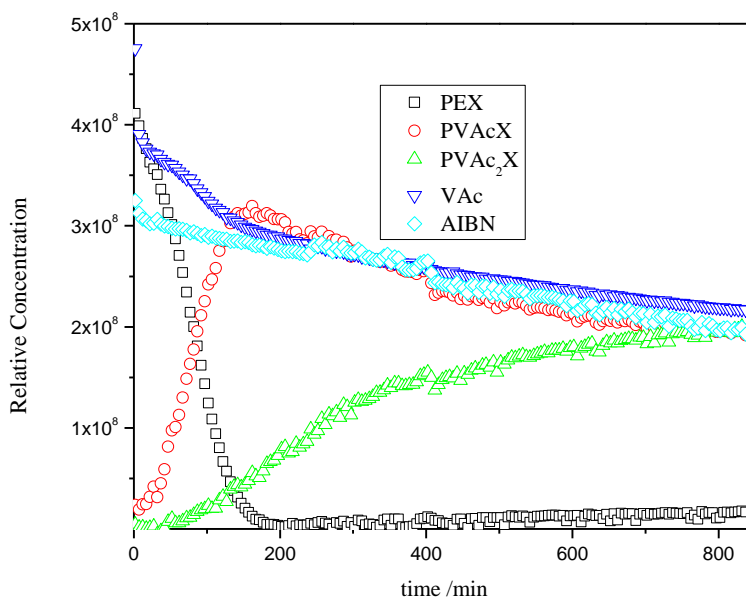


Figure 4.15: The relative concentration of species in the PEX mediated VAc homopolymerization at 60 °C monitored by *in situ* ¹H NMR run for 14 hours at [VAc]:[PEX]:[AIBN] ratios of 5:1:0.2

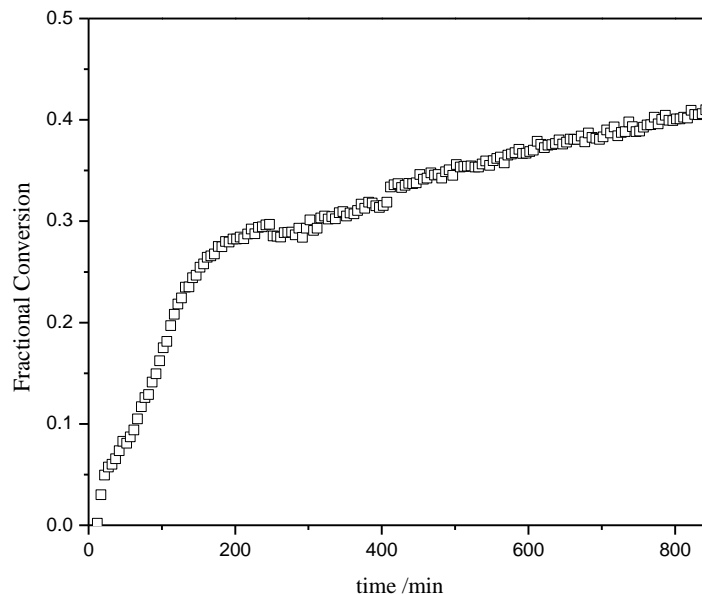


Figure 4.16: VAc fractional conversion as a function of time for the PEX mediated VAc homopolymerization at 60 °C monitored by *in situ* ^1H NMR run for 14 hours at [VAc]:[PEX]:[AIBN] ratios of 5:1:0.2

The rate of polymerization is relatively faster during the initialization period as indicated by the rapid increase of VAc monomer conversion (Figure 4.16). Beyond initialization, beyond 200 minutes, both consumption of the single VAc unit derived transfer agent and the pure VAc monomer slows down, this is indicated by the decrease in the slope of their curves (Figures 4.15-4.16). This phenomenon is ascribed to the poor leaving properties of the VAc adduct group. The final VAc fractional conversion was 41% which is higher than when CDB and ECX are used as transfer agents in VAc homopolymerization.

In the case of PEX mediated AN homopolymerization, the polymer obtained was a solid and the NMR spectra displayed broad bands for all the initial species in the reaction mixture. No indication of oligomerization was observed as none of the PEX peaks seemed to change their resonance positions. Based on this observation and also on the number average molecular weight for this sample obtained by size exclusion analysis using DMAc system against PMMA standards was 3144 gmol^{-1} (target was 550 gmol^{-1}) with a dispersity value of 1.47. It was concluded that

AN here reacted by means of a conventional radical polymerization mechanism, with the xanthate acting as a chain transfer agent with relatively low chain transfer constant.

4.4.4 Side reactions in CDB and ECX homopolymerization

4.4.4.1 Acetaldehyde formation in CDB and ECX mediated VAc homopolymerization

In polymerization reactions involving VAc, a quartet was seen to appear at 9.25 ppm and it increased as a function of time. This peak was assigned to acetaldehyde formed as a result of hydrolysis of the ester bond of VAc. Nonetheless, for freshly distilled monomer, the acetaldehyde was never formed in the reaction. This indicates that VAc is moisture sensitive. As a result, care was taken when doing the experiments in order to exclude moisture from the reaction. These side reactions were obtained in the case of CDB (Figure 4.17) and ECX (Figure 4.18) mediated systems.

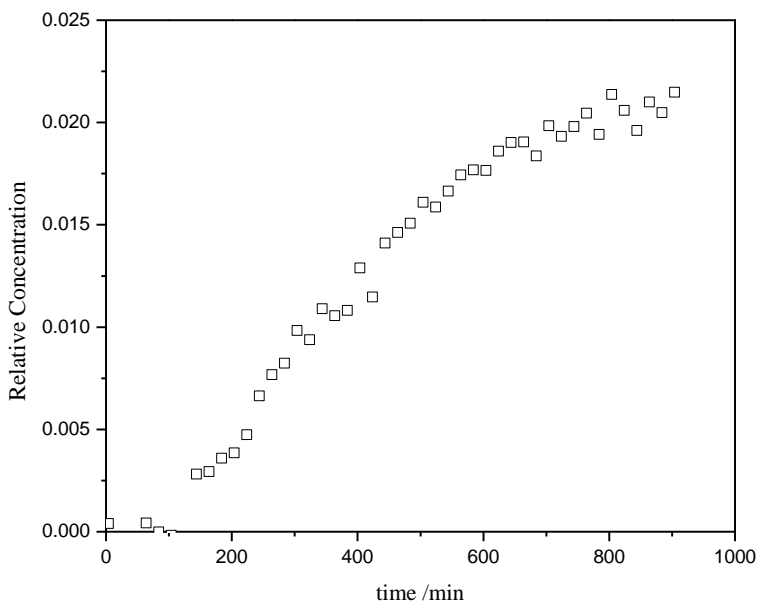


Figure 4.17: Evolution of the acetaldehyde relative to the total ECX concentration as a function of time for the CDB mediated VAc homopolymerization at 60 °C monitored by *in situ* ^1H NMR run for 14 hours at [CDB]:[VAc]:[AIBN] ratios of 5:1:0.2

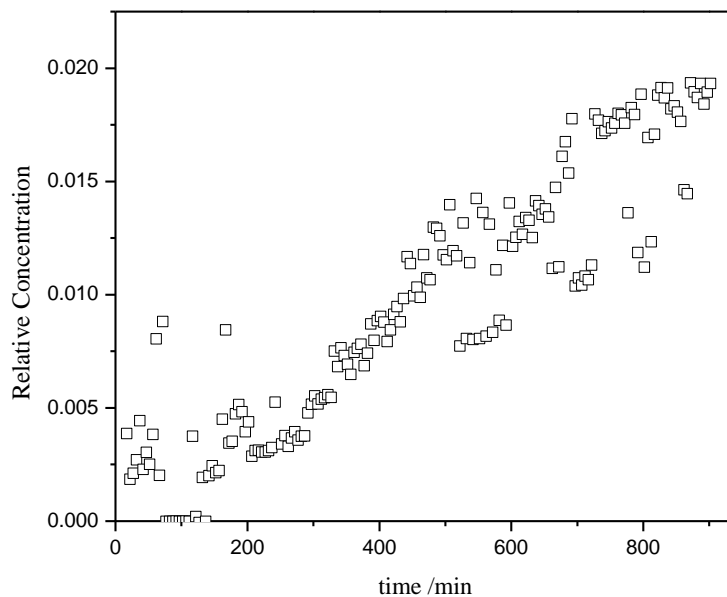


Figure 4.18: Evolution of the acetaldehyde relative to the total ECX concentration as a function of time for the ECX mediated VAc homopolymerization at [ECX]:[VAc]:[AIBN] ratios of 5:1:0.2

4.4 Conclusion

The homopolymerizations of AN and VAc were performed in the presence of three different RAFT agents. CDB showed selective initialization in the case of AN, whereas extreme retardation, in agreement with literature, was observed for CDB mediated VAc homopolymerization. The application of PEX on the other hand showed selective initialization for VAc but no control over AN homopolymerization as was indicated by a solid polymer sample obtained with AN homopolymerization. Thus, relatively long PAN chains were obtained (M_n of 3144 g mol⁻¹) with PEX were found, showing that the polymerization characteristics were similar to those of a conventional radical polymerization. The ECX mediated homopolymerization of VAc consumption was in the form of CiPVAcX species while ECX mediated AN homopolymerization resulted in oligomerization.

4.5 References

1. Moad, G.; Rizzardo, E.; Thang, S. *Aust. J. Chem.* **2005**, *58*, 379-410.
2. Fleet, R.; McLeary, J. B.; Grumel, V.; Weber, W. G.; Matahwa, H.; Sanderson, R. D. *Macromol. Symp.* **2007**, *255*, 8–19.
3. Liu, X.; Li, Y.; Lin, Y.; Li, Y. *J. Polym. Sci., Part A: Polym Chem.* **2007**, *45*, 1272–1281.
4. McLeary, J. B.; McKenzie, J. M.; Tonge, M. P.; Sanderson, R. D.; Klumperman, B. *Chem. Commun.* **2004**, 1950-1951.
5. McLeary, J. B.; Calitz, F. M.; McKenzie, J. M.; Tonge, M. P.; Sanderson, R. D.; Klumperman, B. *Macromolecules* **2004**, *37*, 2383-2394.

CHAPTER 5: RAFT MEDIATED COPOLYMERIZATION

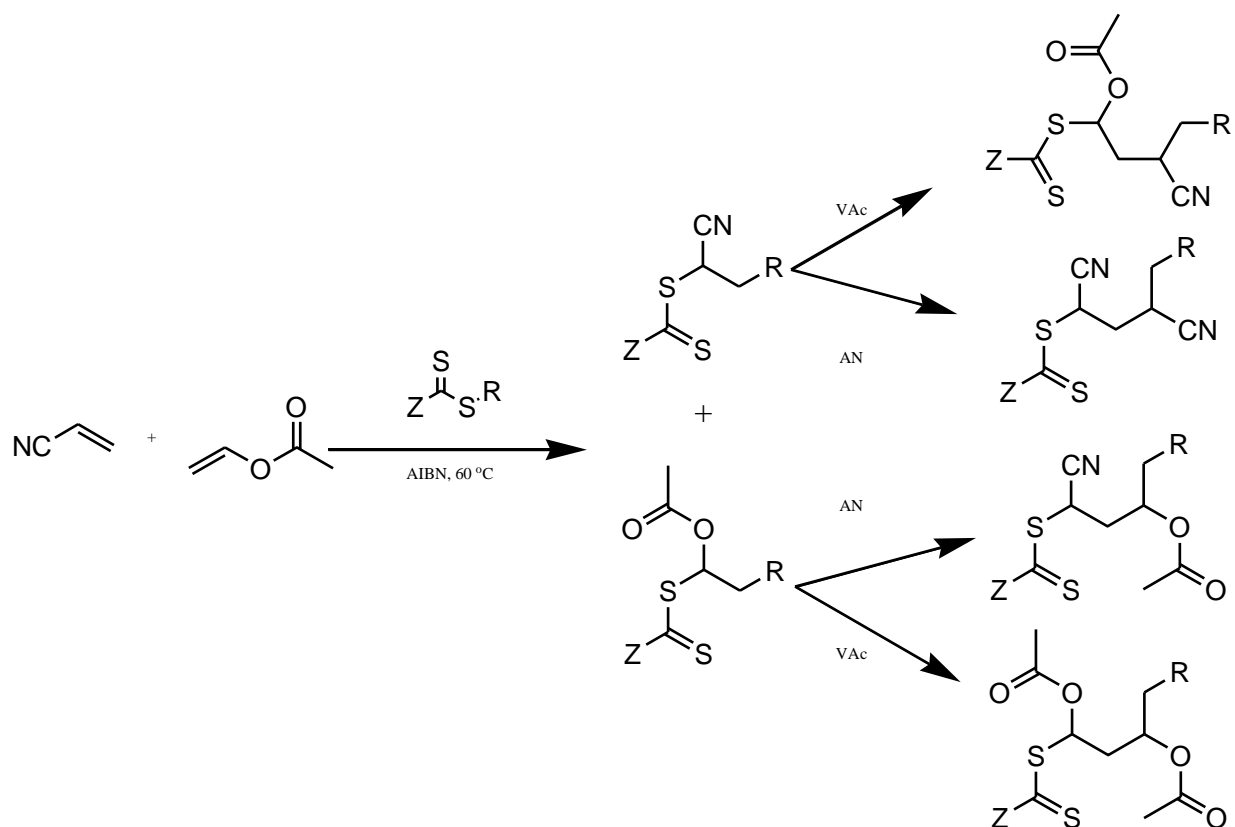
5.1 Introduction

The application of copolymerization has attracted a lot of popularity because of the improved properties which would otherwise not be attainable with the use of homopolymers. The copolymerization of acrylonitrile (AN) with vinyl acetate (VAc) has been studied by Cheetham *et al.* under conventional radical polymerization conditions with determined reactivity ratios of $r_{AN} = 2.7$ and $r_{VAc} = 0.05$.^{1, 2} This group used the combination of spin trapping with Electron Spin Resonance (ESR) spectroscopy to examine propagating radicals in the copolymerization mixture. They found that AN propagating radicals were always in abundance in comparison to VAc propagating radicals. The latter could only be detected in VAc fractional feed compositions above 0.9. AN radicals were proven to be reactive towards VAc monomer while the reverse was less favoured, this was corroborated by the large ratio between addition rate coefficient of AN monomer to VAc radical center, k_{VA} , to the addition rate coefficient of VAc to AN radical center, k_{AV} , ($k_{VA}/k_{AV} = 39$).

Centiner *et al.* studied the free radical copolymerization of acrylonitrile and vinyl acetate using ammonium persulphate in aqueous media while varying the vinyl acetate content and then electrospun the copolymer into nanofibers. They reported that the polymer showed improved thermal properties as compared to polyacrylonitrile (PAN) homopolymer. High VAc feed compositions resulted in nano-fibers of decreased diameter and the nano-fiber mats made from copolymer containing 30% VAc could be applied as membranes for filtration. Also, they could be used as precursors for carbon nano-fibers for energy storage applications due to thin and homogeneous nano-fiber distribution exhibiting high thermal stability and high surface area.³

AN/VAc copolymer has found application in acrylic fibers synthesis where at least 85% by weight of the polymer should be acrylonitrile. It can also be used as a plastic when VAc content is above

15 %.⁴ Increased incorporation of the comonomer in PAN polymer has been found to result in increased mobility of polymer segments, thus the copolymer has a lower glass transition temperature (T_g). In addition, the AN/VAc copolymer was found to be easy to spin and the onset of cyclization temperature during oxidation was found to be significantly reduced as compared to the PAN homopolymer. Furthermore, the crystallinity of the copolymer and the crystal size are significantly reduced relative to pure PAN homopolymer. For the copolymerization of AN with VAc, Scheme 5.1 shows the copolymerization tree diagram of the possible products during the first few monomer additions.



Scheme 5.1: Reaction pathway for RAFT-mediated copolymerization showing the first two monomer insertions.

5.2 Determination of Reactivity Ratios

Monomer reactivity ratios are important parameters that aid in the prediction/description of the copolymer composition for a given feed composition of a monomer pair system. It is however of

importance to be able to estimate the reactivity ratios as accurately as possible. There are two main models used to describe radical copolymerization namely the terminal unit method (TUM) and the penultimate unit model (PUM).⁵ TUM does not consider the penultimate unit effect on reactivity of the chain end radical with the incoming monomer while the PUM takes into account the effects of both the terminal unit and penultimate unit on the reactivity. In situations where the average propagation rate coefficient needs to be determined, PUM should be used since TUM in general fails to describe it correctly.

A number of methods, linear and nonlinear, have been used to determine reactivity ratios. For determination of reactivity ratios at low monomer conversion, Kelen-Tudos^{6, 7} Mayo-Lewis⁸, and Mao-Huglin⁹ have been shown to give reliable results. Extended Kelen-Tudos¹⁰ and Mao-Huglin methods have been used for determination of reactivity ratios at high monomer conversions as they take into account the monomer composition drift.¹¹ What all these methods of determining reactivity ratios have in common is that the copolymers with the fractional composition ratios varied from 0-1 are prepared. This is followed by isolation of the copolymer and then molar feed and copolymer compositions determined. The down side of these approaches is that they are associated with a number of errors including the fact that the copolymer composition is not instantaneous, thus it is the average copolymer formed until termination of the reaction. Most importantly, the error structure of the experimental data may be distorted due to the linearization process. Also, complete isolation of the copolymer from the solvents and residual monomer may be impossible. Reactivity ratios in this work were calculated based on the nonlinear least squares fitting method proposed by Aquilar *et al.*¹² This method has been found to give reliable reactivity ratios especially for the monomer system with high dissimilarity in reactivity. Aquilar's method is based on the instantaneous copolymer compositions as described by TUM, given by the equation 5.1.

$$F_{AN} = \frac{r_{AN}f_{AN}^2 + f_{AN}f_{VAc}}{r_{AN}f_{AN}^2 + 2f_{AN}f_{VAc} + r_{VAc}f_{VAc}^2} \quad (5.1)$$

Where F and f denote the mole fraction of the monomer in the copolymer and feed composition respectively. Integration of equation 5.1 transforms it to the integrated form of copolymerization equation 5.2.

$$\frac{[VAc]}{[VAc]_0} = \left(\frac{[VAc]_0 [AN]}{[AN]_0 [VAc]} \right)^{r_{VAc}/(1-r_{VAc})} \times \left(\frac{(r_{AN}-1) \left(\frac{[AN]}{[VAc]} \right)^{-r_{VAc}+1}}{(r_{AN}-1) \left(\frac{[AN]_0}{[VAc]_0} \right)^{-r_{VAc}+1}} \right)^{(r_{AN} r_{VAc}-1)/[(1-r_{AN})(1-r_{VAc})]}$$

(5.2)

if $\frac{[AN]}{[VAc]} = x$, $\frac{[AN]_0}{[VAc]_0} = x_0$, $[VAc] = y$, $[VAc]_0 = y_0$, $r_{VAc} = a$, $r_{AN} = b$ then equation

5.2 can be rewritten as equation 5.3, factoring out the constant k gives equation 5.4.

$$y = y_0 \left(\frac{[x]}{[x_0]} \right)^{b/(1-b)} \times \left(\frac{(1-b)+(a-1)x}{(1-b)+(a-1)x_0} \right)^{(ab-1)/[(1-a)(1-b)]}$$

(5.3)

$$y = kx^{b/(1-b)} \times ((1-b) + (a-1)x)^{(ab-1)/[(1-a)(1-b)]}$$

(5.4)

Where k is a constant that includes initial conditions and its value is described by equation 5.5, its used as a third parameter in nonlinear fitting of equation 5.4.

$$k = y_0 \left(\frac{1}{[x_0]} \right)^{b/(1-b)} \times \left(\frac{1}{(1-b)+(a-1)x_0} \right)^{(ab-1)/[(1-a)(1-b)]}$$

(5.5)

5.3 Experimental

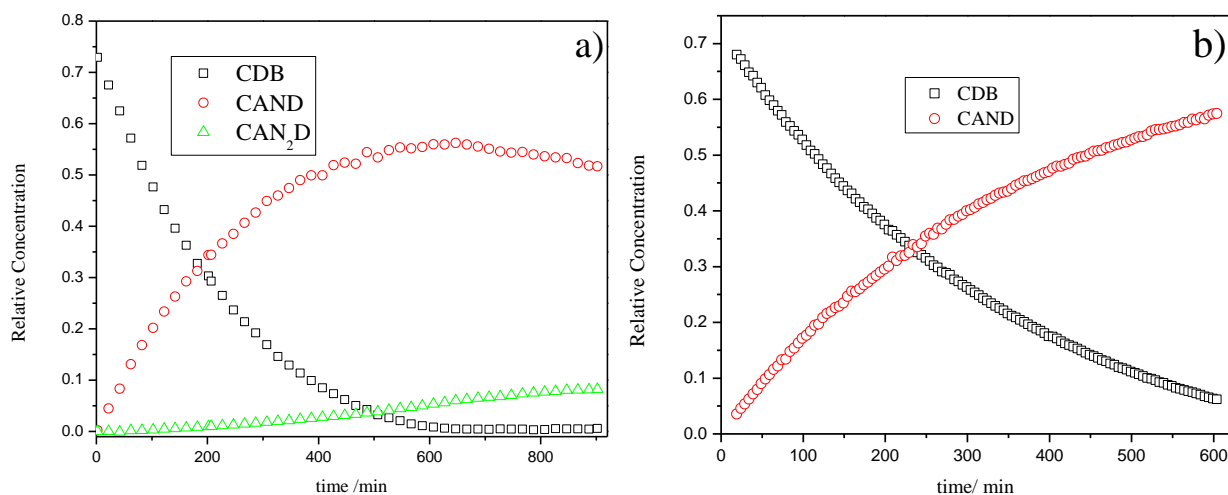
Refer to Chapter 4 section 4.3 and Chapter 3, Table 3.1

5.4 Results and Discussions

5.4.1 CDB-Mediated Acrylonitrile-Vinyl Acetate (AN/VAc) Copolymerization

The copolymerization of AN with VAc was investigated at 60 °C and at 70 °C by *in situ* proton NMR employing CDB as a chain transfer agent at total monomer to CDB to AIBN ([M]:[CDB]:[AIBN]) ratios of 5:1:0.2 and 10:1:0.1. In all the CDB-mediated copolymerization experiments, two first monomer adduct peaks were observed as was the case in the CDB-mediated AN homopolymerization. These two isomeric structures resonated around the same frequencies, 1.13-1.16 ppm and 1.23-1.26 ppm, as in the homopolymerization reactions. However, this first monomer adduct peaks are suspected to be a mixture of AN and VAc adducts since the first adduct peaks of both VAc and AN appeared around the same resonance frequency values as was shown in homopolymerizations (Chapter 4, Figures 4.2 and 4.5). With that in mind, it should be stated that since addition of VAc to CDB is not favoured, the majority of the first monomer adduct species is expected to be composed of AN adduct.

For the CDB mediated copolymerization reactions carried out at 60 °C, two main observations were made. Firstly, when the $f_{AN} \leq 0.5$, the second monomer adduct peaks could not be observed in the ^1H NMR spectra (Figures 5.1(b-c)). For the copolymerization where $f_{AN}=0.9$, second monomer adduct peaks were observed as seen in Figures 5.1(a). Secondly, the rate of CDB consumption was slower than in homopolymerization with initialization time about 600 minutes for the sample where $f_{VAc}=0.1$ was used as opposed to 150 minutes reported for AN homopolymerization reaction (Chapter 4, Figure 4.3). The possible explanation for these observations is the fact that VAc retards the AN polymerization since it competes for CDB and traps it during the repeated addition-fragmentation cycles between VAc units and cumyl radical of CDB.



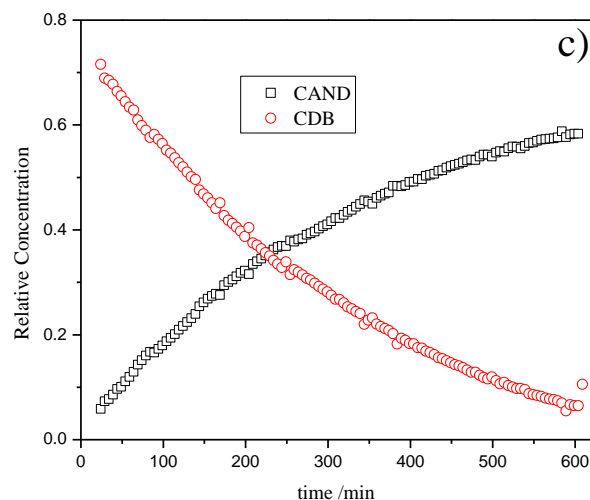


Figure 5.1: The relative concentration of the RAFT species for CDB mediated AN/VAc copolymerization with [M]:[CDB]:[AIBN] ratios of 5:1:0.2 monitored via *in situ* ^1H NMR for 10 hours. at 60 °C a) $f_{\text{AN}}=0.9$, b) $f_{\text{AN}}=0.5$, c) $f_{\text{AN}}=0.25$

AN monomer conversion calculated for above copolymerization reactions at 60 °C with [M]:[CDB]:[AIBN] ratios of 5:1:0.2 were found to be 24%, 47%, 54% for corresponding AN feed composition of 0.9, 0.5, and 0.25 respectively. Higher AN fractional conversion were obtained greater than 17% obtained in the CDB-mediated AN homopolymerization conducted under similar reaction conditions(Section 4.4.1 Chapter 4). This should be expected since the AN content in copolymerization reactions is relatively lower than in AN homopolymerization reaction.

Figure 5.2 shows the plot of fractional conversion of AIBN as a function of time and it shows that AIBN conversion remains more or less the same for all the experiments. The exception was observed for the sample where equal monomer feed compositions were used where after 250 minutes the AIBN decomposition increases drastically. This could have been caused by an abnormal increase or fluctuation in reaction temperature beyond 250 minutes of the reaction time. It was hence concluded that VAc was the main factor causing the retardation in the copolymerization reactions.

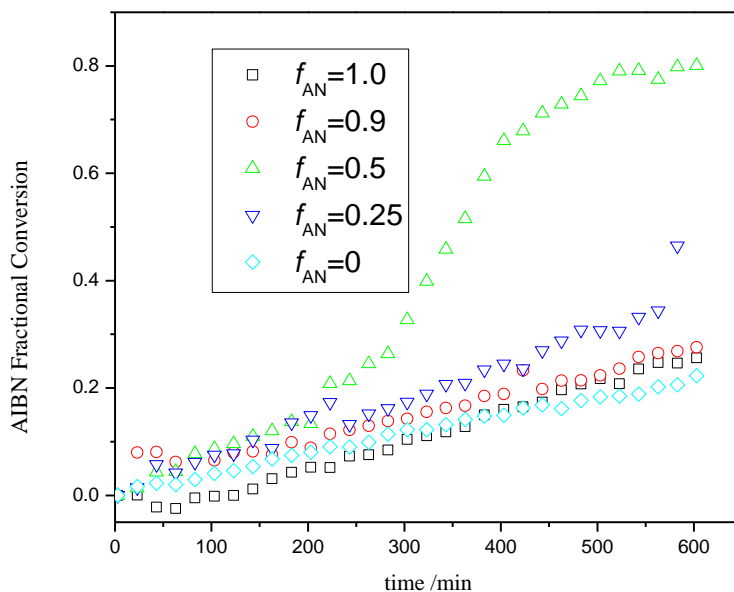


Figure 5.2: The evolution of AIBN fractional conversion with time as a function AN feed compositions for the polymerization reactions with [M]:[CDB]:[AIBN] ratios of 5:1:0.2 monitored via *in situ* ^1H NMR conducted at 60 °C for 10 hours.

5.4.1.1 Temperature effect study

Copolymerization reactions were also conducted at 70 °C using $f_{AN}=0.25$ AN composition feed while still maintaining the 5:1:0.2 total monomer to CDB to AIBN ratio. By increasing the temperature, the aim was to increase rate of decomposition of AIBN and concomitantly increase the rate of monomer consumption. That is, the initialization time, if it exists, would be reduced and the second monomer adduct would be visible within the time of the experiment. Figure 5.3 shows the plot of relative concentration of RAFT species as a function of reaction time for the reaction under-taken at 70 °C. In Figure 5.3, the consumption of CDB was completed within 300 minutes, which is twice faster than at 60 °C. The second monomer was observed but the initialization was not as clear or as sharp as was observed in CBD mediated homopolymerization, thus the reaction still showed significant retardation. The CDB concentrations were believed to be too high to allow observation of the end of initialization period hence further reactions were needed.

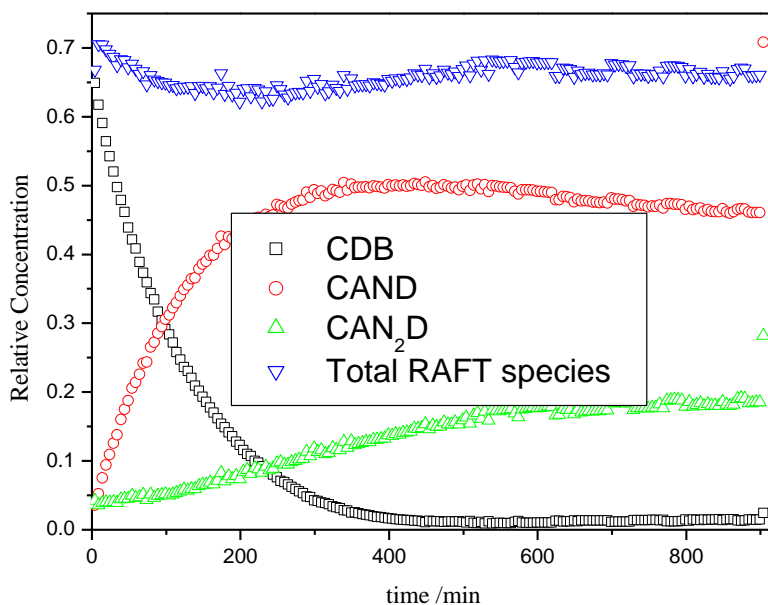


Figure 5.3: The plot of the relative concentration of the RAFT species for the CDB mediated AN/VAc copolymerization at 70 °C and at $[M]:[CDB]:[AIBN]$ ratios monitored by *in situ* ^1H NMR run for 14 hours, $f_{\text{AN}} = 0.25$

5.4.1.2 Increased chain length study

In this subsection, the effect of chain length on the initialization period was studied. The study was motivated by the fact that at longer chain lengths the model RAFT agent concentration will be less as opposed to monomer (more importantly AN) hence it was anticipated that the initialization period would be completed early or within the given reaction time. The experiment was done using 10:1:0.1 monomer to CDB to AIBN ratios with $f_{\text{AN}} = 0.25$ while still maintaining polymerization temperature as 60 °C. Figure 5.4 shows the plot of the relative concentration of RAFT species as a function of reaction time for the CDB mediated AN/VAc copolymerization reaction. It is observed that CDB concentration decreases at a much slower rate than when the same reaction was done at 5:1:0.2 ratios (Figure 5.1 c)) but at the same polymerization temperature. It is also slower than when the reaction was done at 70 °C but maintaining the 5:1:0.2 ratios (Figure 5.3). In the 14 hours of the reaction time, only 47% of CDB was consumed. The reason behind this observation is suspected to be the low radical flux experienced at 10:1:0.1 ratios used in the current study. Another important observation is that the slope of CDB concentration curve is higher than that of appearance of CAND concentration curve. This means that there are other events, other than

addition to AN monomer, leading to consumption of CDB, these include the consumption of CDB by AIBN radicals.

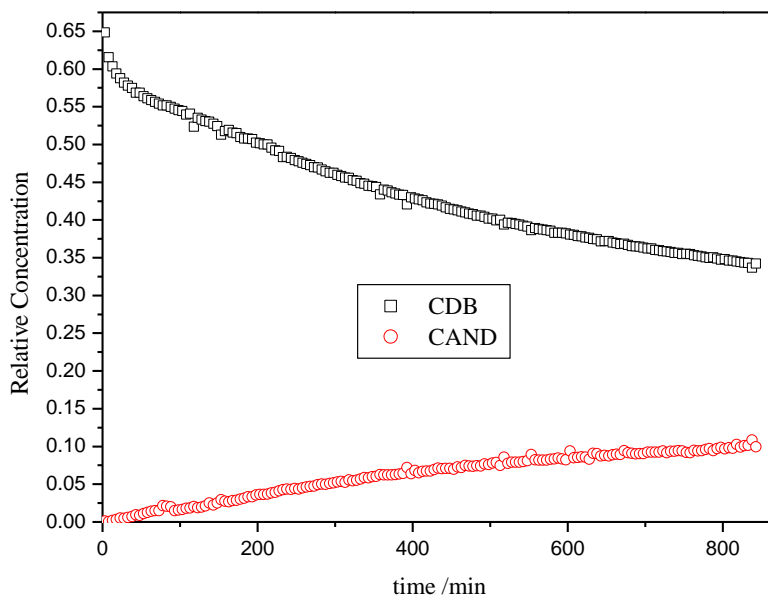


Figure 5.4: The plot of the relative concentration of the RAFT species for the CDB mediated AN/VAc copolymerization at 60 °C and at [M]:[CDB]:[AIBN] ratios of 10:1:0.1 monitored by *in situ* ^1H NMR run for 14 hours, $f_{\text{AN}} = 0.25$

5.4.1.3 Variation of monomer conversion with temperature and chain length

Comparison of individual monomer fractional conversion as a function of time for copolymerization reaction monitored via *in situ* ^1H NMR at $f_{\text{AN}} = 0.25$ were carried out. Figures

5.5, 5.6 and 5.7 show the plots of fractional monomer conversion as a function of time. The VAc conversion is found to be 4% while AN was 54% at the ten hour mark when the polymerization reaction was done at 60 °C (Figure 5.5). For the reaction done at 70 °C but at the same conditions as the previous reaction, VAc conversion was found to be 6% and AN was 60% in five hours (Figure 5.6). This served as further evidence that the reaction rates were improved at higher polymerization temperatures. While increasing the chain length, the VAc conversion was found to be 6% after two hours and it remained constant for the entire reaction time while the AN conversion increased at a slow rate to a final conversion of about 15% when the reaction was done at 60 °C monitored via *in situ* ^1H NMR run for 14 hours at $[\text{M}]:[\text{CDB}]:[\text{AIBN}]$ ratios of 10:1:0.1 (Figure 5.7). Figure 5.7 shows very low conversion of AN as opposed to the previous two cases where 54% and 60% AN conversions were reported. The reason behind the observation may be the fact that in the present case, a lower AIBN concentration is used and hence lower monomer conversions are expected, however the same cannot be said for VAc. The VAc conversion in Figure 5.7 is the same as that reported in Figure 5.6 (6%) and is achieved in short time after the reaction had commenced. The explanation for this behaviour is unknown at the moment.

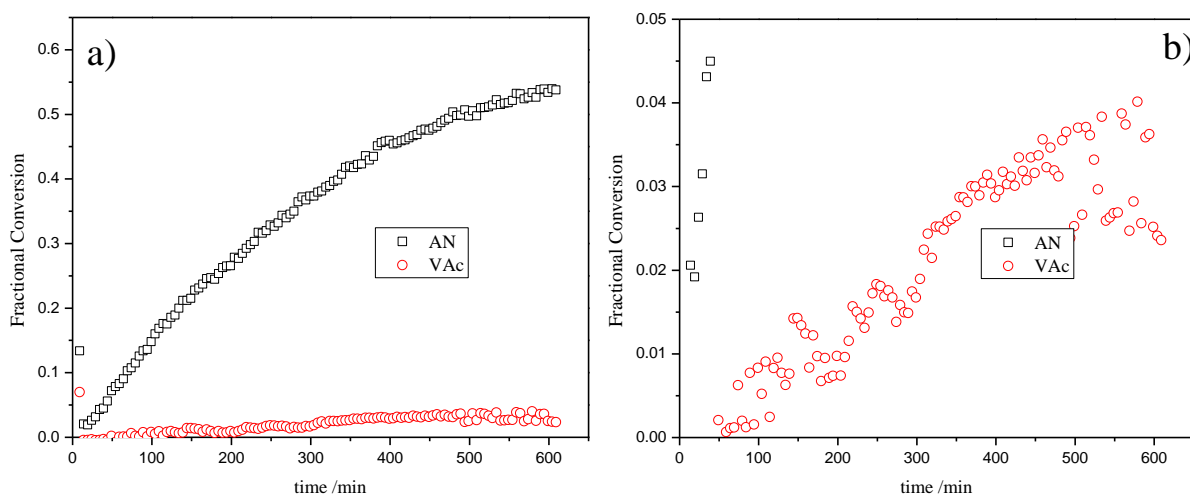


Figure 5.5: a) The evolution of AN and VAc fractional conversion as a function of time for CDB mediated AN/VAc copolymerization at 60 °C monitored by *in situ* ^1H NMR run for 10 hours. $f_{\text{AN}}=0.25$ b) an enlargement in the region of the VAc fractional conversion for the $[\text{M}]:[\text{CDB}]:[\text{AIBN}]$ ratios of 5:1:0.2.

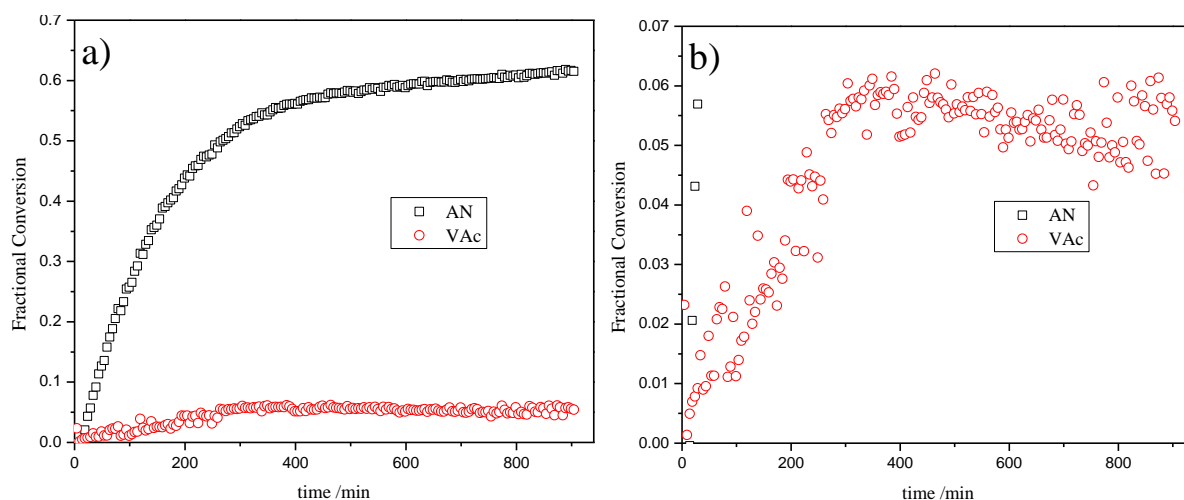


Figure 5.6: a) The evolution of AN and VAc fractional conversion as a function of time for CDB mediated AN/VAc copolymerization at 70 °C monitored by *in situ* ^1H NMR run for 14 hours. $f_{\text{AN}}=0.25$ b) an enlargement in the region of the VAc fractional conversion at $[\text{M}]:[\text{CDB}]:[\text{AIBN}]$ ratios of 5:1:0.2.

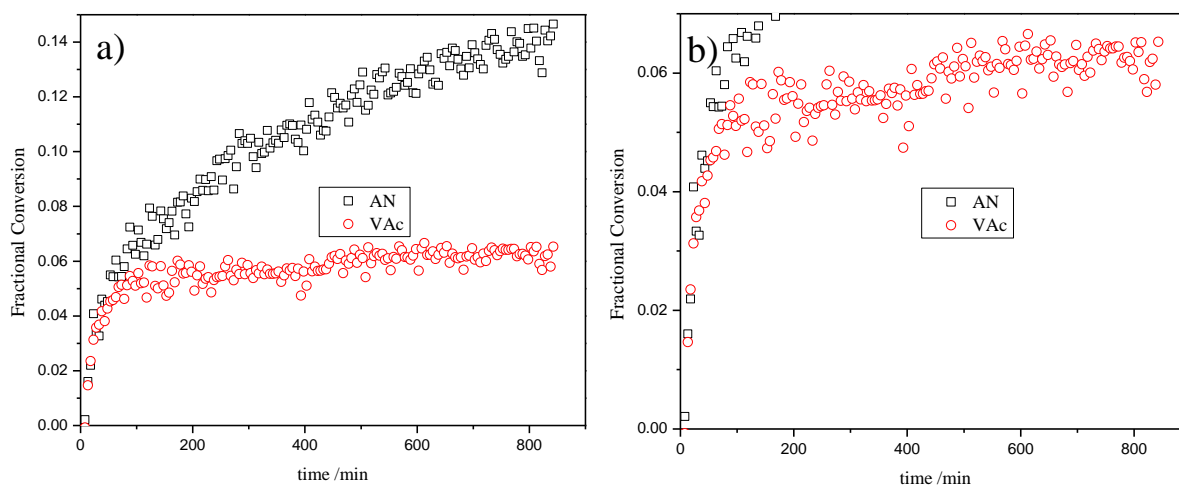
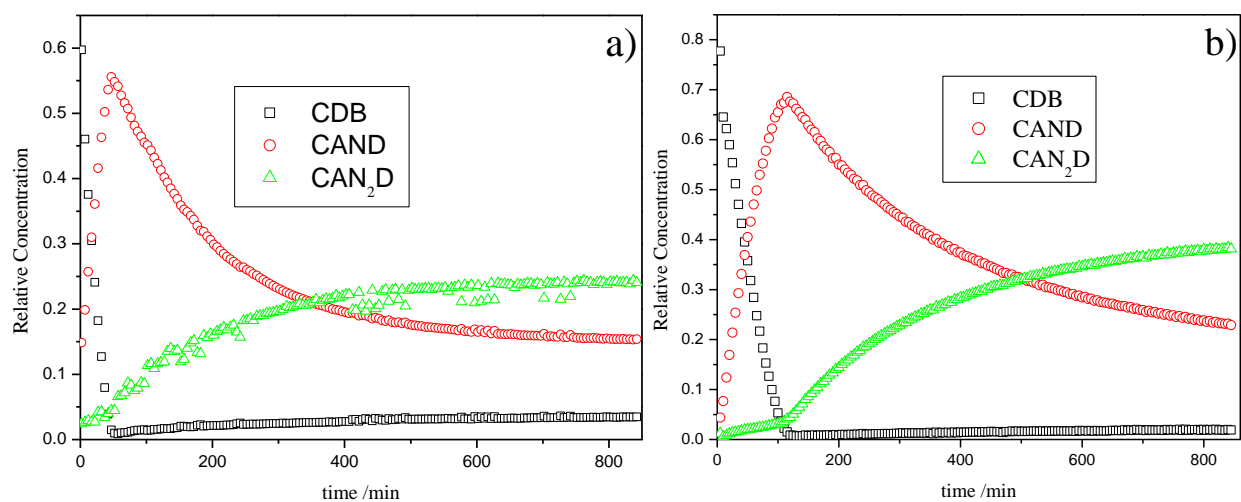


Figure 5.7: The evolution of AN and VAc fractional conversion as a function of time for CDB mediated AN/VAc copolymerization at 60 °C and at $[\text{M}]:[\text{CDB}]:[\text{AIBN}]$ ratios of 10:1:0.1 monitored by *in situ* ^1H NMR run for 14 hours. $f_{\text{AN}}=0.25$ b) an enlargement in the region of the AN fractional conversion

5.4.1.4 Higher temperature and longer chain length studies

In further attempts to try and understand why initialization is retarded in AN/VAc copolymerization, copolymerization reactions were undertaken at 70 °C targeting longer chain lengths ([M]:[CDB]:[AIBN] ratios of 10:1:0.1). Various ratios of AN and VAc were investigated. The plots of relative concentration of various RAFT species as a function of polymerization time are shown in Figure 5.8 (a-c). In these copolymerization reactions, clear initialization and appearance of second adduct species was observed for $f_{AN} = 0.9$ (Figure 5.8 a) and $f_{AN} = 0.5$ (Figure 5.8 b). Conversely, in Figure 5.8 (c) where $f_{AN} = 0.1$, no initialization is observed. The latter scenario can be explained by the fact that the concentration of AN present is less than that of CDB hence AN is depleted before all the transfer agent is consumed. It must be noted that at 10:1:0.1 ratios, the concentrations of CDB and of AIBN are half of that in the case where five monomer units per RAFT agent molecule were targeted. It is believed that this, in combination with high reaction temperature, were the reasons why clear initialization was observed in the 90 and 50 % AN copolymerization reactions at 70 °C.



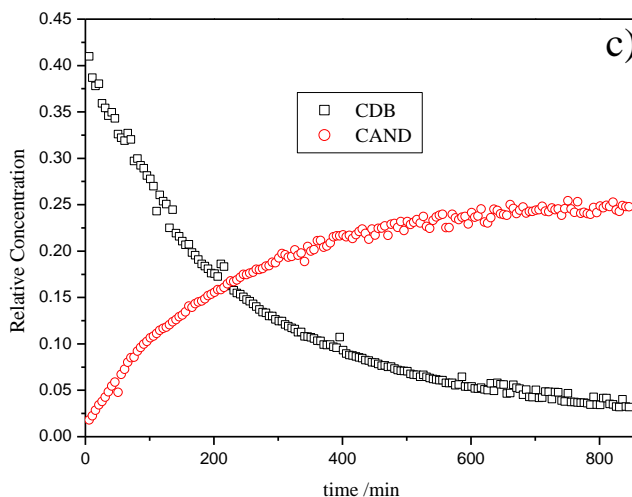


Figure 5.8: The relative concentration of the RAFT species for CDB-mediated AN/VAc copolymerization at 70 °C monitored by *in situ* ^1H NMR run for 14 hours at $[\text{M}]:[\text{CDB}]:[\text{AIBN}]$ ratios of 10:1:0.1 a) $f_{\text{AN}} = 0.9$, b) $f_{\text{AN}} = 0.5$, c) $f_{\text{AN}} = 0.10$.

5.4.1.5 Variation of initialization time as a function of VAc feed composition

The effect of increasing VAc feed composition as function of time was investigated by plotting the CDB fractional conversion as a function of time at shorter chain length and lower temperature, Figure 5.9, as well as at longer chain length and higher temperature, Figure 5.10. In both these graphs, the time for complete CDB conversion increased as a function of decreasing AN in the feed composition (while increasing VAc in the feed) in the copolymerization mixture. The exception was that the $f_{\text{AN}}=0.9$ sample showed the same CDB conversion rate as in $f_{\text{AN}}=1$ for the reaction done at 70 °C and at $[\text{M}]:[\text{RAFT}]:[\text{AIBN}]$ ratios of 10:1:0.1. The explanation here maybe due to the fact that at $f_{\text{AN}}=0.9$ sample, majority of the intermediate radicals in the copolymerization reaction mixture are composed of AN and hence the effect of VAc seems to be negligible. As a result, the fragmentation rates during homopolymerization and copolymerization at 10% VAc do not differ much at 70 °C and $[\text{M}]:[\text{CDB}]:[\text{AIBN}]$ ratios of 10:1:0.1.

However, referring back to Figure 5.9, the copolymerization reactions undertaken at 60 °C and $[\text{M}]:[\text{RAFT}]:[\text{AIBN}]$ ratios of 5:1:0.2, addition of 10% VAc shows major retardation in the reaction time, when compared to that of CDB mediated AN homopolymerization under similar conditions. From there on, not much difference in the initialization periods is observed in

copolymerization where higher ($f_{VAc}=0.5$ and $f_{VAc}=0.25$) VAc content is used. The explanation here for the observation is believed to be due to high CDB concentrations as well as lower reaction temperatures. Thus, under these reaction conditions, the reaction rate of either monomer with CDB is lower and hence it will take longer for CDB to be completely consumed. Thus, in the wide range of VAc feed compositions studied in the present work, $f_{AN} = 0.9-0.25$, at 60 °C the successful addition of cumyl radical to VAc monomer does not differ much.

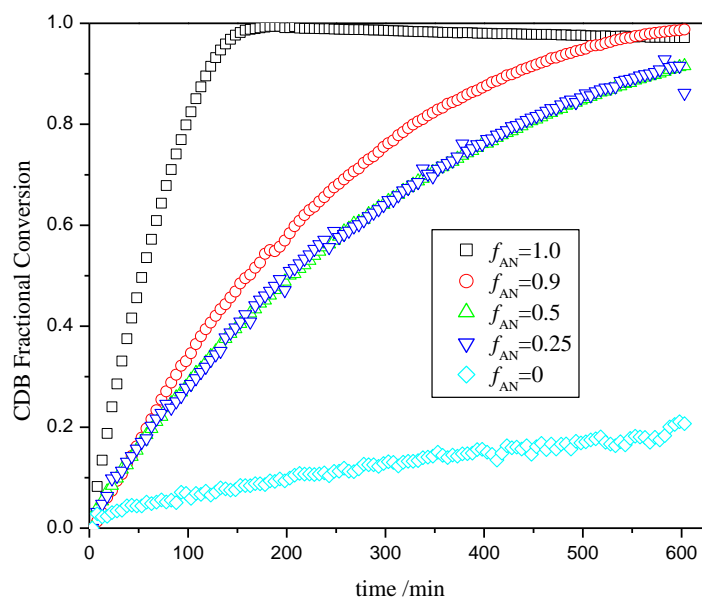


Figure 5.9: The CDB fractional conversion as a function of time at various f_{AN} for the polymerization reactions undertaken at 60 °C and at $[M]:[CDB]:[AIBN]$ ratios of 5:1:0.2 as monitored by *in situ* 1H NMR. Where total $[M]_{oTotal} = 2$ M, $[CDB]_o = 3.5 \times 10^{-1} - 4.5 \times 10^{-1}$ M and $[AIBN]_o = 7.5 \times 10^{-2} - 9.0 \times 10^{-2}$ M.

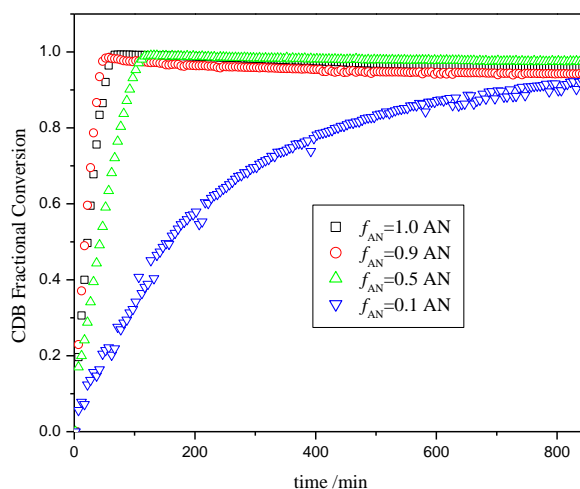


Figure 5.10: The CDB fractional conversion as a function of time at various f_{AN} for the copolymerization reactions at 70 °C and at $[M]:[CDB]:[AIBN]$ ratios of 10:1:0.1 as monitored by *in situ* 1H NMR. Where total $[M]_{oTotal} = 3$ M, $[CDB]_o = 3.1 \times 10^{-1}$ M and $[AIBN]_o = 3.1 \times 10^{-2}$ M.

5.4.1.6 Selectivity Studies with CDB

Methyl acrylate/ vinyl acetate (MA/VAc) and AN/VAc are similar reactivity ratio type systems and as such, one expects that both these systems will tend to give similar reactivity results when it comes to controlled radical copolymerization reactions. A closer examination of AN and MA show that in the presence of VAc, the initialization process is retarded when CDB was used as the RAFT agent. However, this retardation seems to be more severe in the case of AN/VAc copolymerization compared to MA/VAc copolymerization. Figure 5.11 a) and b) show the plots of relative concentration profiles versus time of the cumyl leaving group and its single monomer adduct species in MA homopolymerization and MA/VAc ($f_{VAc} = 0.5$) copolymerization processes, respectively. The initialization process in MA homopolymerization was found to take about 240 minutes as opposed to 260 minutes in MA/VAc copolymerization. For the homopolymerization of AN, initialization took about 60 minutes while it took about 110 minutes for the copolymerization with VAc ($f_{VAc} = 0.5$) as seen in Figure 5.12 a) and b). Thus, the initialization period took about 20 minutes more in the case of MA/VAc copolymerization compared to MA homopolymerization and almost doubled up (50 minutes) in the AN/VAc system compared to AN homopolymerization. This

shows that CDB exhibits higher selectivity in MA/VAc copolymerization than in AN/VAc copolymerization. The possible explanation could be the fact that MA is more electron poor than AN, while the cumyl leaving group of CDB is electron rich. This large difference in electron density around the vinyl double bond of the monomers (MA and AN) means that the cumyl radical will tend to show higher selectivity in the MA copolymerization than in the AN copolymerization.

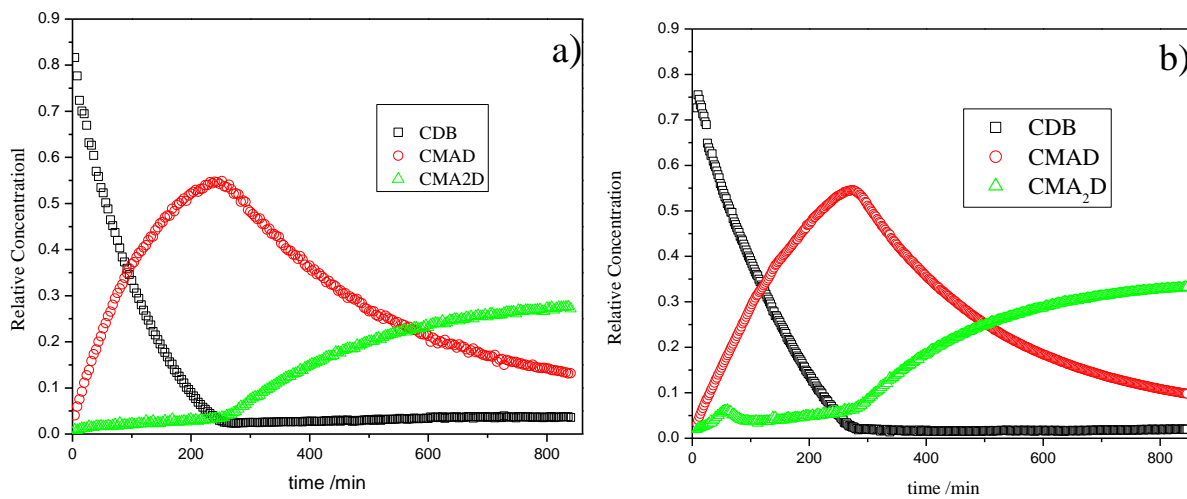


Figure 5.11: Relative concentration of CDB adducts versus time for CDB mediated polymerization at 70 °C and 10:1:0.1 [M]:[CDB]:[AIBN] ratios (a) MA CDB-mediated homopolymerization and (b) MA/VAc CDB-mediated copolymerization, $f_{MA}=0.5$

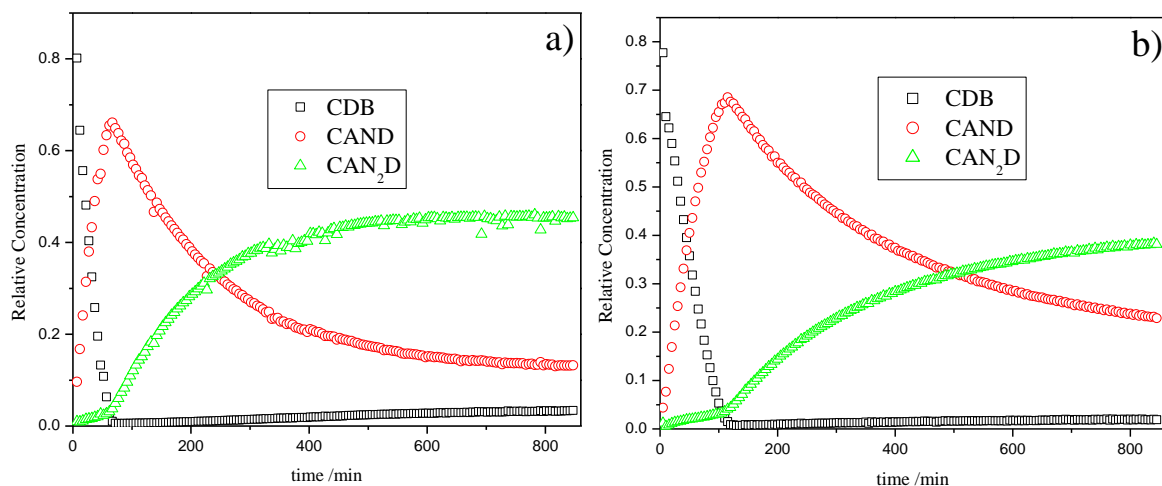


Figure 5.12: Relative concentration CDB adducts versus time CDB mediated polymerization at 70 °C and 10:1:0.1 [M]:[CDB]:[AIBN] ratios a) AN CDB-mediated homopolymerization and b) AN/VAc CDB-mediated copolymerization, $f_{MA}=0.5$

5.4.2 *S*-Cumyl-*O*-Ethyl Xanthate (ECX) Mediated Copolymerization

The ECX-mediated copolymerization reaction was done at equimolar feed compositions of AN and VAc at 60 °C using [M]:[ECX]:[AIBN] ratios of 5:1:0.2. Examination of individual monomer fractional conversion as a function of time (Figures 5.13 a) and b)), shows fast reaction rates in the first 50 minutes of the reaction for both monomers, after which the rate slows down for AN with little or no further consumption of VAc. On the other hand, fractional conversion of ECX as a function of time in homo- and copolymerizations of AN and VAc are plotted in Figure 5.14. No clear initialization was observed in all these experiments and this was ascribed to the hybrid behaviour occurring during the reaction. The results observed in Figure 5.14 are similar to previously observed results in ECX-mediated AN homopolymerization as reported in section 4.4.2 of Chapter 4.

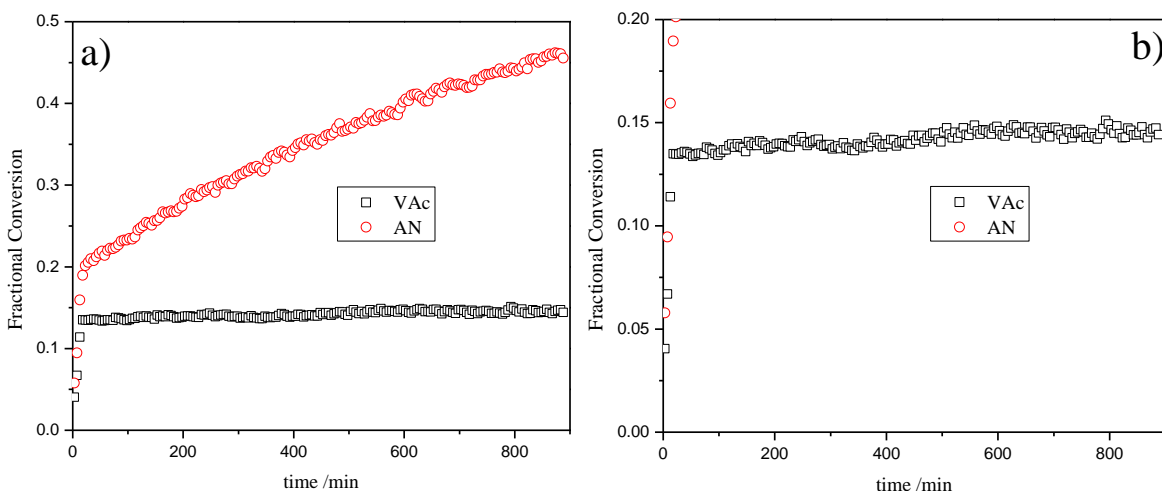


Figure 5.13: a) The fractional monomer conversion as a function of time for ECX-mediated AN/VAc copolymerization at 60 °C monitored via *in situ* ^1H NMR for 10 hours. $f_{\text{AN}} = 0.5$ b) shows an enlargement in the region of the VAc fractional conversion.

From Figure 5.14, it can also be established that the ECX conversion rate is slowed down in the copolymerization (O, Figure 5.14) reaction compared to the homopolymerization (Δ , Figure 5.14) reaction. The ECX conversion was found to be 70 % as opposed to 95% in ECX mediated AN homopolymerization. It must be noted that the *O*-ethyl group is a poorly stabilizing Z-group, which favours fast fragmentation of the intermediate radical. On the other hand, the cumyl leaving group is a highly stabilized electron rich group which will tend to show affinity for the electron deficient AN monomer. Due to destabilizing *O*-ethyl Z-group, oligomeric AN chains will be formed very early in the reaction before the initial ECX is completely consumed. In conclusion, even though xanthates are good RAFT agents for VAc, cumyl R-group makes a bad radical to react with VAc but react favourably with AN. However, the ECX has a low chain transfer constant when it comes to AN. Similar kind of hybrid behaviour was described by Pound-Lana for *N*-vinylpyrrolidone (NVP) polymerization mediated by *S*-*tert*-butyl-*O*-ethyl xanthate.¹³ The hybrid behaviour was confirmed by liquid chromatography mass spectroscopic (LC-MS) analysis; these results are shown and discussed later on in this chapter, (see Figures 5.20 and 5.21).

The LC-MS results showed that the polymer products were composed of a mixture of chains with one to four AN units and an *O*-ethyl xanthate RAFT chain end still intact for the ECX-mediated

homopolymerization. In the ECX-mediated copolymerization, similar results were obtained, but with a presence of chain transfer adducts (CTA) with one VAc unit inserted. The abnormal decrease of ECX (Figure 5.14) conversion in the first few minutes of the reaction for the ECX mediated VAc homopolymerization and for the ECX mediated AN/VAc copolymerization could have been due to errors associated with manual integration.

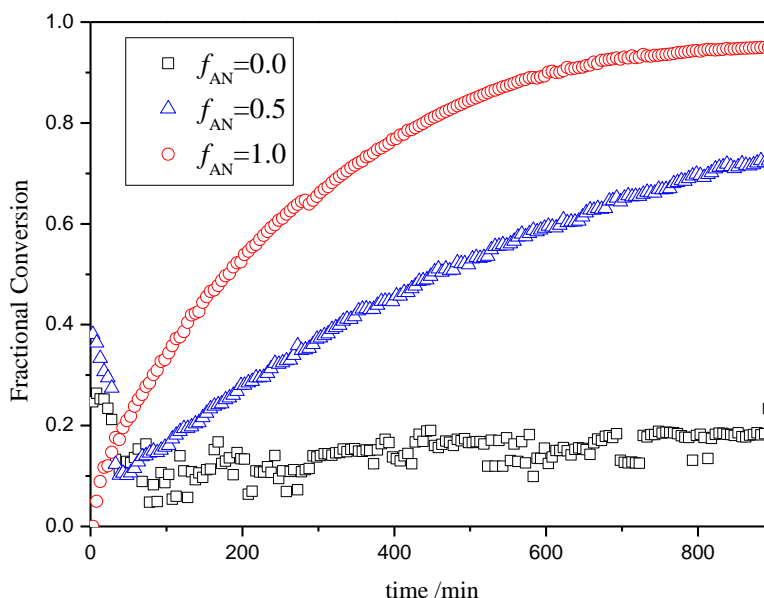


Figure 5.14: ECX fractional conversion for the ECX mediated polymerization at 60 °C in C₆D₆ at [Monomer]:[ECX]:[AIBN] ratios of 5:1:0.2 at 0, 0.5 and 1 AN feed compositions

5.4.3 *S*-sec Propionic acid *O*-Ethyl Xanthate (PEX) Mediated AN-VAc Copolymerization

The PEX-mediated copolymerization was monitored via *in situ* ¹H NMR under similar polymerization conditions used in the case of CDB and ECX. Figure 5.15 shows the variation of concentration of all relevant species in the polymerization mixture as a function of time. It is evident that PEX gets consumed faster than AIBN up until 400 minutes of the polymerization reaction time. Past the 400 minute mark, PEX and AIBN concentrations decrease at the same rate. Studying the monomer concentration profiles, AN is seen to be used up faster than VAc. This behaviour may be explained by the fact that the PEX leaving group radical is quick to react with

VAc monomer to result into the formation of the first VAc adduct species with the PEX transfer agent. The doublet peak associated with the first VAc adduct was observed to appear around 1.622-1.675 ppm. These first VAc adduct peaks appear at the same resonance frequency in both PEX-mediated VAc homo- and copolymerization.

Hence, one can conclude that PEX still shows some specificity towards VAc even in the presence of co-monomer (AN). However, once VAc radicals have been generated, AN can react with them as it was reported that AN is reactive to VAc radicals.² On the other hand, most of AN seems to be undergoing free radical polymerization reaction and this is corroborated by the fact that its reaction rate is faster than that of VAc. It must be mentioned that xanthates have moderate transfer abilities with regards to polymerization of more activated monomers. Destarac *et al.* reported that the *O*-ethyl xanthates mediated polymerization of styrene showed improved transfer ability when the leaving group stability and steric hindrance was increased.¹⁴

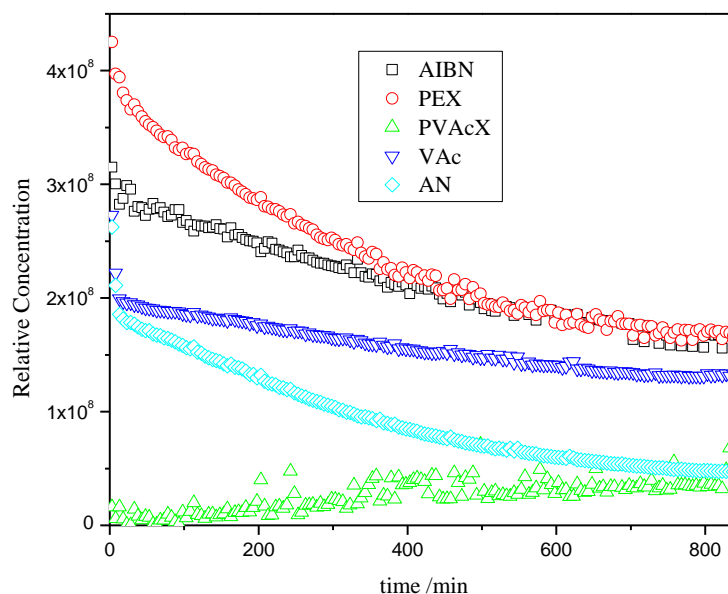


Figure 5.15: The relative concentration versus time for the PEX mediated copolymerization of AN and VAc at 60 °C monitored by *in situ* ^1H NMR using $f_{\text{AN}} = f_{\text{VAc}}$ where $[\text{M}]:[\text{PEX}]:[\text{AIBN}]$ is 5:1:0.2

Upon exploration of fractional monomer conversions, Figure 5.16, it was found that the final VAc fractional conversion was 31% while that of AN was 75%. This further strengthens the argument that most of the AN underwent conventional radical polymerization, the THF SEC analysis of this sample gave D values of 1.7. However, we believe once in a while, the AN oligomer would add a VAc unit which then has a high probability of adding to the S=C double bond of either the original or oligomeric transfer agent to undergo RAFT mechanism until the terminal unit changes to AN.

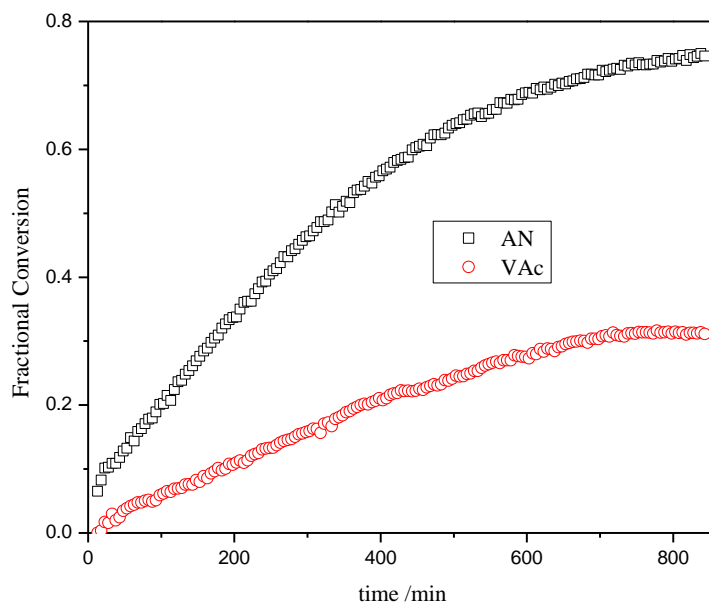


Figure 5.16: Fractional monomer conversion for the PEX-mediated copolymerization of AN and VAc at 60 °C using $f_{AN} = f_{VAc}$ where $[M]:[PEX]:[AIBN]$ is 5:1:0.2

5.4.4 Evaluation of the Reactivity Ratios

The TUM reactivity ratios of the RAFT mediated AN/VAc copolymerization were determined by application of the nonlinear least square fitting procedure where the experimental data extracted from the *in situ* ^1H NMR was fitted to equation 5.4. Figures 5.17-5.19 show the plot of the experimental and fitted data for the three RAFT agents. The fitted data match the experimental data almost perfectly for the PEX mediated system (Figures 5.17) and the reactivity ratios, $r_{AN} = 2.45$ and $r_{VAc} = 0.156$, demonstrate an improved reactivity of VAc as opposed to free radical copolymerization system. However the reactivity of AN has changed slightly, decreased by about 9%. The reactivity ratios of AN and VAc were also successfully estimated for the CDB mediated copolymerization, $r_{AN} = 22.7$ and $r_{VAc} = 0.118$, as seen from the decent correlation of

the experimental data with the fitted data (Figure 5.18). As for the case of ECX mediated system, the fitted data did not adequately fit to the experimental data as it was seen by the slight divergence of the two curves beyond [AN]/[VAc] ratios 0.65 and 0.80 in Figure 5.19. This shows that it is not possible to estimate reliable reactivity ratios for ECX mediated system in the entire experimental [AN]/[VAc] ratios ($r_{AN} = 5.53$ and $r_{VAc} = 0.046$). However, it is worth

mentioning that these experiments were done at short target chain lengths ($[M]:[RAFT]:[AIBN]$ ratios of 5:1:0.2) and also the RAFT agent used in the reaction showed specificity for one monomer in the reaction mixture as such there will be bias in the reactivity ratios. One additional remark is that in all three cases, there is a general trend of deviation of the experimental data from the fitted one at $[AN]/[VAc]$ ratios above 0.95. Experimental fitting was repeated excluding the data points towards the end of the reaction (5 data points), however, no significant improvement was observed in the correlation of the fitted and the experimental data. It was thought that probably the TUM model used in the calculations did not describe the copolymerization system adequately.

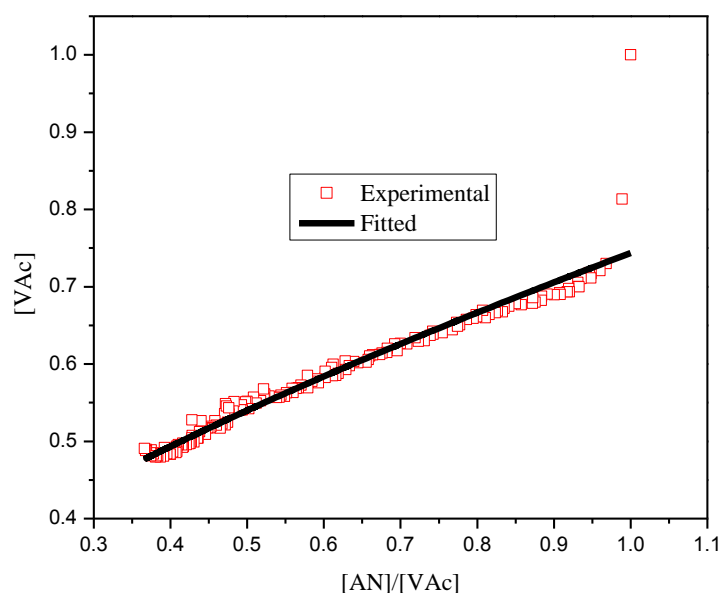


Figure 5.17: Relative concentration of vinyl acetate $[VAc]$ versus the ratio $[AN]/[VAc]$ for the PEX mediated AN/VAc copolymerization at $f_{AN} = 0.5$ and at $[M]:[PEX]:[AIBN] = 5:1:0.2$ for the polymerization undertaken at $60\text{ }^{\circ}\text{C}$ by *in situ* ^1H NMR ($r_{AN} = 2.45$ and $r_{VAc} = 0.156$)

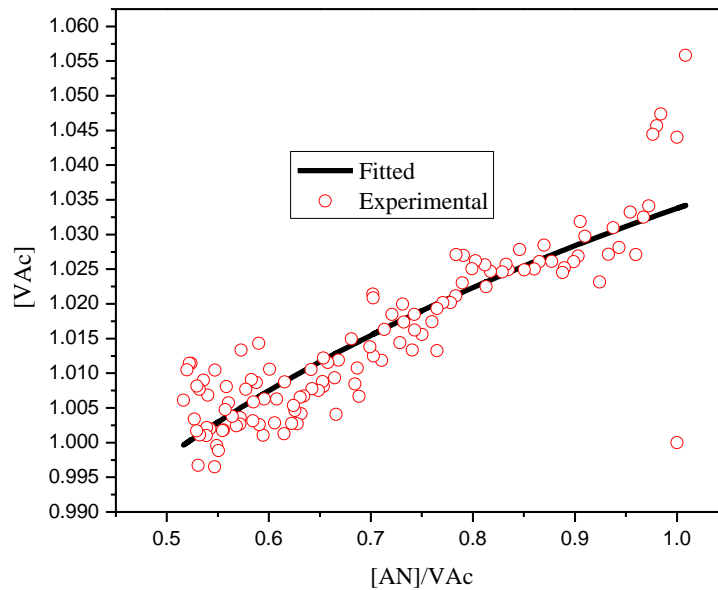


Figure 5.18: Relative concentration of vinyl acetate $[VAc]$ versus the ratio $[AN]/[VAc]$ for the CDB mediated AN/VAc copolymerization at $f_{AN} = 0.5$ and at $[M]:[CDB]:[AIBN] = 5:1:0.2$ for the polymerization undertaken at $60\text{ }^{\circ}\text{C}$ by *in situ* ^1H NMR ($r_{AN} = 22.7$ and $r_{VAc} = 0.118$)

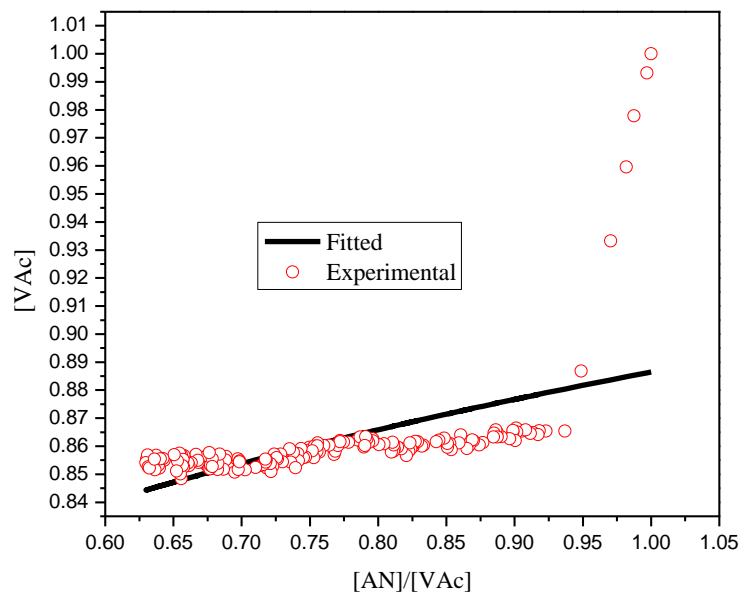


Figure 5.19: Relative concentration of vinyl acetate [VAc] versus the ratio [AN]/ [VAc] for the ECX mediated AN/VAc copolymerization at $f_{AN} = 0.5$ and at $[M]:[ECX]:[AIBN] = 5:1:0.2$ for the polymerization undertaken at 60 °C by *in situ* ^1H NMR ($r_{AN} = 5.53$ and $r_{VAc} = 0.046$)

5.4.5 LC-MS Analysis for RAFT Mediated Copolymerization

The AN/VAc copolymers/oligomers were further characterized by high performance liquid chromatography (HPLC-MS) in order to have an indication of the molecular weight of the species in the final polymerization products. The (co)polymers/oligomers analysed by LC-MS were prepared at 60 °C with $[M]:[RAFT]:[AIBN]$ of 5:1:0.2. Close examination of the LC-MS chromatograms show that only for the ECX-mediated systems, Figures 5.20 and 5.21, the products have oligomer chains ranging from one monomer to five monomer units both in AN homopolymer and copolymer with the ECX end groups at the α and the ω chain ends.

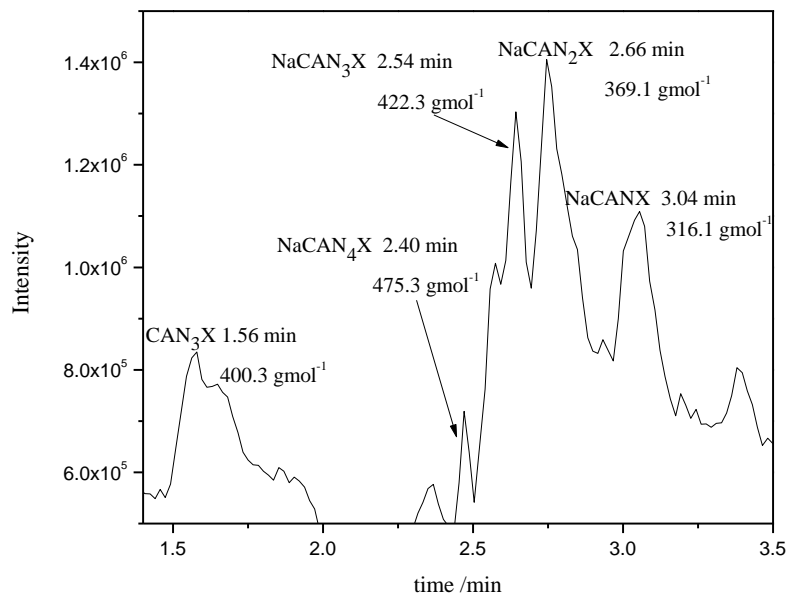


Figure 5.20: LC-MS analysis of ECX-mediated AN homopolymerization at [AN]:[ECX]:[AIBN] ratios of 5:1:0.2 at 60 °C monitored via *in situ* ¹H NMR. The ionization source was ESI+, Capillary voltage 3 kV, Cone Voltage 25 V and the analysis was calibrated against Sodium formate and Lock mass against Leucine enkephalin. Waters UPLC flow rate of 1 mL/min, 100% methanol (Romil), Ascentis[®] C18 column.

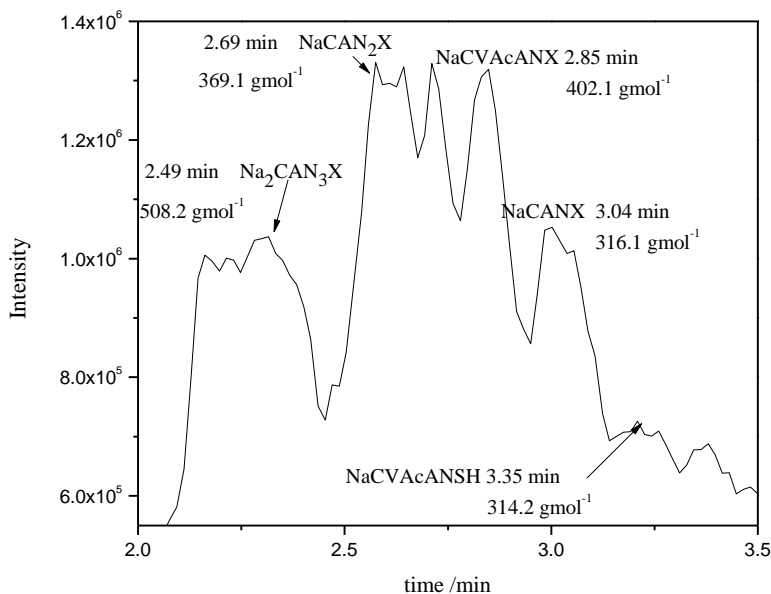


Figure 5.21: LC-MS analysis of ECX-mediated AN/VAc copolymerization at [AN]:[ECX]:[AIBN] ratios of 5:1:0.2 at 60 °C monitored via *in situ* ^1H NMR. The ionization source was ESI+, Capillary voltage 3 kV, Cone Voltage 25 V and the analysis was calibrated against Sodium formate and Lock mass against Leucine enkephalin. Waters UPLC flow rate of 1 mL/min, 100% methanol (Romil), Ascentis[®] C18 column.

In the case of CDB (Figure 5.22) and PEX (Figure 5.23) no RAFT end groups were maintained as was the case with ECX. With CDB, oligomers with three to five monomer units long were obtained. However, the CDB end groups were not observed at all. It is believed that the predominant terminal unit in the chains was VAc, as a result, even soft ionization as ESI initiated bond breakage of such end groups due to weak bond existing between VAc and CDB end groups. All the three copolymers produced with all the three RAFT transfer agents gave UV signal at $\lambda = 290$ nm which is characteristic peak for $-\text{S}-(\text{C}=\text{S})-$ moiety (Figures 1-3 in appendix). Hence this shows that the removal of RAFT chain ends in PEX and CDB produced polymers occurred post the polymerization time (due to ESI ionization). As for the PEX-mediated system, Figure 5.23, oligomer chains with three to five monomer units were obtained. Also, the three 404 g mol^{-1} peaks appearing at different retention times are believed to be due to these oligomer chains having VAc situated as the 1st, 2nd and 3rd positions respectively in the

oligomer backbone hence having different interaction properties with the column. Here, also no RAFT chain ends are maintained for the majority of the chains and it was suspected that the terminal units of the active chains were probably AN monomer. This resulted in PEX end groups not being strongly attached at the oligomer chain ends due to the low probability of addition of AN radicals to PEX. The thiol bearing a (-SH) chains (239 gmol^{-1}) could have been as a result of fragmentation of the chains bearing PEX chain ends. The present result means that the *S*-sec propionic acid readily is a good leaving group but is not as good at reinitiating the polymerization reaction in the copolymerization reaction. This is in contradiction to the PEX mediated VAc homopolymerization where while following the leaving group adduct derivatives, selective initialization was observed.

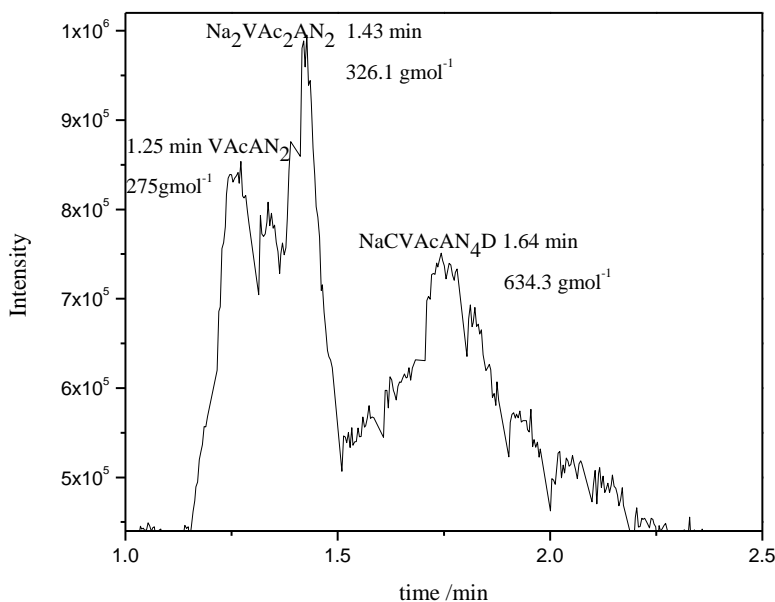


Figure 5.22: LC-MS analysis of CDB-mediated AN/VAc copolymerization at [AN]:[ECX]:[AIBN] ratios of 5:1:0.2 at 60 °C monitored via *in situ* ¹H NMR. The ionization source was ESI+, Capillary voltage 3 kV, Cone Voltage 15 V and the analysis was calibrated against Sodium formate and Lock mass against Leucine enkephalin. Waters UPLC in methanol at a flow rate of 0.2 mL/min using Phenomenex Nucleosil 5 C18, 150x2mm

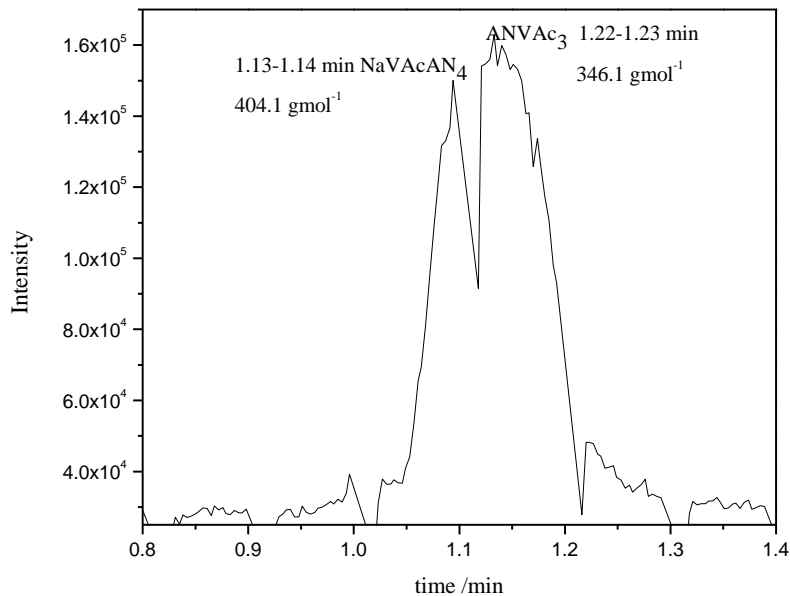


Figure 5.23: LC-MS analysis of PEX mediated AN/VAc copolymerization at [AN]:[ECX]:[AIBN] ratios of 5:1:0.2 at 60 °C monitored via *in situ* ^1H NMR. The ionization source was ESI+, Capillary voltage 3 kV, Cone Voltage 15 V and the analysis was calibrated against Sodium formate and Lock mass against Leucine encephalin. Waters UPLC in methanol at a flow rate of 0.2 mL/min using Phenomenex Nucleosil 5 C18, 150x2mm

5.4.6 High molecular weight RAFT-mediated AN/VAc copolymerization

A set of experiments were done at 70 °C using dimethyl formamide (DMF) as a solvent (in Schlenk flasks and degassing done through bubbling argon gas through the reaction mixture for 10 mins) using [M]:[RAFT]:[AIBN] ratios of 100:1:0.1 while using different RAFT agents, target molecular weight of 5,500 g mol^{-1} . For the experiment done in the absence of the RAFT agent, the same [M]:[AIBN] ratio of 100:0.1 was used. Prior to SEC analysis, the copolymer samples were left in the fume hood for 48 hours to allow the DMF and residual monomer to evaporate. Figure 5.24 shows the DMAc SEC results of these copolymerization reactions. From these three experiments, it is seen that in the case of CDB, PEX and when no RAFT agent was used, multimodal distributions of molecular weight were obtained whereas in the case of ECX, bimodal distribution was obtained.

Thus, even though the overall reaction shows improved dispersity values when RAFT agents were used, as seen from Table 5.1, when looking at the CDB SEC curve, the difference between the retention times of the three distributions is smaller. ECX shows analogous reduction in the difference in the retention times between the two molecular weight distributions as opposed to PEX and in absence of RAFT agent. This shows that even ECX and CDB are not as efficient in controlling the AN and VAc copolymerization at higher molecular weight. Furthermore, in the PEX-mediated copolymerization, the first peak shows a broad molecular weight distribution ($\mathcal{D} = 1.44$) with the number average molecular weight found was $13,117 \text{ g mol}^{-1}$. This behavior was ascribed to the polymerization of AN forming longer chains, after the reaction has commenced, via a mechanism similar to conventional radical polymerization and once in a while attaching a VAc unit. When the terminal unit of the chain is VAc, it is presumed that the polymerization process undergoes RAFT mechanism with PEX and back to conventional radical mechanism when the terminal unit changes to AN.

All the components of the multimodal distributions were suspected to be AN/VAc copolymers but with various AN sequence chain length. It is suspected that the first distribution has longer AN oligomer sequence than second peak and in a similar fashion, the second distribution has longer AN sequence than the third one. If this holds, all the copolymers should be completely soluble in organic solvents. This was tested by dissolving the copolymer samples showing multimodal distributions in pentane and in THF. None among PEX, CDB and no RAFT copolymers dissolved in pentane. The CDB copolymer dissolved completely in THF while the PEX produced copolymer and the one produced in the absence of the RAFT agent showed that some copolymer dissolved but still left polymer residue floating around. It is suspected that the floating residue was probably AN homopolymer but further studies need to be done on these samples in order to study the chemical composition of these copolymers in detail.

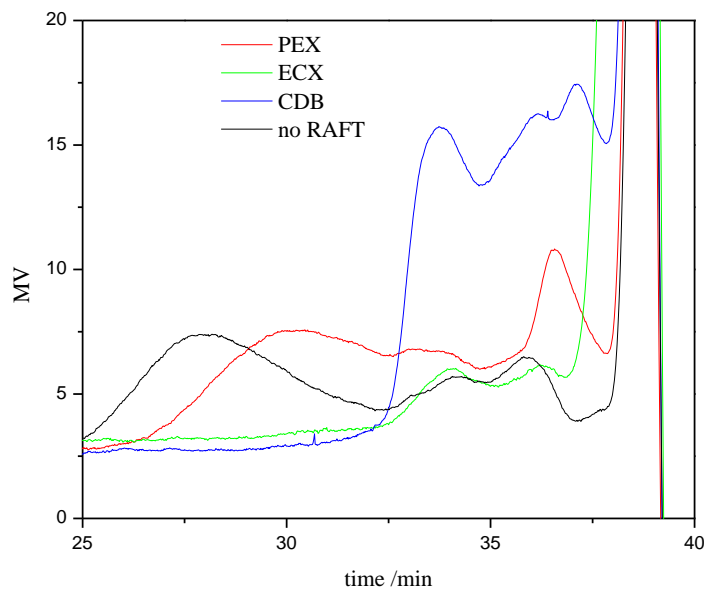


Figure 5.24: DMAc SEC analysis of AN/VAc copolymers produced using different RAFT agents at $[M]:[RAFT]:[AIBN]$ ratios of 100:1:0.1 and $[M]:[AIBN]$ ratio of 100:0.1 in absence of RAFT agent at 70 °C.

Table 5.1: DMAc SEC analysis against polymethyl methacrylate (PMMA) standards

EXPERIMENT	Target M_n / $g\text{mol}^{-1}$	SEC M_n / $g\text{mol}^{-1}$ (t_R /min)	SEC M_w / $g\text{mol}^{-1}$	\bar{D}
16 ^c $f_{AN} = 0.50$ PEX	5,500	13,117 (30.442) 3,085 (33.262) 1,129 (36.571)	18,911 3,498 1,210	1.44 1.13 1.07
17 ^b $f_{AN} = 0.50$ ECX	5,500	1,788 (36.216)	2,375	1.33 overall
18 ^a $f_{AN} = 0.50$ CDB	5,500	1,600 overall 2,751 (33.741) 1,098 (36.397)	2,145 3,080 1,161	1.34 overall 1.12 1.058
19 $f_{AN} = 0.50$ No RAFT	$\geq 10,000$	20,674 (28.175) 1,586 (35.817)	33,945 2,218	1.64 1.40

NB: Target M_n were calculated based on equation 2.1 in Chapter 2 and also was based on AN homopolymerization

^a Cumyl dithiobenzoate (CDB)

^b *O*-ethyl-*S*-cumyl xanthate (ECX)

^c *S-sec* propionic acid *O*-ethyl xanthate (PEX)

where t_R is retention time

5.5 Conclusion

The RAFT-mediated copolymerization of AN and VAc was done where CDB, ECX and PEX were used as chain transfer agents. In the CDB-mediated copolymerization, when the reaction was undertaken at low temperature (60 °C) and at 5:1:0.2 ratios, the initialization period was found to be extremely long. Thus, introduction of 10% VAc in the copolymerization mixture resulted in the initialization period being four times (600 minutes) longer than when homopolymerization of AN was done under the same reaction conditions. The retardation was thought to be caused by repeated addition-fragmentation cycles of the first VAc unit to cumyl leaving group of CDB. Thus, this makes some of the CDB not immediately available for AN to react with.

Also the second monomer adduct was not observed when the AN feed composition was 50% and 25%. While doing the copolymerization reaction of the 25% AN feed composition at increasing polymerization temperature 70 °C resulted in reduction in the retardation time by about 200 minutes and the second monomer adduct peaks were also picked up by the ¹H NMR instrument. This retardation was consistent even while changing both the chain length and temperature at the same time. It was hence concluded that initialization still occurs in CDB mediated AN/VAc copolymerization even though VAc imparts some retardation to the process.

The use of xanthates, ECX and PEX, in the copolymerization resulted in the oligomerization of AN in both cases. With PEX, a small percentage of the first VAc adducts were observed. From this study, it was concluded that *S-sec* propionic acid leaving group of PEX adds VAc to undergo RAFT polymerization whereas once the AN unit attaches to the chain, then a process similar to conventional radical polymerization occurs due to low transfer properties of xanthates when it comes to controlling more activated monomers. ECX, on the other hand, has a leaving group suitable for reaction with AN but not VAc, while the transfer constant is high enough for VAc and not for AN, this still resulted in telomerisation of AN monomer.

LCMS analysis of the polymers revealed an interesting observation; the polymer where ECX was used as the RAFT agent gave the oligomer chains containing one VAc unit with chain length distribution from one to five monomer units. Again, the RAFT chain ends were maintained in all the polymer/oligomer chains. In the case of PEX and CDB, much narrower chain length distributions were found, which were three to five monomer units long for both, but all without RAFT chain ends. It is speculated that PEX produced copolymer chain had AN as the terminal unit and CDB ones probably had VAc terminal units, which both resulted in a weak bond with the RAFT chain ends. On exposure of the samples to ESI ionization energy of the LC instrument, these bonds were easily destroyed.

For the CDB, ECX and PEX mediated systems, the LC-MS results revealed that some form of control was observed in both systems. Thus, the number average molecular weight of the resultant polymer product in all the three studied cases were close to or less than the theoretically targeted one (500 g mol^{-1}). This means that, the polymer grew in a controlled manner, however increasing the target molecular weight to $5,500 \text{ g mol}^{-1}$ resulted in the polymer with three distributions (PEX and CDB) and two distributions (ECX) as determined by DMAc SEC against PMMA standards. This was suspected to be due to propagation and initialization events occurring at the same time. This last study revealed that of all the three RAFT agents, CDB gave a much better control over AN/VAc copolymerization while PEX gave the poorest control over number average molecular weight when higher molecular weight values were targeted.

5.6 References

1. Cheetham, P. F.; Huckerby, T. N.; Tabner, B. J. *Eur. Polym. J.* **1994**, *30*, 581-587.
2. Cheetham, P. F.; Tabner, B. J. *Eur. Polym. J.* **1994**, *30*, 1367-1373.
3. Cetiner, S.; Sen, S.; Arman, B.; Sarac, S. A. *J. Appl. Polym. Sci.* **2012**, *127*, 1-9.
4. Zhang, C.; Du, Z.; Li, H.; Ruckenstein, E. *Polymer* **2002**, *43*, 2945-2951.
5. Zetterlund, P. B.; Tagashira, S.; Izumi, K.; Nagano, Y.; Azukizawa, M.; Yamazoe, H.; Kumagai, M.; Yamada, B.; . *Macromolecules* **2002**, *35*, 8209 - 8215.
6. Kelen, T.; Tüdös, F. *J. Macromol. Sci. Chem.* **1975**, *A9(1)*, 1-27.
7. Semsarzadeh, M. A.; Daronkola, M. R. R. *Iranian Polymer Journal* **2006**, *15*, 829-839.
8. Mayo, F. R.; Lewis, F. M. *J. Am. Chem. Soc.* **1944**, *66*, 1594-1601.
9. Mao, R.; Huglin, M. B. *Polymer* **1993**, *34*, 1709-1715.
10. Tudos, F.; Kelen, T.; Foldes-Bereznich, T.; Turcsanyi, B. *J. Macromol. Sci. Chem.* **1976**, *A10*, 1513.
11. Abdollahi, M.; Mahdvavian, A. R.; Nouri, A. *J. Macromol. Sci. Chem Part A* **2007**, *44*, 839.
12. Aguilar, M. R.; Gallardo, A.; Fernandez, D. M.; Roman, J. S. *Macromolecules* **2002**, 2036-2041, 2036-2041.
13. Pound, G. Reversible Addition Fragmentation Chain Transfer (RAFT) Mediated Polymerization of N-vinylpyrrolidone. PhD Thesis, Stellenbosch University, Stellenbosch, South Africa, 2008.
14. Destarac, M.; Brochon, C.; Catala, J.; Wilczewska, A.; Zard, S. Z. *Macromol. Chem. Phys.* **2002**, *203*, 2281-2289.

Chapter 6: Conclusions and Recommendations

6.1 Overall conclusions

In the present study the RAFT copolymerization of two monomers of strongly different reactivity and also preferring completely different RAFT transfer agents were studied. This study's focus was initially to evaluate if in presence of a RAFT agent specific for addition of one of these monomers, whether this transfer agent would selectively react with it in such a manner similar to such monomers RAFT homopolymerization. Also, to evaluate which of AN or VAc monomer will subsequently follow the addition of the first monomer unit. But first of all the RAFT agents of choice were synthesized according to the procedures stipulated in the literature and are discussed in Chapter 3.

Chapter 4 deals with RAFT homopolymerization of the monomers with the use of all the three RAFT agents. It was found that CDB controlled AN but not VAc while PEX on the other hand gave good control over VAc molecular weight.

Following this, in Chapter 5, the RAFT copolymerization was done to study specificity of RAFT agents in the presence of both monomers in the reaction medium. The most interesting results reported in this work show that CDB mediated systems showed slowed down consumption rates of this transfer agent with addition of VAc to the polymerization mixture. However, varying the fraction of VAc in the feed between 0.1-0.90 did not produce much difference in the retardation of the initialization process and the poor compatibility of VAc with the cumyl radical of CDB was believed to be the main reason for this observation.

In the present study we studied the feed compositions 10%, 50% and 90% in relation to CDB mediated copolymerization. It was concluded that the retardation imparted by VAc did not differ a lot in the various feed compositions.

6.2 Recommendations

It is recommended that further studies be done using CDB but this time put more emphasis on the reactions where $f_{VAc} \geq 0.9$ and $f_{VAc} \leq 0.1$ in order to try and explain the source of retardation better.

We recommend that for high target number average molecular weight samples that a 2D LCMS analysis be done in order to characterize what the polymer products in each distribution are composed of.

From the current study, it was shown that VAc retards AN polymerization when CDB was used as the transfer agent and most chains were found to have a VAc unit. This presents a possibility of end functionalizing AN homopolymer with an ester end by undertaking the CDB mediated homopolymerization and then adding VAc at a desired AN conversion to stop the reaction and at the same time introducing the ester at the chain end of well controlled PAN. It is recommended that studies be done in order to proof these speculations.

APPENDIX

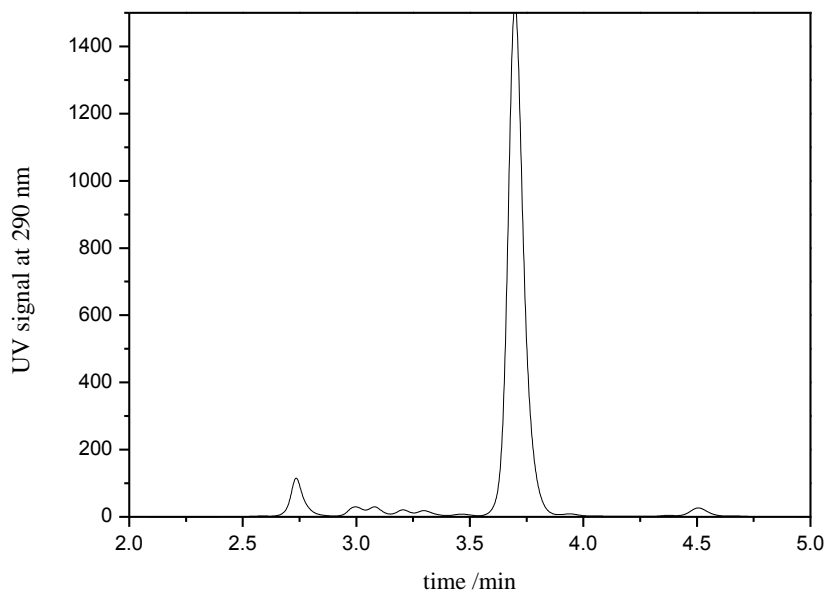


Figure 25: HPLC analysis of CDB-mediated AN/VAc copolymerization at [AN]:[ECX]:[AIBN] ratios of 5:1:0.2 at 60 °C monitored via *in situ* ^1H NMR. UV detector signal at 290 nm. Agilent 1260 LC flow rate of 1 mL/min, 100% methanol (Romil), Ascentis[®] C18 column

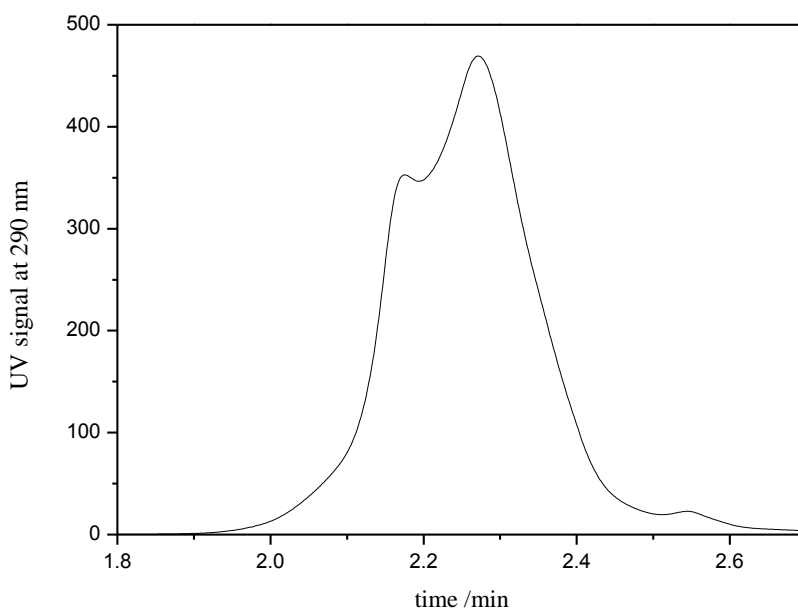


Figure 26: HPLC analysis of PEX-mediated AN/VAc copolymerization at [AN]:[ECX]:[AIBN] ratios of 5:1:0.2 at 60 °C monitored via *in situ* ^1H NMR. UV detector signal at 290 nm. Agilent 1260 LC flow rate of 1 mL/min, 100% methanol (Romil), Ascentis[®] C18 column

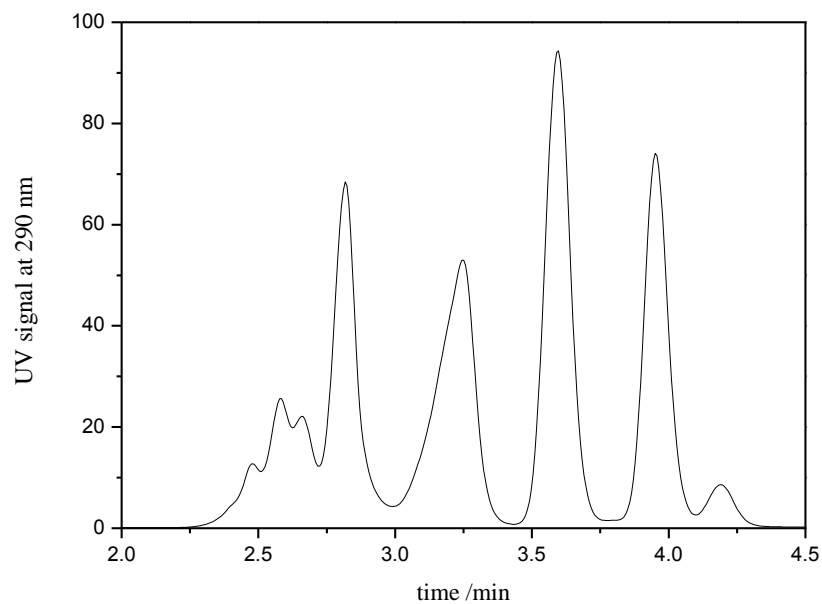


Figure 27: HPLC analysis of ECX-mediated AN/VAc copolymerization at [AN]:[ECX]:[AIBN] ratios of 5:1:0.2 at 60 °C monitored via *in situ* ^1H NMR. UV detector signal at 290 nm. Agilent 1260 LC flow rate of 1 mL/min, 100% methanol (Romil), Ascentis[®] C18 column